

SPECIATION AND TRANSPORT OF
ANTHROPOGENIC ^{129}I IODINE AND NATURAL ^{127}I IODINE
IN SURFACE AND SUBSURFACE ENVIRONMENTS

A Dissertation

by

KATHLEEN A. SCHWEHR

Submitted to the Office of Graduate Studies of
Texas A&M University
in partial fulfillment of the requirements for the degree of

DOCTOR OF PHILOSOPHY

May 2004

Major Subject: Oceanography

© 2004

KATHLEEN A. SCHWEHR

ALL RIGHTS RESERVED

SPECIATION AND TRANSPORT OF
ANTHROPOGENIC ¹²⁹IODINE AND NATURAL ¹²⁷IODINE
IN SURFACE AND SUBSURFACE ENVIRONMENTS

A Dissertation

by

KATHLEEN A. SCHWEHR

Submitted to Texas A&M University
in partial fulfillment of the requirements
for the degree of

DOCTOR OF PHILOSOPHY

Approved as to style and content by:

Peter H. Santschi
(Chair of Committee)

Luis A. Cifuentes
(Member)

Gary A. Gill
(Member)

Ethan Grossman
(Member)

Laodong Guo
(Member)

Wilford D. Gardner
(Department Head)

May 2004

Major Subject: Oceanography

ABSTRACT

Speciation and Transport of
Anthropogenic ^{129}I and Natural ^{127}I
in Surface and Subsurface Environments. (May 2004)

Kathleen A. Schwehr, B.S., Montana College of Mineral Science and Technology;

M.S., University of Houston

Chair of Advisory Committee: Dr. Peter H. Santschi

Iodine is a biophilic element with one natural long-lived isotope, ^{129}I ($t_{1/2} = 15.6$ million years), and one stable isotope, ^{127}I . The inventory of ^{129}I in surface environments has been overwhelmed by anthropogenic releases over the past 50 years. The objective of this study is to utilize the elevated concentration and biophilic nature of ^{129}I and the isotopic ratio of iodine ($^{129}\text{I}/^{127}\text{I}$) as a tracer of water mass movement and organic matter. Additionally, the significantly elevated values of $^{129}\text{I}/^{127}\text{I}$ could provide a geochronometer, similar to the way ^{14}C is used, particularly for terrestrial organic matter that is less than 50 years old.

A series of laboratory experiments and field investigations were carried out to characterize the dominant chemical forms of dissolved iodine, i.e., iodide (I^-), iodate (IO_3^-), and organic iodine (DOI) in natural waters. Sensitive methods were developed for the analysis of nanomolar quantities of ^{127}I species in a variety of environmental systems

using high performance liquid chromatography (HPLC) and an organic iodine decomposition technique, dehydrohalogenation.

The potential use of $^{129}\text{I}/^{127}\text{I}$ as a hydrological tracer was evaluated through measurements of ^{129}I and ^{127}I , which were carried out in wells in the artificially recharged ground water basin of Orange County, California. Literature values of aquifer ages based on $^3\text{H}/^3\text{He}$ and $\delta^{18}\text{O}$ tracer data, as well as time-series data of chloride and Santa Ana River flow rates over the past decade were compared to values for ^{129}I and ^{127}I . The iodine isotopes demonstrated a conservative behavior in these aquifers, suggesting that the observed variations of these isotopes reflect past river flow conditions during the time of recharge.

The feasibility of using $^{129}\text{I}/^{127}\text{I}$ ratios to trace terrestrial organic matter across an estuary was tested. A novel analytical technique to determine $^{129}\text{I}/^{127}\text{I}$ ratios in DOI was developed for this investigation. The results of a Galveston Bay transect clearly show that $^{129}\text{I}/^{127}\text{I}$ ratios in DOI can remain elevated up to salinity of about 15, but that $^{129}\text{I}/^{127}\text{I}$ values of inorganic iodine species do not show any trend with change in salinity gradient due to fast isotopic and chemical equilibration in the estuarine waters.

ACKNOWLEDGMENTS

I would like to express my deepest appreciation to Dr. Peter H. Santschi, Chairman of the Advisory Committee, for presenting me with the opportunity to study at Texas A&M University, and for his encouragement, guidance and support throughout the entire research. I would also like to thank my committee members, Drs. Gary G. Gill, Ethan Grossman, Luis A. Cifuentes, and Laodong Guo, for their constructive suggestions and guidance for my dissertation.

I owe a special thanks to Dr. Gary Gill and Ron Lehman of the Mercury Lab for sharing their facilities and expertise. I gained invaluable insight and experience in assisting Dr. Gary Gill with teaching an EPM lab and observing his techniques in action.

My sincerest appreciation goes to Drs. Degui Tang, Seunghee Han, Kent Warnken, and Key-Young Choe, for their incredible help in the field and in the laboratory. Also, the shared field experience, whether aboard the RV/Gyre or the flat-bottomed 14' skiff in the Galveston Bay with Drs. Jay Pinckney, Erla Ornlófsdóttir, and Beth Lumsden, was rewarding, productive, and memorable. All of these friends provided invaluable technical discussion and insights. I wish to thank Drs. Laodong Guo and Degui Tang for their assistance in my early experimental work; their guidance provided a framework throughout this research. A special thanks to Jan Gerston, and Drs. Jean E. Moran, Chin-Chang Hung, and Sarah D. Oktay-Quigley for sharing their experiences and knowledge. The efforts of Kim Roberts in providing an orderly lab and procedures for radioisotope safety were appreciated. Mary Howley and Sheri Shaklovitz were

always available for invaluable administrative assistance and general advice.

This research was supported by grants from the Texas Water Research Institute, and the Texas Institute of Oceanography Graduate Fellowship, and a Graduate Assistantship through Dr. Peter H. Santschi. The generous provision of $^{129}\text{I}/^{127}\text{I}$ sample analysis via Accelerator Mass Spectrometry was through Dr. David Elmore and Xiu Ma of the Purdue Prime Lab. I also received financial support through Teaching Assistantships from Texas A&M University at College Station and Galveston.

Special appreciation is reserved for Dr. Penny Taylor who has been an inspiration in research and life.

Finally, this dissertation is dedicated to Sherry L. Smotherman, my Aunt Jacquelyn R. Edens, the Smotherman family, Darla Bond, and my Parents, Richard and Sybilla Schwehr, with deepest regards for their unconditional and infinite love, prayers and sacrifice.

TABLE OF CONTENTS

	Page
ABSTRACT	iii
ACKNOWLEDGMENTS	v
TABLE OF CONTENTS	vii
LIST OF TABLES	ix
LIST OF FIGURES.....	x
CHAPTER	
I INTRODUCTION TO THE PROBLEM.....	1
Introduction	1
Hypotheses	19
Objectives.....	20
Approach.....	21
II A SENSITIVE DETERMINATION OF IODINE SPECIES, INCLUDING ORGANO-IODINE, FOR FRESHWATER AND SEAWATER SAMPLES USING HIGH PERFORMANCE LIQUID CHROMATOGRAPHY AND SPECTROPHOTOMETRIC DETECTION	23
Introduction	23
Methodology	26
Results and Discussion.....	45
Conclusions	56
III ¹²⁹ IODINE: A NEW HYDROLOGIC TRACER FOR AQUIFER RECHARGE CONDITIONS INFLUENCED BY RIVER FLOW RATE AND EVAPOTRANSPIRATION.....	57
Introduction	57
Methodology	67
Results and Discussion.....	70

CHAPTER	Page
Conclusions	91
IV THE DISSOLVED ORGANIC IODINE SPECIES OF THE ISOTOPIC RATIO OF $^{129}\text{I}/^{127}\text{I}$: A NOVEL TOOL FOR TRACING TERRESTRIAL ORGANIC MATTER IN THE ESTUARINE SURFACE WATERS OF GALVESTON BAY, TEXAS	93
Introduction	93
Methodology	94
Results and Discussion	103
Conclusions	121
V CONCLUSIONS AND RECOMMENDATIONS FOR FUTURE RESEARCH	122
Conclusions	122
Recommendations for Future Research	126
REFERENCES	128
VITA	143

LIST OF TABLES

TABLE	Page
1.1 Summary of ^{129}I fluxes from some major rivers of the world (Moran et al., 2002).....	3
1.2 Concentrations (ng m^{-3}) of iodine species in aerosols (as cited in Yoshida and Muramatsu, 1995)	6
2.1 Range of total iodine values in geological matrices.....	29
2.2 Mobile phase gradient elution profile	30
2.3 Iodine speciation in the vertical profile of a warm core ring, Gulf of Mexico, $26^{\circ} 0.04' \text{ N}$, $95^{\circ} 20' \text{ W}$. Collection was July 9, 2000, aboard the R/V Gyre.	42
2.4 Iodine speciation in estuarine surface waters from Galveston Bay	43
2.5 Iodine speciation in surface and ground waters from central and southeastern Texas. Gorman Springs and CO_2 Alley (Gorman Cave) are in the Colorado Bend State Park. The Trinity River is the major inflow into Galveston Bay.....	53
3.1 Iodine and water age data for the Orange County study wells.....	65
3.2 Comparison of ^{129}I , ^{127}I , Cl concentrations and flux for regional rivers and the recharge ponds.....	71
3.3 Statistics for TOC (mg/L) from May 1990 through April 2001. Data provided by G. Woodside, OCWD.....	74
4.1 Concentration of ^{127}I species in the surface waters of the Galveston Bay, Dec. 2001	105
4.2 ^{129}I , ^{127}I , and DOC for the linear mixing model end-members, i.e., the Trinity River and the Gulf of Mexico (GOM)	107
4.3 Concentration of ^{129}I and $^{129}\text{I}/^{127}\text{I}$ species in the surface waters of the Galveston Bay, Dec. 2001	115

LIST OF FIGURES

FIGURE	Page
1.1 Iodine biogeochemical cycling in aquatic systems (Baker, 2002)	5
1.2 Iodine species concentration (nM) profile in a Warm Core Ring in the Gulf of Mexico (Schwehr and Santschi, 2003). (TI): total iodine, (TII): total inorganic iodine, (I ⁻): iodide, (IO ₃ ⁻): iodate, (DOI): dissolved organic iodine. Values for DOI are higher than those published for oceans. Additionally, values for TII are equivalent to values for TI (which includes DOI) in other studies, demonstrating that published operational methods for determining DOI may not be quantitative.....	7
1.3 (a) Normalized input functions (to 1988 values) of ¹²⁹ I in Western Europe, showing constant values for ¹²⁹ I in rainwater in the 1990's, while discharges to the ocean greatly increased (Schnabel et al., 2001); (b) ¹²⁹ I/ ¹²⁷ I ratios in rainfall over Western Europe, showing constant values in the 1990's (Szidat et al., 2000).	16
2.1 Peak height for the same concentration of iodide, as a function of NaCl concentration	27
2.2 Chromatograms depicting a change in % B NaCl mobile phase component. A slower elution and better I ⁻ peak resolution evolves as the % B is decreased from chromatogram "a" to chromatogram "c"	32
2.3 Analytical sample processing scheme for the determination of iodine species	33
2.4 HPLC chromatograms showing standard additions to a 200 nM TI solution of certified reference material, powdered milk, NIST SRM 1549. The letters "a" through "d" represent the overlain chromatograms of progressively increasing concentrations. The effective concentrations of the standard additions were a) no addition (sample concentration plus blank iodide solution), b) 17.8 nM, c) 71.3 nM, and d) 142.6 nM. Calculations are presented in the text.	38

FIGURE	Page
2.5 Sea water sample from 1787 m depth from a WCR in the Gulf of Mexico that displays TII analysis using an isocratic mobile phase. The chromatogram curves “a” and “b” represent blanks run before and after the sample which are much higher than blanks using the recommended gradient, Table 2.2. Chromatogram “c” is the diluted sample (DF = 7.25 in a 0.1M NaCl solution) “c”, and the Γ standard additions to the diluted sample of 35.6 nM for “d” and 142.6 nM for “e”.....	48
2.6 This chromatogram series depicts the measurement of TI in the Galveston Bay sample with a salinity of 18, Table 2.4. Chromatogram “a” is the blank. The sample has been diluted 12.2 times and is shown in the “b” chromatogram with no Γ addition. The “c” chromatogram is the sample with an addition of 20 nM of Γ in a 0.1M NaCl solution, and the additions to the “d” and “e” injections are 40 nM and 160 nM, respectively.....	51
2.7 Surface water sample from the Trinity River near its mouth to Galveston Bay, Table 2.5. This overlay of chromatograms depicts the standard additions method for determining Γ concentration. Standard additions were made to a 0.1M NaCl solution, wherein the dilution factor was 10. Chromatogram “a” is the blank and “b” is the sample with no Γ addition. The standard additions of Γ are 3.6 nM (0.6 ppb) for “c”, 17.8 nM for “d”, 35.6 nM for “e”, and 142.6 nM for “f”	54
3.1 Map showing (a) the general location of the study area, the Santa Ana River Basin; (b) the Santa Ana River Basin indicating the Unconfined Forebay recharge area, the Santa Ana River, Prado Dam, Anaheim Lake and Kraemer Basin, and the location of the cross section shown in Fig. 3.2; and (c) a detailed map showing the cross section location.	61
3.2 Cross-section showing the study wells and the artificial recharge ponds. Contours represent ground water age as determined from ($^3\text{H}/^3\text{He}$ for waters >1 yr) and $\delta^{18}\text{O}$ and Xe tracer tests. All ground waters are < 10 yrs old with the exception of AMD 9-3, for which there is no water age data available, and AMD 9-4, which is in a separate aquifer system	64

FIGURE	Page
3.3	Mixing diagram showing iodine isotopic ratios as a function of the inverse of the stable iodine values for surface and ground waters on a log-log scale. The squares represent values for surface waters, i.e., Anaheim Lake (An Lk), Kraemer Basin (Kr Bs), river drainages, and the median for U.S rain (Moran et al., 2002). Dots indicate values for the study wells with the AMD 9 perched aquifer wells delineated as a circled group. The triangle is the AMD 9-4 well, which is in an older, deeper aquifer system than the other wells 76
3.4	The $^{129}\text{I}/^{127}\text{I}$ (10^{-11}) and ^{129}I (10^7 atoms/L) values for ground waters, as a function of ground water age. Vertical error bars represent 10%. 83
3.5	Inverse correlation for chloride concentration (meq/L) in the Santa Ana River at the Prado Dam (SARPD) as a function of discharge at the dam (m^3s^{-1}). The diamonds and the dashed regression line represent monthly values for both flow and $[\text{Cl}^-]$. The inset shows the annual median of the monthly values discussed in the text 84
3.6	(a) The $^{129}\text{I}/^{127}\text{I}$ (10^{-11}) and ^{129}I (10^7 atoms/L) values for ground waters as a function the Santa Ana River Prado Dam (SARPD) mean monthly outflow (m^3s^{-1}). Vertical error bars represent 10%. (b) Also, shown are the chloride concentrations for the ground waters, yet these show no apparent correlation to SARPD flow 86
3.7	The log $[\text{Cl}^-]$ (meq/L) in meteoric precipitation (PPT) as a function of the log $[\text{Cl}^-]$ (meq/L) in ground water (GW) and that of the log $[\text{Cl}^-]$ (meq/L) in the SARPD. The contrast in slope shows the buffered response in $[\text{Cl}^-]_{\text{GW}}$ to changes in $[\text{Cl}^-]_{\text{PPT}}$. The riverine response in changes of $[\text{Cl}^-]_{\text{SARPD}}$ to $[\text{Cl}^-]_{\text{PPT}}$ is much faster as expected. The buffered response of $[\text{Cl}^-]_{\text{GW}}$ explains the lack of correlation in $[\text{Cl}^-]$ to SARPD flow in Fig. 6. $[\text{Cl}^-]_{\text{PPT}}$ data is for monthly precipitation-weighted concentrations from the National Atmospheric Deposition Program for the water years 1982 to 1999 (NADP/NTN, 2002). 89
3.8	Similar to Fig. 3.6, but showing the correlation of ^{127}I values for ground waters as a function the Santa Ana River Prado Dam (SARPD) mean monthly outflow (m^3s^{-1}). Unlike in the case of ^{129}I , there is no apparent correlation to SARPD flow, suggesting that ^{127}I and ^{129}I have different mobilities in ground water 90

FIGURE	Page
4.1	Sampled locations in Galveston Bay Estuary on Dec. 14, 2001 96
4.2	Distribution of ^{127}I species concentrations in the Galveston Bay, December 14, 2001 104
4.3	(a) Comparison of observed (squares) and modeled (triangles) data for [DOC] ($\mu\text{M C}$). The line of short dashes indicates a conceptual conservative linear mixing between the Trinity River and GOM end-members. The shaded area shows the range of variability for the Trinity River input (Guo and Santschi, 1997; Wen et al., 1999; Tang et al., 2002; Warnken and Santschi, 2003). (b) Comparison of observed transect (diamonds) and modeled (triangles) data for [TI] (nM) 108
4.4	Distribution of nutrient concentrations, irradiance (K_d), and biomass as chl a for the sampled transect of Galveston Bay. Data provided by J.L. Pinckney and S.E. Lumsden..... 112
4.5	Distribution of ^{129}I species concentrations in Galveston Bay, December 14, 2001 114
4.6	Comparison of observed (diamonds and solid lines) and modeled (triangles and dashed lines) data for (a) ^{129}I -TI and (b) $^{129}\text{I}/^{127}\text{I}$ for TI 118
4.7	Mixing diagram for the values of the isotopic ratio $^{129}\text{I}/^{127}\text{I}$ (10^{-12}) plotted against $1/^{127}\text{I}$ (ppb^{-1}). Values are shown for $^{129}\text{I}/^{127}\text{I}$ (10^{-12}) median of U.S. rains (diamond), U.S. rivers (circle), and the Gulf of Mexico (GOM, triangle) are all for the iodine species TI for both isotopes. The squares indicate the observed data values for the species DOI for both isotopes. This plot emphasizes the terrestrial source of DOI for Stations 4 and 1, which compare to mixing between U.S. rains and rivers. Stations 3 and 5 show values approximating the ocean waters of GOM with limited dilution from U.S. rivers 120

CHAPTER I

INTRODUCTION TO THE PROBLEM

INTRODUCTION

Sources of iodine isotopes

Iodine is a biophilic element with several short-lived isotopes (^{131}I , with $t_{1/2}$ of 8 days), one long-lived isotope (^{129}I $t_{1/2}$ = 15.6 million years), and one stable isotope, ^{127}I . The environmentally low concentrations of ^{129}I in North America are measured accurately by Accelerator Mass Spectrometer, AMS (Fehn et al., 1986). However, the higher concentrations of ^{129}I in Europe may also be determined by Neutron Activation (Hou et al., 2000). A better understanding of the biogeochemistry of iodine and its isotopes in the environment is important for iodine deficiency disorders, mineralization in exploration geochemistry, migration of radionuclides from the nuclear industry, and the transfer of volatile organic greenhouse-active and ozone-destroying iodine species from the oceans to the atmosphere.

This dissertation follows the journal style of *Geochimica et Cosmochimica Acta*.

Sources of ^{129}I

The total inventory of natural ^{129}I from cosmic ray-induced spallation of Xe in the atmosphere and spontaneous fission of ^{238}U in the earth's crust is $\sim 100\text{-}260$ kg (Fabryka-Martin et al., 1985). Atmospheric bomb testing (1953-1962) added about 50-150 kg to this inventory (USA: ~ 4 kg) (UNSCEAR, 1982; Raisbeck et al., 1995; Eisenbud and Gesell, 1997), while the Chernobyl reactor accident (1986) contributed only ~ 1.3 kg (Paul et al., 1987). The atmospheric releases by the Hanford nuclear facility in Washington (1944-1972) added ~ 260 kg (Hanford website, cited in Schnabel et al., 2001). Fuel reprocessing releases from facilities in La Hague in France and Sellafield in England, however, exceed all these sources, having provided ~ 2600 kg (460 Ci) to the ocean (Raisbeck and Yiou, 1999; Schnabel et al., 2001), and currently ~ 6 kg/yr to the atmosphere (Schnabel et al., 2001). As is evident from Fig.1.1, the nuclear fuel reprocessing discharges to the ocean have increased greatly over the past decade (Raisbeck and Yiou, 1999), while releases to the atmosphere have remained nearly constant (Szidat et al., 2000; Schnabel et al., 2001).

The most important documented sources of ^{129}I have been and still are the fuel reprocessing facilities at La Hague and Sellafield; however, other ^{129}I sources, such as from the former Soviet Union, have also been identified. Estimated ^{129}I fluxes in the Siberian rivers, Ob and Yenisei, which drain former nuclear-weapons-test sites, amount to less than 0.3 kg/yr (Cochran et al., 2000; Moran et al., 2002), but are considerably higher than ^{129}I fluxes in other European and US rivers (Table 1.1).

Table 1.1. Summary of ^{129}I fluxes from some major rivers of the world (Moran et al., 2002).

River	Mean Annual Discharge Rate ($10^3 \text{ m}^3/\text{s}$)	^{129}I conc. (10^7 atoms/L)	^{129}I flux (g/yr)	Reference
Columbia	7.5	16	8	Moran et al., 2002
Savannah	0.28	1,600	28	Moran et al., 2002
Rhine	1.8	37	4.5	Moran et al., 2002
Rhone	1.4	240	22	Moran et al., 2002
Mississippi	18.4	8	15	Oktay et al., 2000
Yenisei	17.6	36	41	Beasley et al., 1997
Ob	13.4	272	235	Moran et al., 1995; Cochran et al., 2000

These sources of anthropogenic ^{129}I are potentially important for several reasons.

1) The largest fraction of the short-term and long-term dose from nuclear releases and fallout is from iodine isotopes. If all the 2500 Ci of ^{129}I produced by the nuclear power industry up to year 2000 would disseminate in the environment, the collective dose equivalent to the world's population will be large, about 10^8 person-thyroid rem on the order of 10^6 person-thyroid Sv (Eisenbud and Gesell, 1997). 2) ^{129}I is one of only two (the other is ^{99}Tc) long-lived nuclides with high mobility in stored radioactive waste (Eisenbud and Gesell, 1997). 3) ^{129}I could provide the scientific community with a new geochemical tracer and geochronometer, similar to anthropogenic ^{14}C .

Because the atmospheric residence time of iodine is about two weeks, it can easily travel around the globe. In fact, anthropogenic ^{129}I from reprocessing emissions is currently found in rainwater (Moran et al, 1999a, b; Lopez-Gutierrez et al., 2000) and river water of the northern hemisphere (Schink et al., 1995b; Oktay et al., 2001; Moran

et al., 2002). These measurably high anthropogenic ^{129}I emissions are found not only in their source area in western Europe, but also in the USA, where known atmospheric releases currently are negligible, as well as in the southern hemisphere (Fehn and Snyder, 2000).

Sources of ^{127}I

Atmospheric and terrestrial sources of stable ^{127}I , Fig. 1.1, originate from aerosols formed from sea spray as inorganic iodide (I^-) or iodate (IO_3^-) species (Heumann, 1993) or from the release of volatile organic iodine (VOI) compounds by algae (Kolb, 2002; O'Dowd et al., 2002; Baker, 2002; Baker et al., 2000). Bacteria and phytoplankton are thought to use enzymes to reduce IO_3^- , the most thermodynamically stable form of iodine in seawater to I^- . In turn, it is speculated that macroalgae and seaweed use I^- in the production of alkyl iodides or VOI, which are emitted as a defense mechanism against grazers. Compounds of VOI in the surface oceanic microlayer are easily photolyzed into reactive iodine species. The most significant concentration of VOI species is CH_3I , which is found in concentrations of 1 to 30 ppt (Stutz, 2000) and has a photolytic span of about 14 to 18 days (Moran et al., 1999a, 1999b). Once photolyzed, the VOI form a reactive pool of iodine oxides, i.e., HOI , I_2O_2 , IO_2 , which either form condensable vapors as nuclei for aerosols, or which react with ozone (Kolb, 2002; O'Dowd et al., 2002), or perhaps cycle as short-term intermediates which re-form VOI, predominantly as CH_3I .

of ^{127}I concentrations are likely low by a factor of 2-3, as early analytical techniques did not quantitatively include organic iodine in their determination of total iodine concentrations. Assessments of organic iodine quantification in estuarine and seawaters showed discrepancies of up to 40% (Wong and Cheng, 2001) or higher (Schwehr and Santschi, 2003), depending on the processing method used. Difficulties in the determination of organic iodine concentration are similar for both of the isotopes, ^{129}I and ^{127}I .

For ^{129}I , ranges in concentrations in aquatic systems are even larger; $10^5 - 10^9$ atoms L^{-1} in freshwaters (summarized in Snyder and Fehn, 2003) and $10^5 - 10^{10}$ atoms L^{-1} in seawater (summarized in Raisbeck and Yiou, 1999). Concentrations of ^{129}I in the atmosphere, range from $10^6 - 10^{10}$ atoms m^{-3} , or in rainwater, range from $10^6 - 10^{10}$ atoms L^{-1} , are dependent on latitude and distance from the European nuclear reprocessing source locations (Tsukada et al., 1991; Lopez-Gutierrez et al., 1999; Moran et al., 1999; Szidat et al., 2000; Schnabel et al., 2001, and references therein).

Table 1.2. Concentrations (ng m^{-3}) of iodine species in aerosols (as cited in Yoshida and Muramatsu, 1995).

Location	Organic	Inorganic	Particulate	Reference
Kansas, Arizona, Canada, Bermuda	3 – 28	0.4 – 17	0.2 – 3.7	Rahn et al., 1976
Hawaii	2.7	5.5	0.5	Butler, 1986
Hawaii	4.4	13	6.4	Butler, 1986
Japan	7.8 – 20.4	1.2 – 3.3	0.3 – 3.4	Yoshida and Muramatsu, 1995

Chemical speciation of iodine isotopes

Since anthropogenic ^{129}I has not had time that ^{127}I has had to equilibrate in environmental surface compartments, these isotopes may not be in isotopic equilibrium. While inorganic I^- and IO_3^- species of both may reach isotopic equilibration rapidly, organic iodine isotopes are expected to equilibrate much more slowly. The slower isotopic equilibration of organic iodine species are due to the biogeochemical cycling of iodine from inorganic chemical species to labile organic forms, such as proteins (half life of days to weeks) and labile humics (half life of weeks to months), then eventually to refractory organic forms (half life in years) (Schwehr and Santschi, 2004). The non-equilibration of organic isotopic anthropogenic ^{129}I to natural ^{127}I may provide new applications for using $^{129}\text{I}/^{127}\text{I}$ ratios as a source tracer or as a geochronometer. However, such applications will require a better understanding of the chemical speciation i.e., I^- , IO_3^- , and especially, organic iodine, for both ^{129}I and ^{127}I .

Chemical speciation schemes for both fresh and marine waters have only recently been reported (Krupp and Aumann, 1999; Hou et al., 2001; Wong and Cheng, 2001; Farrenkopf and Luther, 2002, Schwehr and Santschi, 2003). Organic iodine species can be expected to be important, based on the biophilic nature of iodine. Indeed, in terrestrial surface waters and in the oceans, organic iodine species have been found to be a more significant pool than previously expected. This is demonstrated in Fig.1.2, where the oceanic profile values for total inorganic iodine (TII) correspond very closely to salinity-corrected total iodine (TI) values of other investigators (Schwehr and Santschi, 2003), thus demonstrating the difficulties of accurately assessing dissolved organic iodine

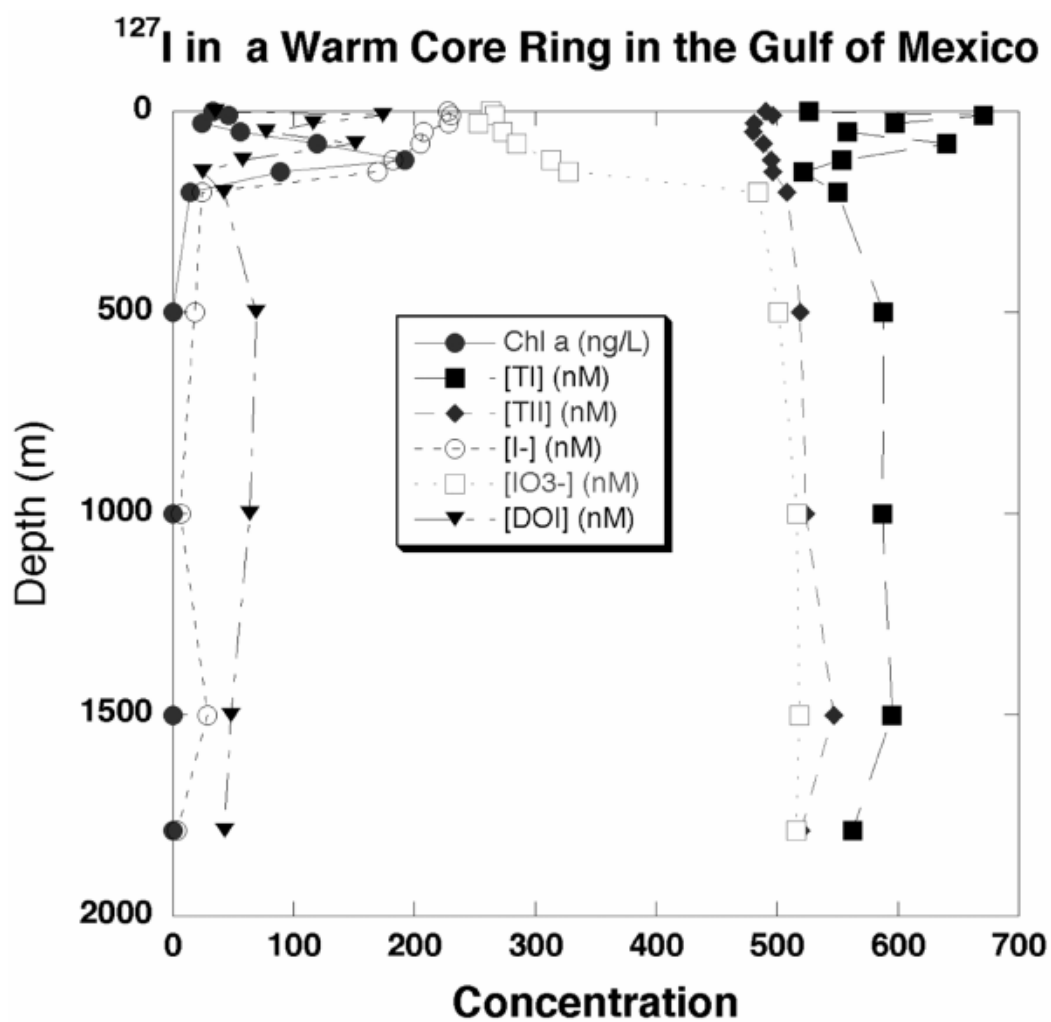


Fig. 1.2. Iodine species concentration (nM) profile in a Warm Core Ring in the Gulf of Mexico (Schwehr and Santschi, 2003). (TI): total iodine, (TII): total inorganic iodine, (I⁻): iodide, (IO₃⁻): iodate, (DOI): dissolved organic iodine. Values for DOI are higher than those published for oceans. Additionally, values for TII are equivalent to values for TI (which includes DOI) in other studies, demonstrating that published operational methods for determining DOI may not be quantitative.

(DOI) values. However, retention of colloidal DOI species in near-surface soils makes DOI the least important iodine species in ground waters where the most mobile species is expected to be iodide (Santschi et al., 1999; Schwehr et al., 2003).

Interactions between water and soil, however, play a key role in the terrestrial iodine cycle. This is the most complex and least studied part of the biogeochemical cycle of I. The chemical forms of iodine in soils and soil water are especially poorly known, but have great bearing on retention versus mobility of both ^{127}I and ^{129}I . These isotopes are expected to have different behaviors and perhaps different chemical forms since the recently introduced anthropogenic ^{129}I may not have isotopically equilibrated with natural ^{127}I in surface environmental compartments.

Chemical forms of anthropogenic ^{129}I from nuclear fuel reprocessing emissions

^{129}I Iodine released to atmosphere from nuclear fuel reprocessing facilities at La Hague and Sellafield is thought to be in the form of CH_3I , which is relatively inert enough (or repeatedly cycles through photolytically-formed reactive intermediates back to CH_3I) that it may be transported in the troposphere of the northern hemisphere within about 14 days (Moran et al., 1999a, 1999b). In this form it may even be long lived enough to be transported to the stratosphere (Wayne et al., 1995). Within the troposphere the chemistry may involve complex cycling due to photolysis and reactions with atmospheric volatile active radicals, i.e., peroxides, hydroxides, ozone, activated oxygen, which form iodine oxides. In summary, both iodine isotopes follow similar chemical pathways, although the concentrations of total ^{129}I are much lower than those of ^{127}I .

Determination of ^{127}I

Iodine in the atmosphere occurs in both gaseous and particulate (bound to aerosols) forms. There is no study documenting the speciation of radioiodine in the atmosphere, and there are only a few documenting that of ^{127}I (Table 1.2). Data given in Table 1.2 show that the organic iodine fraction is an important reservoir. For example, Yoshida and Muramatsu (1995) and Baker et al., (2000) emphasize that 75-90 % of the atmospheric iodine is in a gaseous form, mostly organic.

In aquatic systems (including rain water), very few studies have used reliable procedures to determine the total iodine concentration including organic iodine. In the absence of certified aquatic standard reference materials, the total concentration (wherein organics are totally decomposed) can only be accurately measured using ICP-MS. Recently, Schwehr and Santschi (2003) have presented a speciation scheme for iodine in aquatic samples based on HPLC techniques. Moreover, their HPLC measurements after dehydrohalogenation were within 3-5% of ICP-MS values for total iodine determination. This work suggests that past iodine measurements have only quantified the inorganic speciation and concentrations of iodine, yielding uncertain results for organic iodine concentrations. We speculate that the reason is likely that previous methods relied on oxidation methods, such as UV irradiation, H_2O_2 , or NaClO , to decompose organic iodine compounds. However, such methods are also known to iodinate phenolic compounds or amino acids contained in natural organic matter (SeEVERS and Counsell, 1982; Lassen et al., 1994; Hussain et al., 1995; Bichsel and von Gunten, 1999; 2000) and are not quantitative for DOI decomposition techniques (Spokes

and Liss, 1996; Wong and Cheng, 1998; 2001). This potential analytical artifact illuminates the need for further studies of the biogeochemistry of iodine in the environment.

Summary of chemical and physical behavior of iodine isotopes

What is currently known about the chemical and physical behavior of iodine isotopes in two contrasting continents, North America and Western Europe, can be summarized as follows:

1) The atmospheric depositional flux of ^{129}I in Western Europe is $\sim 3 \times 10^{12}$ at $\text{m}^{-2} \text{yr}^{-1}$ (~ 760 g/yr) (Schnabel et al., 2001), compared to a much smaller flux of about 1×10^{10} at $\text{m}^{-2} \text{yr}^{-1}$ (30 g/yr) (Moran et al., 2002) to the contiguous USA (see Fig. 4 in Santschi and Schwehr, 2003).

2) As a consequence of the transfer pathway of ^{129}I and ^{127}I from air to water to soil to rivers to groundwater, and the recent introduction of ^{129}I to environmental reservoirs, the present-day $^{129}\text{I}/^{127}\text{I}$ ratios in both USA and Western Europe decrease in the direction from rainwater > surface water > near-surface groundwater (Lopez-Gutierrez et al., 2000; Szidat et al., 2000; Schnabel et al., 2001; Buraglio et al., 2001; Moran et al., 2002; Schwehr et al., 2003). ^{127}I concentrations generally decrease from seawater (~ 600 nM) > freshwater (~ 10 -200 nM) > rainwater (~ 20 nM).

3) ^{129}I concentrations in rainwater are higher than in river water in Western Europe due to iodine removal in soils and high local atmospheric source input. ^{129}I concentrations in rain of the USA, however, are much lower than in river water due to

evapotranspirative concentration processes in catchments (Moran et al., 2002; Oktay et al., 2001).

4) In the USA, ^{129}I from bomb fallout still mainly resides in soils, while ^{129}I in rivers is likely from reprocessing sources. In contrast, in Western Europe both sources of ^{129}I reside mainly in soils. Positive correlations between ^{129}I concentrations and chloride and DOC, DON or total phosphate concentrations in Swedish rivers suggest that ^{129}I in rivers is from both atmospheric sources as well as from soil erosion (Kekli et al., 2003).

5) ^{129}I in European groundwater decreases, as expected, with water residence time of 1 d to 2 years. In the USA, ^{129}I concentrations decrease from surface to groundwater due to retention of macromolecular organic iodine, but increase in ground waters with water residence time of 0.1 to 7 years. The mechanism for this striking difference between European and USA groundwater is possibly due to the more inert behavior of the predominant ^{129}I species in USA rivers and semi-arid soils than in Europe (see Fig. 5 in Santschi and Schwehr, 2003).

6) In the surface environment, it appears that there are contrasting physico-chemical responses in iodine isotopic behavior, between anthropogenic ^{129}I and ^{127}I . As stated earlier, the slower isotopic equilibration of organic iodine species are due to the biogeochemical cycling of iodine from inorganic chemical species to labile organic forms, such as proteins (half life of days to weeks) and labile humics (half life of weeks to months), then eventually to refractory organic forms (half life in years) (Schwehr and Santschi, 2004). In addition there is also different speciation between ^{129}I from bomb fallout (more reactive iodine) and ^{129}I from nuclear fuel reprocessing (less reactive

iodine) (Oktay et al., 2001; 2000).

7) ^{129}I (Smith et al., 1998; Cooper et al., 2002; 1998) and other radioisotopes (Baskaran et al., 1995, 1996) in Russian Arctic waters are mainly from the European reprocessing plants of La Hague and Sellafield. However, the amounts of ^{129}I carried by the Ob River to the Arctic Ocean, due to releases from nuclear facilities in its drainage basin, are some of the highest of any world river (Table 1.1).

^{129}I as a new environmental tracer and geochronometer in environmental archives

If certain conditions are met, ^{129}I could be used as a new environmental radioactive tracer, i.e., as a process proxy or analogue. These conditions include: 1) ^{129}I must trace a single environmental process with a defined time scale. 2) ^{129}I must be equilibrated with the stable isotope, ^{127}I . If it is not equilibrated, the extent to which this is the case needs to be defined. 3) The predominant chemical species of ^{129}I and their geochemical properties must be known. These conditions appear to be met in some studies, where the different iodine species and isotopes all have similar properties (i.e., soluble and mobile), are equilibrated, or have defined geochemical properties. ^{129}I looks promising as a tracer for recent North Atlantic water and ocean mixing (see Fig. 6 in Santschi and Schwehr, 2003), sedimentation (Oktay et al., 2000), evapotranspiration in a large watershed (Oktay et al., 2001), and as a tracer and dating tool of infiltrating river water and recharge ponds to ground water (Santschi et al., 1999; Schwehr et al., 2003).

One of the most promising potential applications for the $^{129}\text{I}/^{127}\text{I}$ ratio is as a new source tracer and geochronometer for terrestrial organic matter, on time scales less than

50 years. This is especially attractive since radiocarbon can at times be an ambiguous chronometer for the 50-year time-scale.

Since iodine has a 40,000 year mean oceanic residence time, and thus behaves almost “conservatively” (Wong, 1991), it can be used as an oceanographic upper ocean water mixing tracer in the Northern hemisphere (summarized in Raisbeck and Yiou, 1999) and to distinguish the contributions of different down-welling regions in the North Atlantic Ocean (Santschi et al., 1996) or large rivers in the Arctic Ocean. ^{129}I is being transported with currents from the Northern to the Southern hemisphere, where it has been recently detected (Fehn and Snyder, 2000). Because of its long mean oceanic residence time, it is reasonable to assume that little ^{129}I has been transferred from the surface ocean to underlying sediments. However, ^{129}I has been detected in ocean margin sediments (Fehn et al., 1986). Oktay et al. (2000) ascribed the presence of ^{129}I and the $^{129}\text{I}/^{127}\text{I}$ profile in Mississippi Delta sediments to close-in tropospheric particle-bound fallout. The basis for the interpretation was the low $^{240}\text{Pu}/^{239}\text{Pu}$ ratios in that core, and that the $^{129}\text{I}/^{127}\text{I}$ ratios track the $^{239,240}\text{Pu}$ and ^{137}Cs nuclides without exhibiting extra mobility. These results suggest that it may be possible to date North American aquatic sediments using iodine isotope ratios on time scales of about 50 years (relating to the beginning of the nuclear bomb-testing era).

The behaviour of ^{129}I in other environmental archives, however, is not straightforward. In Europe, recent results have shown that ^{129}I in glacier ice recorded progressively increasing inputs rather than a bomb peak (Wagner et al., 1996; Lopez-Gutierrez et al., 2000). Also in Europe, ^{129}I in tree rings showed enhanced mobility

(Hauschild and Aumann, 1985; Rao et al., 2002), and there were significant offsets in $^{129}\text{I}/^{127}\text{I}$ ratios between bovine thyroids and vegetation or soils (Frechou et al., 2002).

While ^{129}I profiles in European alpine glaciers (Wagner et al., 1996) or coastal sediments (Lopez-Gutierrez et al., 2000) are mainly marked by atmospheric nuclear fuel reprocessing emissions (Fig. 1.3), this is not the case in the USA. In the USA, ^{129}I from bomb fallout is likely a more important source than in Europe. This is evident from a comparison of the ^{129}I inventory in an undisturbed soil core taken from Marlin, TX, with that expected from bomb fallout (Santschi and Moran, unpublished results shown as Fig. 10 in Santschi and Schwehr, 2003).

The ^{129}I inventory in the Marlin (TX) soil core is about 1×10^8 at/cm², which is very similar to the inventory in the Mississippi River delta sediment core of Oktay et al. (2000). If extrapolated to the area of the contiguous USA, it would amount to a total of 2 kg of ^{129}I , which is similar to the inventory of ~ 4 kg from bomb fallout deposited over the USA. Regardless of soil type, climate, or vegetation, many locales show a rapid decrease in ^{129}I concentration with depth, such that a major fraction of the ^{129}I inventory is found in the top 10 cm of the soil profile (Schmitz and Aumann, 1995).

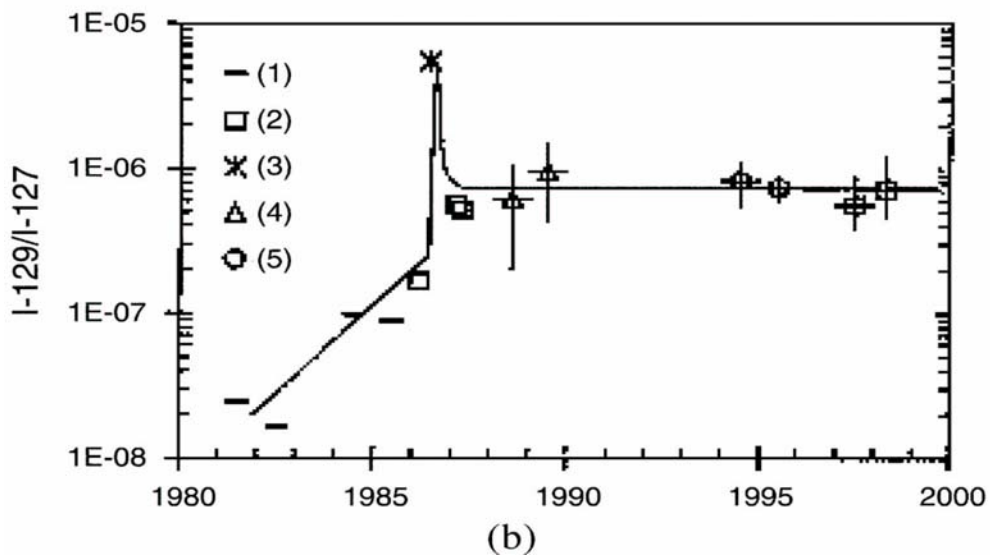
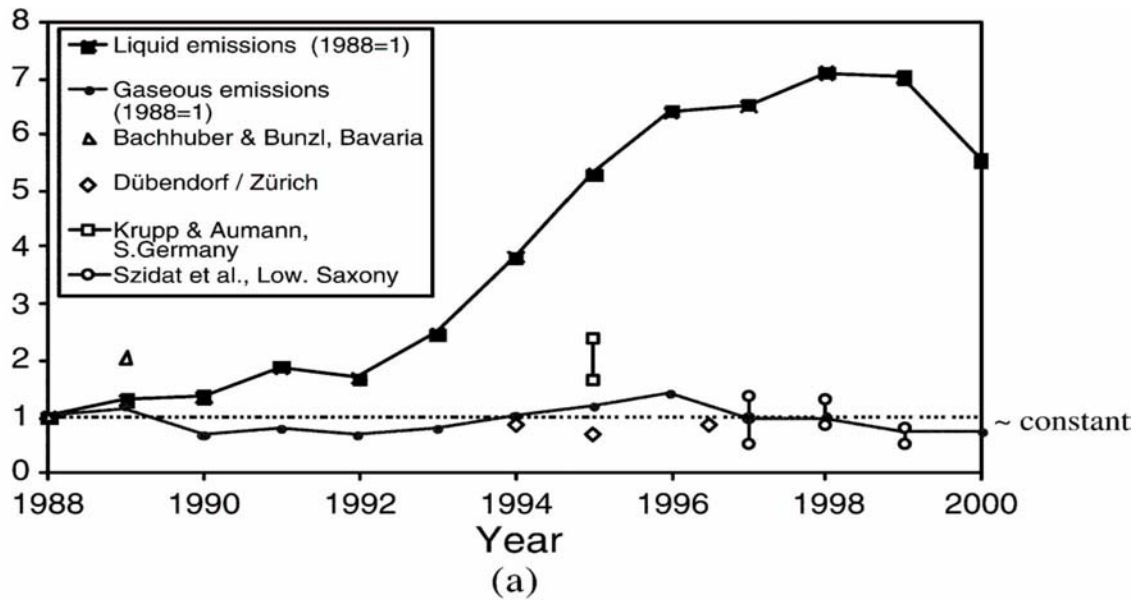


Fig.1.3. (a) Normalized input functions (to 1988 values) of ^{129}I in Western Europe, showing constant values for ^{129}I in rainwater in the 1990's, while discharges to the ocean greatly increased (figure from Schnabel et al., 2001); (b) $^{129}\text{I}/^{127}\text{I}$ ratios in rainfall over Western Europe, showing constant values in the 1990's (figure from Szidat et al., 2000).

Biophilic nature of iodine and coupling of iodine cycling with the organic carbon cycle

Iodine is significantly involved in the cycle of organic matter in the surface environment. The biophilic nature of iodine is demonstrated by a high enrichment factor of iodine to organic matter, 5×10^5 to 10^6 L/kg (Schink et al., 1995b; Hou et al., 1997; Oktay et al., 2001) in the environment, leading to high concentrations not only in seaweed (20 - 250 ppm) but also in detrital macromolecular organic matter (Oktay et al., 2001). Large fractions of ^{127}I and ^{129}I were associated with organic matter in fresh, estuarine and surface ocean water (Krupp and Aumann, 1999; Szidat, 2000; Oktay et al., 2001; Schwehr and Santschi, 2003).

Mechanisms of iodination of organic matter

Iodination of organic matter can be accomplished in the laboratory by electrophilic substitution of benzene ring, phenol, or alkenes by I^+ (or H_2OI^+). This iodine species is produced by promoters, such as hydrogen peroxide, H_2O_2 , or CuCl_2 (creates Cu^+), chloramines, or ICl (creates I^+ and Cl^-). Also, iodine reacts with alpha-methylcarbonyl, which involves the initial conversion of the alpha-methylcarbonyl to the enol. The enol then reacts with IOH . Enolization of the alpha-methylcarbonyl is promoted by both H^+ and OH^- .

In environmental systems, much less is known about iodination of natural organic matter. While it has been shown that humic matter could be iodinated by extracellular peroxidases, the exact mechanisms has not been unequivocally elucidated, as the reactions appears to be only partly reversible at low, environmentally relevant

concentrations of iodide (Christiansen and Carlsen, 1991). In seaweed, the majority of iodine appears to be in proteins (Hou et al., 2000). In humic acids, the majority of iodine appears to be in methoxy-phenols (Warner et al., 2000). In experiments where natural organic matter in river water is exposed to inorganic I⁻ for ~ 2 months, the majority of I cycles into refractory high molecular weight organic matter. However, 1-2 months later the iodine fraction existed primarily as transitory low molecular weight organic matter species, particularly after exposure to bacterial cultures (Rädlinger and Heumann, 2000).

While kelps and other Pacific algae can contain up to 90% of the iodine in a water-soluble form, mainly as iodine ions, 5% to 37% can be present as organic iodine, of which about 50% can be in the form of iodo-amino acids (Hou et al., 1997). In *Sargassum* and *Laminaria* sp., iodinated forms of thyroxine and tyrosine may comprise up to 0.1% dry weight of *Sargassum* (Nisizawa, 1979). Studies of Pacific seaweeds suggest that the mechanism of iodine enrichment is different for various algae and that its bioavailability also varies. The mechanisms by which seaweeds concentrate, store, or use iodine from seawater are not well understood.

Macroalgae and phytoplankton produce volatile halogenated substances, such as iodomethane, diiodomethane, chloriodomethane, propyl iodide or butyl iodide in the ocean (Schall et al., 1997). However, these volatile species are generally present at concentrations of considerably less than a few ng/L. Therefore, even though these species are important atmospheric gases exerting some control on climate and ozone, they constitute much less than 1 permil of the total iodine in seawater. According to Schall et al. (1997), the concentration of volatile organic iodine species do not relate

well to chl. *a* concentration, while those of organic bromine do. This might be due to the greater sensitivity of organic iodine species to UV light transformation reactions.

Photochemical decomposition of dissolved organic iodine (DOI) in seawater has been shown to produce iodide (Wong and Cheng, 2001; Schwehr and Santschi, 2003). On the other hand, UV irradiation can also produce new organic iodine species (Schwehr and Santschi, 2003). Photochemical processes can directly (photolysis) or indirectly (through radical formation) influence iodine speciation and transport. For example, the photochemical formation of hydrogen peroxide (Zika et al., 1985) likely promotes the iodination of organic matter. While some organic iodine compounds in aquatic systems are destroyed by photolysis, others are newly formed upon UV radiation. While UV oxidation of natural water samples does not appear to totally destroy organic iodine species, these species are totally decomposed when using dehydrohalogenation (Schwehr and Santschi, 2003). Photochemical processes can be expected to have numerous effects on the speciation and transport of iodine within aquatic systems, at the ocean-atmospheric boundary and within the atmosphere (Stutz, 2000; Kolb, 2002; O'Dowd et al., 2002). Our understanding of these processes is still very limited.

HYPOTHESES

The main hypotheses for this study are: 1) Values of $^{129}\text{I}/^{127}\text{I}$ can be used for tracing water movement. The ratio works as a tracer because ^{127}I behaves conservatively during transport, while fractionation processes and concentration variations for ^{129}I should occur

during transport. These isotopes are expected to have different behaviors and perhaps different chemical forms since the recently introduced anthropogenic ^{129}I may not have isotopically equilibrated with natural ^{127}I in surface environmental compartments.

2) Concentrations of ^{129}I and $^{129}\text{I}/^{127}\text{I}$ values can be used as tracers of terrestrial organic matter due to the elevated anthropogenic addition of ^{129}I and the biophilic nature of iodine. This is true particularly because DOI is expected to be a more significant fraction in fresh water and coastal marine waters than reported in studies using operational methods of measurement.

OBJECTIVES

The main objective of this research was to evaluate the usefulness of the isotopic ratio of iodine ($^{129}\text{I}/^{127}\text{I}$) for tracing and dating waters and organic matter in the surface environment through a series of laboratory experiments and field measurements. This study initially focused on the development of a method for characterizing the dominant chemical forms of dissolved iodine in natural waters. Once the methodology was established, concentrations and distributions of stable and radioactive iodine species were investigated to elucidate the possible role these forms play in iodine cycling in the surface environment.

The specific objectives of the proposed research included: 1) Develop methods for establishing the concentration for total dissolved iodine and the dissolved species of iodine as iodide (I^-), iodate (IO_3^-), and organic iodine (DOI) for both isotopes ^{127}I and ^{129}I in a variety of aquatic environments. The matrices investigated include fresh surface and ground waters, estuarine surface waters, and surface sea waters. 2) Determine the concentration and relative distribution for total iodine (TI) and the dissolved species (I^- , IO_3^- , DOI) for both isotopes ^{127}I and ^{129}I in various waters in the surface and subsurface environment. 3) Determine whether isotopic fractionation processes, changes in species distributions, and changes in concentrations of ^{129}I are useful in tracing water mass interactions and organic matter.

APPROACH

An evaluation of iodine speciation may elucidate how useful variations in the isotopic $^{129}I/^{127}I$ ratio can be used for tracing and dating waters and organic matter. The main questions to be addressed by this study are: 1) Can a quantitative process be developed for determining DOI? How significant is the surface (~ 10 cm water depth) DOI pool in various aquatic settings? 2) In fresh waters, will ^{127}I show conservative behavior, while ^{129}I demonstrates fractionation processes and concentration variations?

Will the different behaviors for the iodine isotopes provide a potential hydrological tracer? 3) Can the anthropogenic elevation of ^{129}I concentrations and the biophilic nature of iodine be coupled in $^{129}\text{I}/^{127}\text{I}$ to provide a tracer of organic matter?

To address these questions, a series of investigations are carried out combining both field studies and controlled lab experiments. After intensive methodological investigations to work out the quantitative determination of ^{127}I and ^{129}I species, a series of field studies are conducted. In the first field study, the total iodine $^{129}\text{I}/^{127}\text{I}$ ratios are measured for fresh surface and ground waters from the Anaheim Basin, California, for which collaborators from Lawrence Livermore provide water residence times using alternate techniques for dating the samples. This study provides some insight into the question regarding whether or not iodine is conservative. A second field project addresses the question of non-conservative estuarine mixing across a salinity gradient in the Galveston Bay with regard to changes in $^{129}\text{I}/^{127}\text{I}$ for I^- , IO_3^- , DOI, and TI, in which the utility of DOI in $^{129}\text{I}/^{127}\text{I}$ ratios is shown to be a tracer of terrestrial organic matter.

CHAPTER II

A SENSITIVE DETERMINATION OF IODINE SPECIES, INCLUDING ORGANO-
IODINE, FOR FRESHWATER AND SEAWATER SAMPLES USING
HIGH PERFORMANCE LIQUID CHROMATOGRAPHY AND
SPECTROPHOTOMETRIC DETECTION*

INTRODUCTION

Recent studies have employed ^{129}I and the isotopic ratio of $^{129}\text{I}/^{127}\text{I}$ as a tracer of water mass mixing in oceanography and hydrology (Hou et al., 2002; Raisbeck and Yiou, 1999; Smith et al., 1998; Santschi et al., 1996; 1999; Schink et al., 1995b). Another study has applied inorganic speciation to $^{129}\text{I}/^{127}\text{I}$ ratios for tracing the transport and mixing of marine sources for ^{129}I (Hou et al., 2002). The possible use of the iodine isotopic ratio as a tracer in other aquatic systems (Moran et al., 1997; Schink et al., 1995a) as well as the extension of its current use to provide a new geochronometer for organic matter (Oktay et al., 2001; Moran et al., 1997) will require a thorough characterization of iodine speciation. There are only a few methods sensitive enough to

*Reprinted with permission from “A sensitive determination of iodine species, including organo-iodine, for fresh water and seawater samples using high performance liquid chromatography and spectrophotometric detection” by Schwehr K.A. and Santschi P.H. (2003) *Analytica Chim. Acta*, **482**, 59-71. Copyright 2002 by Elsevier Science.

accurately quantify iodine species (including organo-iodine) at nanomolar concentrations and these do not apply to the whole range of matrices found in aquatic systems, nor do they quantify organic iodine.

Many methods to measure iodine species have been proposed in the literature, but most are applicable only to one particular matrix, e.g., specifically to fresh water, blood, urine, or seawater. A review shows that these literature methods are not applicable to a range of matrices. Analysis of iodine and trace elements in seawater by inductively coupled plasma-mass spectrometry (ICP-MS) is often impractical due to the loss of sensitivity from the build-up of salts (Warnken et al., 2000). However, recently developed methods using IC-ICP-MS for iodine speciation in fresh waters have successfully been employed (Pantsar-Kallio et al., 1998; Heumann et al., 1998). Ion chromatography (IC) and high performance liquid chromatography (HPLC) methods for iodide analysis at trace levels in seawater face the difficulty of separation of high matrix concentrations of chloride and bromide from the much smaller iodide peak (Ito, 1999; 1997). Some IC methods use the addition of NaCl to the mobile phase to remove interferences by the variability in the composition of inorganic ions in the matrix, but require a post-column reaction (Brandao et al., 1995) or large volume samples of 2 to 6 ml with a pre-concentrator column (Ito, 1999; 1997). IC or HPLC methods have been developed to improve the detection limit of iodide in mineral water samples, but again involve post-column reactions for iodide and for iodate (Bichsel and von Gunten, 1999). None of these methods are flexible enough to measure iodine species, including organo-iodine, in both fresh water and seawater samples. Results from reverse phase columns

are generally not as robust as anion exchange; however, a method using a zwitterionic surfactant coating as the stationary phase was shown to measure iodide at ppb levels, albeit with a long retention time (Hu et al., 1999). IC methods using anion exchange and coulometric detection are subject to interferences from natural organic matter (Moran et al., 1995) that reduce the exchange capacity of the column or foul the electrodes. Voltammetry methods, while suitable for open ocean waters with relatively high concentrations of iodate and total inorganic iodide (reduced fraction used to measure iodide by difference) (Wong and Cheng, 1998; Luther and Campbell, 1991) are subject to similar organic fouling of the electrodes (Farrenkopf et al., 1997) in estuarine and fresh waters, and are very time-consuming. In addition, voltammetry of fresh water samples requires even more argon purge time than seawater in removal of oxygen for iodide analysis (Campos, 1997; Tian and Nicolas, 1995). Voltammetry for fresh water samples also requires the addition of electrolyte and trace level metal clean techniques in order to avoid a decrease in signal to noise ratio to a level too low to adequately detect trace iodine species concentrations (Campos et al., 1996). Neutron activation methods are more expensive, not readily accessible to all labs, and have potential interference problems from bromide (Schmidt et al., 1998).

The purpose of this chapter is therefore to develop a practical, sensitive method for the quantification of iodide, iodate, and organic iodine species for fresh water and seawater samples.

METHODOLOGY

Reagents and standards

Eluents, standard solutions, and reagent solutions were all made up with doubly distilled de-ionized waters of 18.3 M Ω resistance produced from two sequential Barnstead NANOpure systems.

All chemicals used were salts of sodium and were analytical grade or equivalent. The iodide and iodate salts were purchased from Fluka and the metabisulfite, chloride, phosphates, perchlorate, hypochlorite, and hydroxide were purchased from Fisher and Spectrum Corporation.

Reagent solutions were made with water degassed by ultrasonication, particularly the iodide solutions. All iodide and iodate solutions were stored in amber polyethylene bottles that were capped, sealed with parafilm, and refrigerated until use. A primary iodide stock solution of 10 mM was freshly made every three weeks, while the secondary and working solutions of 200 μ M and 2 μ M were made each day. Large volume standards for iodide were made up daily when many samples were run. It was determined that peak heights for the same concentration of iodide were dependent on chloride concentration (Fig. 2.1). Since the peak heights were equivalent for the range of 0.1 to 0.3 M NaCl (salinity range of approximately 8 to 20), sample, blank, and standard solutions were made up in a 0.1 M NaCl solution to optimize sensitivity and to approach standardization of samples to the same salinity. Iodide concentrations in samples from differing environments can be quantified through standard additions of a

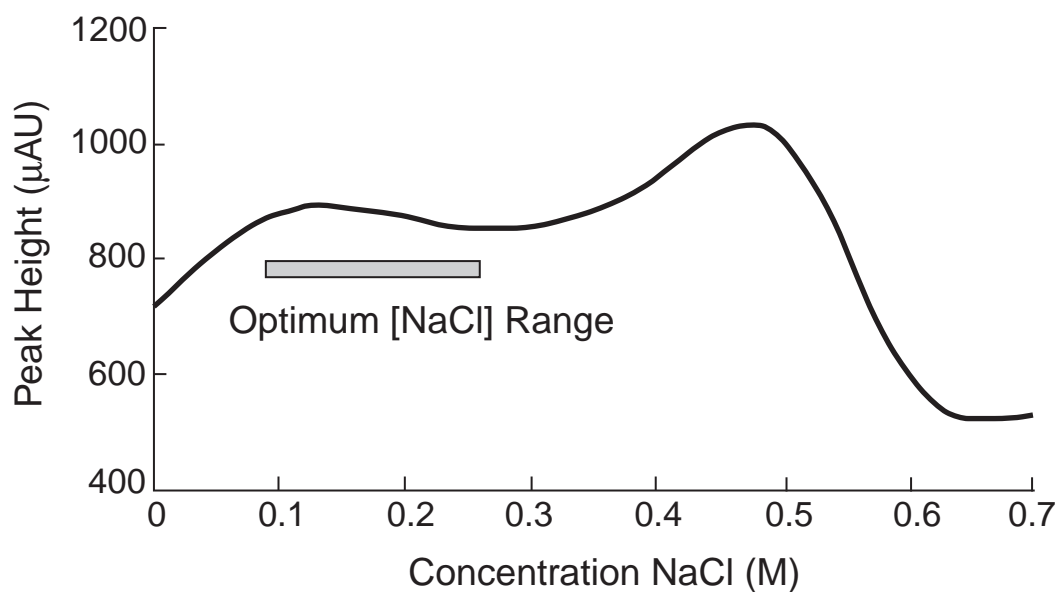


Fig. 2.1. Peak height for the same concentration of iodide, as a function of NaCl concentration.

solution of iodide in 0.1 M NaCl, while iodide in samples with a similar matrix, e.g., open ocean seawater, can be calibrated to the same standards curve.

Instrumentation

Iodine species were separated, identified, and quantified by means of a Waters HPLC. Millennium³² software was utilized to operate the system components and to acquire and integrate the chromatograms. Components used for the analysis of iodine species were a 600S gradient controller, a 626 non-metallic pump, a 200 μL sample loop, a 717-plus auto-sampler, and a dual wavelength 2487 UV spectrophotometer. The UV wavelength used was 226 nm.

The column used was a strong anion exchanger, 250 x 4 mm Dionex AS11, 13 μm particle size, preceded by a 50 x 4 mm Dionex AG11 guard column. The guard and analytical columns were kept at ambient temperature, about 22°C. After each 46-sample tray, the column was cleaned with 0.5 h rinses each of water, 20 mM NaOH, water, 20 mM HNO₃, water, 20% methanol, water, 10% acetonitrile, with a final water rinse to extend the column life and maintain resolution when analyzing waters containing natural organic matter.

The injection volume used for iodide concentrations of 0 to 350 nM was 140 μL . Sample dilutions were, at times, required to fit into this concentration range, or lower injection volumes were used at higher iodide concentrations in order to avoid overloading the column. Table 2.1 shows ranges of total iodine values for Texas soils (Moran et al., 1997; Schink et al., 1995a) and rains (Moran et al., 1997; Schink et al., 1995a), United States rivers (Moran et al., 2002; 1999; 1997; Oktay et al., 2001; 2000; Santschi et al., 2000) and sediments (Oktay et al., 2000), and seawater (Schwehr and Santschi, 2003; Farrenkopf and Luther, 2002; Santschi et al., 2000; Moran et al., 1999; 1997; Wong and Cheng, 1998; Rue et al., 1997; Tian and Nicolas, 1995; Luther and Campbell, 1991) taken from the literature.

Table 2.1. Range of total iodine values in geological matrices.

Sample type	Range of Iodine (nM) Values	Median of Iodine (nM) Values	References
Texas soils	840 – 5600	1911	(Moran et al., 1997; Schink et al., 1995a)
Mississippi River Delta sediments	10000 – 270000	85000	(Oktay et al., 2000)
Texas rains	0.6 – 12	2	(Moran et al., 1999; 1997; Schink et al., 1995a)
Mississippi River	2.2 – 16.9	5.7	(Oktay et al., 2001; 2000; Moran et al., 2002; 1999)
United States Rivers	0.5 – 212	10.7	(Moran et al., 1997; 1999; 2002; Oktay et al., 2001; 2000; Santschi et al., 2000)
United States South Coast Rivers	5.5 – 212	16.6	(Moran et al., 2002)
Surface seawater, Gulf of Mexico	–	500	(Santschi et al., 2000; Moran et al., 1997)
Seawater, North Atlantic	354 – 512	440	(Wong and Cheng, 1998)
Seawater, Arabian Sea	545 – 945 ^a	545	(Farrenkopf and Luther, 2002)
Seawater, specific iodine (total iodine ^b normalized to salinity) (nM/‰)	12.7 – 14.9	~13	(Luther and Campbell, 1991; Campos et al., 1996; Farrenkopf and Luther, 2002; Rue et al., 1997; Schwehr and Santschi, 2003)

^aValues (> 545 nM) in excess of specific iodine in this study are attributed to lateral transport of iodide diffusing out from margin sediments (Farrenkopf and Luther, 2002). ^bTotal iodine refers to total inorganic iodine in most previous studies; see discussion in text.

The mobile phase gradient consisted of a unique selection and application of elements from other published methods. The mobile phase had 4 components used in a gradient elution that included column regeneration and equilibration phases. Mobile phase A was 18.3 MΩ water, B was 200 mM NaCl (Ito, 1999; Brandao et al., 1995), C was 10 mM NaOH (in a solution that was degassed and exposed to the atmosphere as little as possible to avoid carbonate absorption from the air) (Martin, 1999), and D was 75 mM sodium perchlorate and 12.5 mM sodium phosphate (Ito, 1999; 1997). A stock solution for D was prepared by adding 47.5 g of NaClO₄, 5.5 g Na₂HPO₄ and 2.1 g NaH₂PO₄, into 2 L, adjusting the pH to 6.1, and finally diluting the solution by 50% with the addition of 18.3 MΩ water. These solutions were run as the gradient profile shown in Table 2.2.

Table 2.2. Mobile phase gradient elution profile.

Time (min)	Flow rate (mL/min)	Mobile phase solution				Comment
		% A	% B	% C	% D	
0.1	1	76.5	8	10	5.5	Analysis
10	1	68	15	10	7	
11	1	58	15	20	7	Regeneration
13	1	76.5	8	10	5.5	
25	1	76.5	8	10	5.5	Equilibration

Mobile phase solution A is distilled water, B is 0.2 M NaCl, C is 10 mM NaOH, and D is 75 mM NaClO₄ in 12.5 mM phosphate buffer of pH 6.1.

Unlike other applications, the mobile phase is primarily deionized water with dilute reagent solutions, which were more cost effective and easier to fine-tune when necessary. If the large volume blank and standard solutions of iodide are not used, or if the sample matrices are very different from those analyzed here, the iodide peak resolution can be adjusted. Change in the amount of mobile phase B, sodium chloride, adjusted for changes in sample ionic strength, modified the retention time of the iodide peak. Fig. 2.2 is an example of optimizing the percent gradient and concentration of mobile phase B. In Fig. 2.2, chromatogram “a” represents a change from the gradient in Table 2.2 to a gradient of 14% B at 0 minutes and 20% B at 10 minutes; chromatogram “b” is a change to 10% B at 0 minutes and 18% B at 10 minutes; and chromatogram “c” is a decrease to 8% B at 0 minutes and 15% B at 10 minutes. Since the % composition of all the components in the mobile phase solution must equal 100%, the difference in solution was made up in the deionized water, or % A. The decrease in the mobile phase B (NaCl) concentration produces chromatograms showing progressively slower elution with increasing resolution of the iodide peak.

Regulation of the mobile phase C, sodium hydroxide, changed the peak shape of other solution components and enhanced separation from other matrix components. An increased percentage of mobile phase D, sodium perchlorate and phosphate buffer, can sharpen the iodide peak shape.

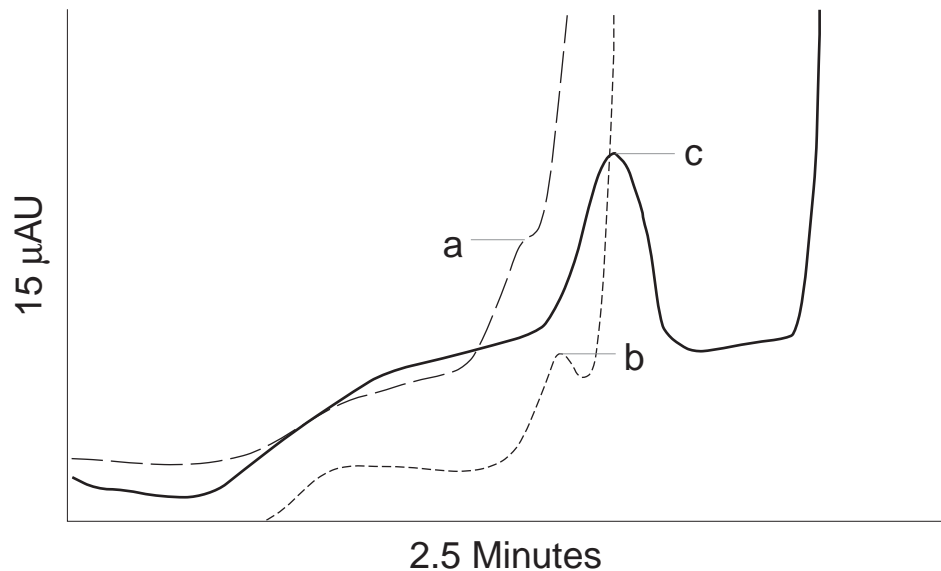


Fig. 2.2. Chromatograms depicting a change in % B NaCl mobile phase component. A slower elution and better I⁻ peak resolution evolves as the % B is decreased from chromatogram “a” to chromatogram “c”.

Method

The analytical scheme is described in Figure 2.3. Iodide was measured directly diluted in standard and blank solutions of 0.1 M NaCl solution to optimize sensitivity and to approach standardization of samples to the same salinity.

Iodate was analyzed directly as a separate peak in some waters, but most often was difficult to resolve due to its early elution and the significant interference by other anions. The procedure used to determine iodate concentrations in this study was, therefore, first to quantify iodide, next to reduce iodate to iodide by NaHSO₃, and finally to calculate iodate as the difference between iodide and the total inorganic iodine (TII)

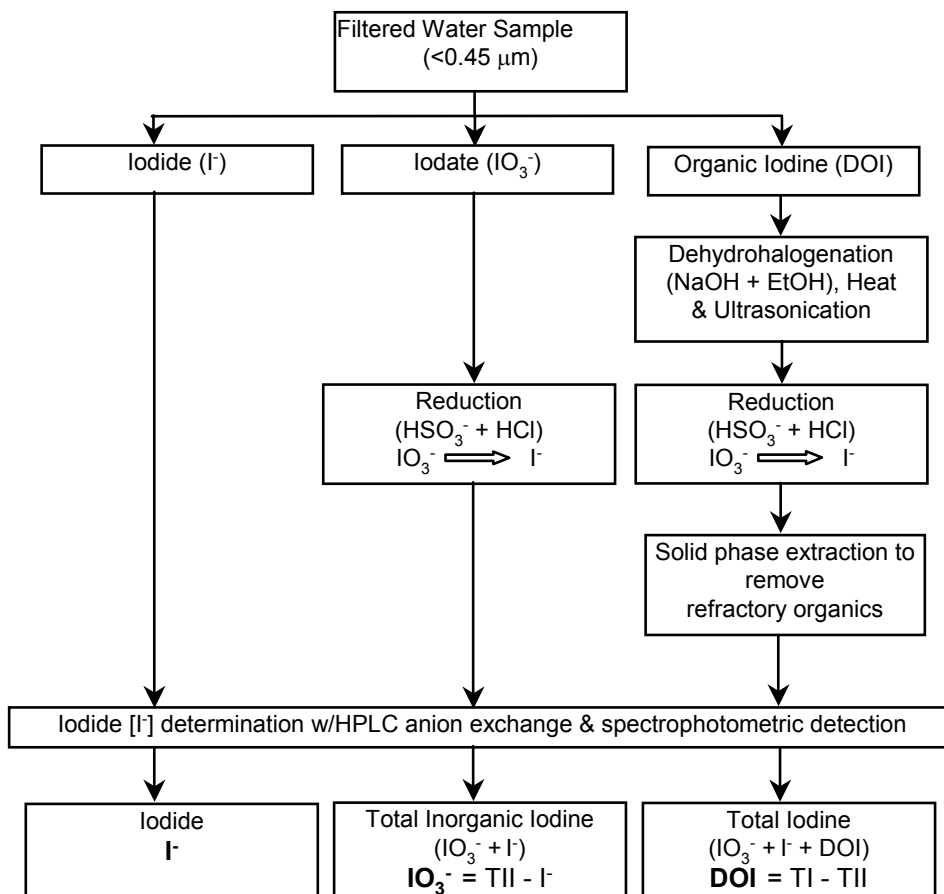


Fig. 2.3. Analytical sample processing scheme for the determination of iodine species.

concentration. Iodate was reduced to iodide by NaHSO₃ addition to a final concentration of 0.07 mM NaHSO₃. After vortexing for a few minutes, the solution was heated at 95°C for 0.5 h in Teflon[®] bombs that were set into the wells of an Environmental Express Hot Block. After the sample was cooled to room temperature, it

was acidified to a final solution concentration of 0.24 mM HCl for less than 5 min. (both amounts of reductant and acid were for an estimated concentration of 500 nM iodate). Then, the treated sample was neutralized with NaOH and diluted to an estimated concentration of 150 nM, and analyzed by HPLC. Analysis should take place as soon as possible after the addition of the SO_3^{2-} , in order to minimize the potential for breaking C-I bonds (Wong and Cheng, 1998), which could cause an overestimation in the inorganic IO_3^- concentration and an underestimation in the organic iodine fraction. There was no significant difference ($\leq \pm 3\%$) between our duplicate runs from the same container of prepared sample, but the potential for slow decomposition of more labile DOI may be there even at neutral pH (Wong and Cheng, 1998). This potential error, which may be sample-dependent, would cause an overestimation of inorganic IO_3^- and an underestimation of DOI. Such an effect, however, was not seen in our data as our DOI values were high relative to other published values, and in agreement with ICP-MS measurements (see Results and Discussion section).

Organic iodine was determined by the difference of total iodine (TI) and total inorganic iodine (TII) after dehydrohalogenation. For the determination of total iodine, 2 mL of 5M NaOH and 2 mL of Pharmco 200 proof ethanol were added to 7 mL of sample in Teflon[®] bombs. The bombs were ultrasonicated for three hours at 65°C and allowed to react overnight. An additional 1 mL of 5 M NaOH and 1 mL of Pharmco 200 proof ethanol were added and the solution was again ultrasonicated for three hours at 65°C. The bombs were placed in the wells of an Environmental Express hot block and heated for 0.5 h at 60°C, after the addition of 0.7 mL 1 M NaHSO_3 for the reduction of

iodate species to iodide. Next, the samples were placed in a freezer for 0.5 h to cool. The process of alkaline hydrolysis, ultrasonication and heating, and finally cooling, was intended to disaggregate colloidal micellular material and break ester bridges in macromolecular humic and fatty acids (Wakeham, 1999; Buldini et al., 1997).

After the addition of 3 mL 6 M HCl, the bombs were weighed, heated while uncapped for 1 h at 80°C to drive off ethanol (boiling point, 78°C), and reweighed. The samples were prepared for HPLC analysis by loading the sample onto a pre-conditioned Waters solid-phase extraction (SPE) tC18 cartridge. The tC18 cartridge was prepared by wetting with 9 mL each of deionized water, methanol, and deionized water. The first 2 mL of sample were discarded, and the remaining effluent retained for analysis. Refractory organic matter and remaining ethanol were retained on the tC18 cartridge, which was then disposed of in an appropriate manner.

Iodide standard solutions and calibrations were run before and after every 15 to 20 samples. Two blanks were run before each sample to insure that no memory effect was present. All samples were run in duplicate, except for fresh water samples of low iodide concentration, which were run in triplicate.

Certified reference material and standard additions

The organic decomposition technique, and the accuracy of the HPLC analysis was first tested with certified reference organic material, SRM 1549, powdered milk (NIST). The milk solution was prepared by using 500 mg for a stock solution, as recommended by NIST, then diluted to 200 nM of iodide. A 15-mL aliquot of the 200-

nM iodide milk solution was adjusted to pH 12 with 120 μL 5 M NaOH, after which 200 μL 4-6% NaClO was added. The solution was ultrasonicated for 20 minutes, and placed into a screw-top Teflon[®] bomb that was heated to 95°C in an Environmental Express Hot Block for 6 h. After cooling, the milk solution was then transferred to a clear-50 mL Teflon[®] bottle with an addition of 500 μL 50% Spectrum Ultrapurex H₂O₂. The milk solution in the Teflon[®] bottle was then irradiated with two 15-W 254 nm UV tubes and a 15-W 185 nm UV tube. The Teflon[®] bottles were exposed to 9 h of UV irradiation that was applied in three repetitions of 3 h of irradiation at 85°C, followed by 2 h of cooling.

Then 1 mL of the sample solution, 50 μL of 1 M HSO₃, and 50 μL of 6 M HCl were added to 9 mL of iodide standard additions solutions in 0.1 M NaCl. The respective concentrations of iodide in the standard addition solutions were a) 0 (blank solution), b) 17.8, c) 71.3, and d) 142.6 nM. The blank solution with the sample was run twice, so the respective chromatogram peak height for each of these standard additions was a) 175 and 169, b) 322, c) 799, and d) 1467 μAU . The standard additions curve for the milk had a correlation coefficient of 0.9997 with a slope of 9 and a y-intercept of 166. Procedures for performing standard additions calculations are described in (Skoog et al., 2000). Examples on how to carry out these calculations and how to calculate the standard error using an Excel spreadsheet are given in (Zellmer, 1998).

The calculations for recovery determination were as follows: 15 mL of 200 nM milk solution were diluted with 120 μL 5 M NaOH, 200 μL 4-6% NaClO, and 500 μL 50% Spectrum Ultrapurex H₂O₂, to a new iodide concentration of 189.6 nM in 15.82

mL. The x-intercept of the standard additions curve is the value of the negative of the intercept over the slope, which represents a diluted concentration of 18.32 nM. Since 1 mL of the 15.82 mL was added to 9 mL of standard solution with the added 50 μ L of 1M HSO₃ and 50 μ L of 6M HCl, the final dilution factor was 10.1 mL to 1 mL. When corrected for dilution, the calculated recovery is 18.32 nM multiplied by 10.1/1 or 185 nM. The 185 nM iodide recovered from a 189.6 nM iodide concentration in the milk solution represented a 98% recovery with a standard error of ± 0.84 nM.

The chromatograms for iodide in the milk solution are shown in Fig. 2. 4. The initial iodide concentration or sample in blank standard addition solution is designated as “a”. The respective iodide standard solutions, where “b” was 17.8 nM, “c” 71.3 nM, and “d” 142.6 nM, were overlain to indicate the ease of iodide peak identification using this method.

While this organic UV decomposition technique in the presence of H₂O₂ yielded an excellent recovery for iodide in milk, the recovery was not quantitative for aquatic samples. The dehydrohalogenation technique using the NaOH/ethanol digestion, described in section 2.3, gave, however, excellent results for all aquatic systems, and therefore became the method of choice for organic iodine determinations.

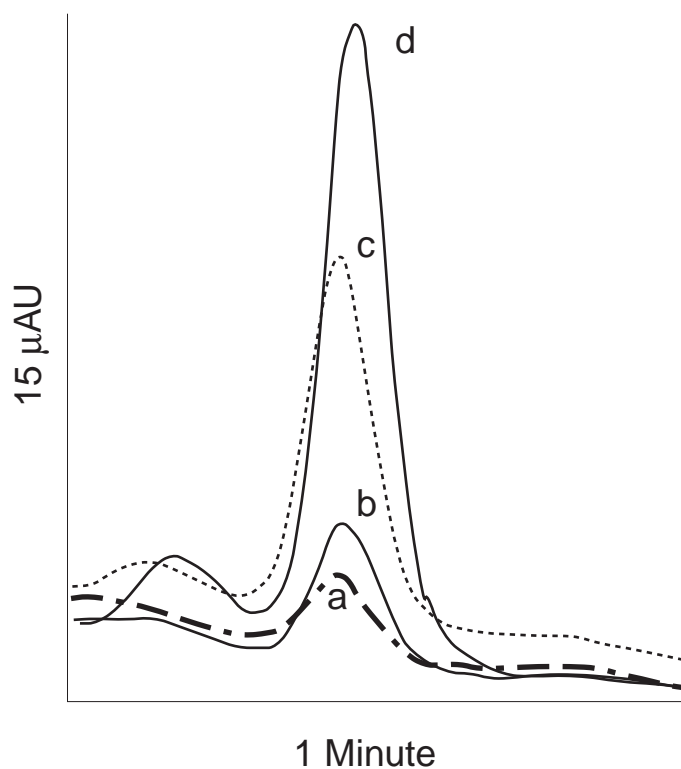


Fig. 2.4. HPLC chromatograms showing standard additions to a 200 nM TI solution of certified reference material, powdered milk, NIST SRM 1549. The letters “a” through “d” represent the overlain chromatograms of progressively increasing concentrations. The effective concentrations of the standard additions were a) no addition (sample concentration plus blank iodide solution), b) 17.8 nM, c) 71.3 nM, and d) 142.6 nM. Calculations are presented in the text.

Comparison with measurements by ICP-MS

The recovery of total iodine, used for the determination of dissolved organic iodine (DOI), was compared with measurements by ICP-MS. Given the high temperature of the ICP-MS plasma, all organic sample material was completely and quantitatively digested. Other published methods currently used to determine TI, i.e., by UV irradiation (Wong and Cheng, 2001; 1998; Spokes and Liss, 1996), chlorination (TI determination by oxidizing I^- to IO_3^- using NaClO (Luther et al., 1991)), TI by reduction of IO_3^- to I^- using ascorbic acid, or by catalytic reduction of IO_3^- to I^- using As^{3+} - Ce^{4+} under acidic conditions, were primarily for the total inorganic species and do not quantitatively convert the organic iodine species to a measurable inorganic form (Wong and Cheng, 1998; Truesdale et al., 1991).

While our UV irradiation technique gave good results for DOC, we did not find it to be quantitative for organo-iodine. However, our UV source was two 15-W 254 nm tubes and a 15-W 185 nm tube versus the 700-W mercury lamp used by Wong and Cheng (Wong and Cheng, 1998) or the 1000-W mercury lamp used by Truesdale et al. (Wong and Cheng, 2001). Although our UV irradiation apparatus was different, we maintain that after a longer irradiation time, our method resulted in DOC values equivalent to those of Wong and Cheng (~1 ppm), while recoveries of $^{125}\text{I}^-$ from radio-iodinated humic material remained relatively low at 60 to 85%. In a similar experiment, Spokes and Liss (1996) removed ~ 85% of the absorbance from organic matter (Aldrich humic acid) in seawater after 3 h of irradiance from a mercury arc lamp. Furthermore, Wong and Cheng (2001) determined that, while artificial UV irradiation or natural

sunlight effectively release inorganic iodide from some subfractions of DOI, as much as 60 nM remained in other samples having an expected (initial) DOI value of 120 nM. Truesdale et al (2001) reported that some anoxic waters turned yellow immediately after UV irradiation, and then yielded lower apparent iodine concentrations than untreated samples. This suggests that while some inorganic iodine species were liberated from organic iodine, other organic iodine species were either too recalcitrant for decomposition by this method, or more likely, were newly formed through UV-induced radical reactions.

The lack of quantitative evaluation of organic iodine speciation in fresh waters suggests that many reported TI values are underestimated. Therefore, an optimized dehydrohalogenation technique using the NaOH/ethanol digestion, described in section 2.3, was developed and applied for quantitative organic iodine determinations and was tested by comparison to measurements by ICP-MS.

The comparison is shown for end-member waters, deep sea (1787 m) and surface sea (1 m) waters from the Gulf of Mexico (Table 2.3), and fresh surface water from the Trinity River (Table 2.4). The total iodine average value (TIAV) for the surface seawater sample for ICP-MS was $494.5 \text{ nM} \pm 2\%$ relative standard deviation (RSD) and 4.8% precision (n=2), whereas the TI value for the HPLC was $526.2 \text{ nM} \pm 0.5\%$ RSD (n=1), which is +6% of the ICP-MS value. The TIAV for the deep seawater sample was $537.0 \text{ nM} \pm 2\%$ RSD, with a 4.8% precision (n=2) by ICP-MS versus $562.6 \text{ nM} \pm 0.5\%$ RSD (n=2) by HPLC, with a 1.1% precision, which is within 5% of the ICP-MS value. The TIAV for the Trinity River fresh water sample was $280.3 \text{ nM} \pm 0.4\%$ RSD (n=1) by ICP-MS, compared to $294.7 \text{ nM} \pm 0.4\%$ RSD with 2.6% precision (n=2) by HPLC, which is within 5% of the ICP-MS value.

Comparison of HPLC iodide concentrations to those measured by ICP-MS for the same aquatic samples was always within 6% recovery of the ICP-MS values. Therefore, the recovery of TI including the organic iodine species by the dehydrohalogenation technique (described in section 2.3) was shown to be quantitative and superior to the UV irradiation and chlorination method described in section 2.4.

Table 2.3. Iodine speciation in the vertical profile of a warm core ring, Gulf of Mexico, 26° 0.04' N, 95°20' W. Collection was July 9, 2000, aboard the R/V Gyre.

Depth (m)	Salinity	DOC ^a ($\mu\text{M-C}$)	Chl a ^b ($\mu\text{g L}^{-1}$)	(TI) ^c (nM)	(TII) ^d (nM)	(I ⁻) (nM)	(IO ₃ ⁻) (nM)	(DOI) ^e (nM)	% (DOI)
1	36.7	90	0.033	526.2 ^f	491.0	227.8	263.2	35.2	7.2
10	36.7	64	0.046	670.8	496.5	230.0	266.7	174.1	35.1
30	36.7	73	0.024	597.5	481.3	228.4	252.9	116.2	24.1
50	36.5	72	0.056	557.9	480.3	207.6	272.6	77.6	16.2
80	36.5	72	0.119	640.3	489.1	204.8	284.3	151.2	30.9
121	36.5	67	0.192	553.6	495.5	182.4	313.1	58.1	11.7
150	36.4	59	0.089	521.6	496.7	169.1	327.6	24.9	5.0
200	36.4	67	0.014	550.6	508.3	24.3	484.0	42.3	8.3
500	36.8	53	n.d.	588.1	519.3	18.2	501.1	68.8	13.2
1001	34.9	53	n.d.	587.2	523.5	6.7	516.8	63.7	12.2
1501	35.0	47	n.d.	595.1	547.1	28.6	518.5	48	8.8
1787	35.0	43	n.d.	562.6 ^f	519.7	3.4	516.3	42.9	8.3

^aData provided by Hung et al., 2002); ^bData provided by J.L. Pinckney and S.E. Lumsden, n.d. represents concentrations not detectible; ^c(TI): concentration of total iodine; ^d(TII): concentration of total inorganic iodine; ^e(DOI): concentration of dissolved organic iodine; ^f(TI): independently analyzed by ICP-MS and HPLC.

Table 2.4. Iodine speciation in estuarine surface waters from Galveston Bay.

Location	Distance from mouth of Bay (km)	Date	Salinity	Chl a ^a (µg/L)	(TI) ^b (nM)	(TII) ^c (nM)	(I) (nM)	(IO ₃ ⁻) (nM)	(DOI) ^d (nM)	% (DOI)
29.7°N, 94.7°W	45 (near Trinity River mouth)	Sep. 1999	16.5	< 5	300.5	280.6	213.5	67.1	19.9	6.6
29.6°N, 94.8°W	40	Nov. 1999	9	< 5	241.0	127.0	103.6	23.4	114.0	47.3
29.5°N, 94.9°W	22 (mid-Bay)	Sep. 1999	21	10 – 17	438.0 ^e	219.0	112.0	107.0	219.0	50.0
29.5°N, 94.9°W	22 (mid-Bay)	Oct. 1999	12	7	295.4	106.7	54.1	52.6	188.7	63.9
29.5°N, 94.9°W	22 (mid-Bay)	Nov. 1999	18	< 5	331.5	271.4	135.1	136.3	60.1	18.1

^a Reference (Ornolfsdottir, 2002) and E. Ornolfsdottir, J. Pinkney, S. Lumsden, unpublished data; ^b (TI): concentration of total iodine; ^c (TII): concentration of total inorganic iodine; ^d (DOI): concentration of dissolved organic iodine; ^e (TI): concentration independently analyzed by ICP-MS and HPLC.

Linear dynamic range, detection limits, and relative standard deviation

The linear dynamic range for iodide analysis, 6 μAU or 0.44 nM (lower limit equal to twice the detector background) to beyond 2700 μAU or 300 nM, was determined as the linear response to concentration for iodide in 0.1 M NaCl solution. However, with other anions in the sample matrix, the best iodide peak separation was within the iodide concentration range of 0 to 150 nM. Sensitivity, as the slope of the linear range for the response to concentration curve was 9 to 12 $\mu\text{AU}/\text{nM}$, depending on sample matrix. The background within the first 10 minutes of elution (iodide retention is between 4.8 to 6 minutes depending on sample matrix) was very stable at 3 μAU or less. Blanks, 0.1 M NaCl solution with no added iodide, were usually equal to background for fresh waters. For salt waters, however, the background may run as high as 12 μAU , which is equivalent to 0.87 nM or 0.14 ppb. Detection limits (e.g., 3 times relative standard deviation for five samples) for iodide and iodate (as TII) were less than 0.3 nM (0.05 ppb) for fresh water, and lower than 3 nM (0.5 ppb) for seawater samples. The relative standard deviation (RSD) for the inorganic iodide species in all waters was about 4% for a concentration of 3 nM (0.5 ppb) iodide in a 0.1 M NaCl blank solution, and 3% for an iodide concentration of 20 nM (3.3 ppb). Total iodine values had a detection limit of 3 nM or 0.5 ppb and RSD of 7% for the initial concentration of 3 nM in a 0.1 M NaCl blank solution, and 5% for an iodide concentration of 20 nM (3.3 ppb). On average over all aquatic samples, the detection limit was ~ 1 nM (0.2 ppb), with less than 3% RSD, when determined using standard additions to an iodide solution of 20 nM in 0.1 M NaCl.

Precision was lower than 10% for all species, but usually was $\leq 5\%$ for a clean column.

RESULTS AND DISCUSSION

Sample preparation and storage

All containers, polyethelene, fluorcarbonated-polyethylene, or Teflon[®], and Teflon[®] tubing for sample collection were pre-cleaned by ultrasonication at 40°C in a 2% Micro-90[®] cleaning solution for 1.5 h, triple-rinsed with 18 MΩ water, soaked in 2% Micro-90[®] solution for 1 week, triple-rinsed with 18 MΩ water, then cleaned with 6 M HCl using the same procedures, and finally, dried in a clean bench. If the cleaned bottles were not used immediately, they were stored in cleaned, sealed plastic bags with a 0.1% HNO₃ solution in the bottle. Prior to collection, the bottles were again triple-rinsed with 18 MΩ water, then triple-rinsed with the sample water down-stream or down-current from the collection site. Since this study was done in tandem with collection for ¹²⁹I species, large volume samples were obtained (from 5 to 20 L). The filters used for large volume collection were in-line, hydrophilic polysulfone capsule filters in a polypropylene housing, from Supor or Gellman. The filters were also cleaned by soaking in and pumping through several liters each of Micro-90[®] solution, 18 MΩ water, 2 M HCl solution, 18 MΩ water, then conditioned with sample water prior to retaining waters for collection.

Samples were either filtered immediately after collection or transported on ice and filtered within a few hours of collection using a 0.45 μm or a 0.1 μm filter. Iodide was run after filtration. The samples were then stored refrigerated or in a dark cool room, after the addition of the NaHSO_3 reductant until the remaining species were measured. Some samples were frozen for later analysis. All samples chosen for freezing were filtered with the 0.1 μm filter, stored in containers larger than 250 ml (Campos, 1997), and showed no significant change in iodide or total iodide after three years storage, which is in agreement with other literature (Campos, 1997).

Sample data

Sample data for iodide, iodate, total inorganic iodine, organic iodine, and total iodine are presented in Tables 2.3, 2.4, and 2.5, respectively, for seawaters, estuarine, and fresh water samples. Chromatograms for the three types of sample waters are shown as an overlay of standard additions in Figures 2.5 through 2.7 for the different iodine species, I, TII, and TI. These figures are described with the sample types they represent.

The seawater samples measured were from a vertical profile in a nutrient-poor warm core ring (WCR) in the Gulf of Mexico, Table 2.3. Since other studies have effectively used total inorganic iodine (TII) as an operational measurement for total iodine (TI), we expected results that show TI values that are slightly higher than 500 nM, with specific iodine (iodine normalized to salinity) values higher than 13 nM. The TI values measured ranged from ~ 522 to 671 nM, with a median value of 575 nM. This was 5.5% higher than the average Arabian Sea value of 545 nM (30) and 12.3% higher

than the highest value reported for the North Atlantic (Wong and Cheng, 1998). The specific iodine values for the WCR samples were 16.1 nM for the samples from 0 to 121 m depth, and 15.7 nM for the samples deeper than 121 m. Our TI values for both surface and deep water samples have been verified independently by ICP-MS, a method that completely combusts organic iodine species. In support of our contention that other studies have reported TI values equivalent to our TII values, we compare their specific iodine values (of TI), normalized to salinity, to our specific TII values. Our TII concentrations, listed in Table 2.3, ranged from 480 to 547 nM with a median value of 497 nM, which correspond well to TII literature values, listed in Table 2.1. The specific iodine values for TII normalized to salinity were 13.4 nM for a depth range of 0 to 121 m and 14.5 nM below 121 m. These specific iodine values are in excellent agreement with 12.0 to 13.4 for 0-100 m, 13.0 to 14.4 for 100-500 m, and 14.4 to 14.8 for 500-800 m water samples (Farrenkopf and Luther, 2002, and references therein).

To our knowledge, this is the first presentation of a vertical profile of all three species, iodate, iodide, and dissolved organic iodine in the ocean. Note that while Tian and Nicolas (1995) pioneered the measurement of vertical profile for organic iodine in seawater using NaClO oxidation, their method does not, as we show here, recover the more resistant organic iodine compounds, e.g., L-thyroxine (Wong and Cheng, 1998; Luther and Campbell, 1991).

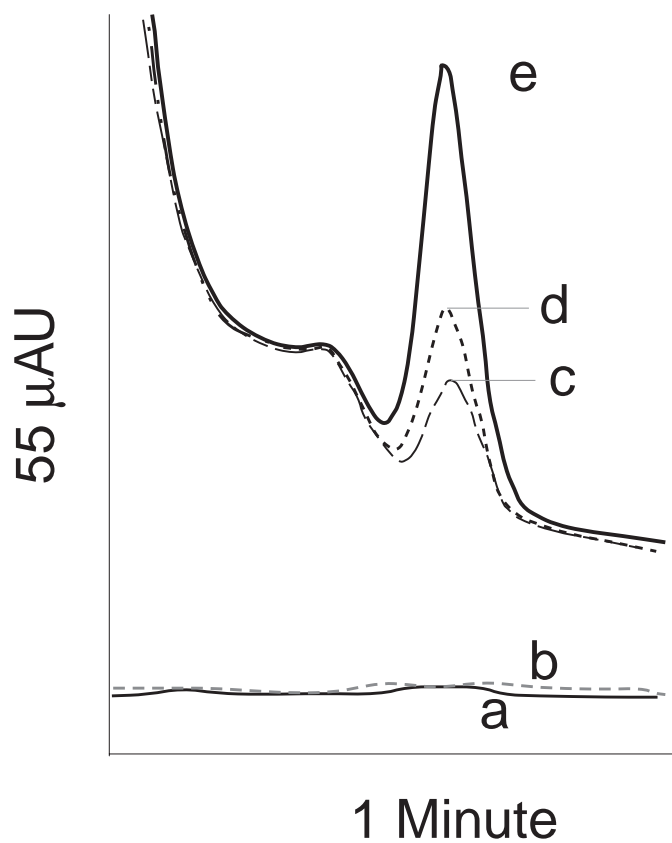


Fig. 2.5. Sea water sample from 1787 m depth from a WCR in the Gulf of Mexico that displays TII analysis using an isocratic mobile phase. The chromatogram curves “a” and “b” represent blanks run before and after the sample which are much higher than blanks using the recommended gradient, Table 2.2. Chromatogram “c” is the diluted sample (DF = 7.25 in a 0.1M NaCl solution) “c”, and the I⁻ standard additions to the diluted sample of 35.6 nM for “d” and 142.6 nM for “e”.

Figure 2.5 is an example of TII in the Gulf of Mexico WCR sample collected at 1787 m. This sample was run for 12 min., using an isocratic mobile phase as described for the 0.1 min. portion of the gradient mobile phase in Table 2.2. Without the regeneration and equilibration stages for the gradient mobile phase in Table 2.2, blanks show a “memory” effect from sample to sample. Therefore, the sample TII concentration has been corrected in a ramp fashion for the blanks “a” which has a peak height value of 70 μ AU and “b”, peak height value of 107 μ AU, Figure 2.5. The chromatograms for the sample in Figure 2.5 are the diluted sample (DF = 7.25 in a 0.1M NaCl solution) “c”, and the I⁻ standard additions to the diluted sample of 35.6 nM for “d” and 142.6 nM for “e”. The uncorrected peak heights in μ AU are 1297 (n = 2) for “c”, 1874 for “d”, and 3633 for “e”. Since blank “b” was run before the sample and “a” after the sample, the blank-corrections for “c” through “e” are 107, 88.5, and 70 μ AU, respectively, yielding blank corrected peak height values of 1190, 1785.5, and 3563 μ AU. The linear regression line for the plot of peak height versus concentration is $y = 16.6x + 1191$ ($R^2 = 1$) and the calculated concentration for “c” is then the intercept

divided by the slope or 71.6 nM. The TII for this deep sea water sample is the DF multiplied by the “c” concentration or 519.3 nM, which is < 1% deviation from the average TII value of 519.7 nM listed in Table 2.3.

The results from our estuarine water samples, presented in Table 2.4, appear to be very similar to values for other coastal waters (Wong and Cheng, 2001; 1998). Iodide concentrations are slightly higher or similar to iodate values. Organic iodine concentrations ranged from about 7% to 64% of the total iodine, with an average value of 37% and a median of 42%.

Interestingly, TI in the estuarine samples, excluding the Trinity River sample, is inversely related to salinity ($TI = -13.7 \text{ Salinity} + 111$, $R^2 = 0.8$). Since the Trinity River value was different, this implies that the Bay and riverine TI did not have the same source during the autumn season. Also, the specific iodine value is similar to values for the open ocean. Iodate is proportional to salinity, but with a low specific iodate value, $IO_3^- = 5.5 \text{ Salinity} - 4$, $R^2 = 0.7$, which suggests microbial reduction of iodate to iodide during the oxidation of organic matter.

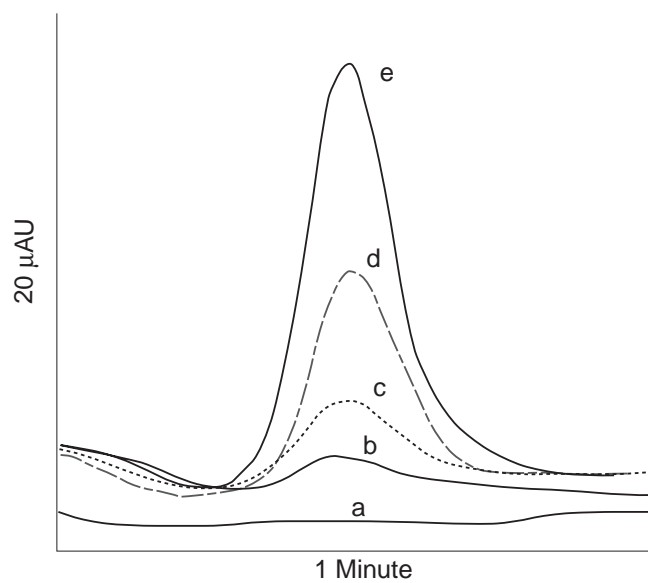


Fig. 2.6. This chromatogram series depicts the measurement of TI in the Galveston Bay sample with a salinity of 18, Table 2.4. Chromatogram “a” is the blank. The sample has been diluted 12.2 times and is shown in the “b” chromatogram with no I^- addition. The “c” chromatogram is the sample with an addition of 20 nM of I^- in a 0.1M NaCl solution, and the additions to the “d” and “e” injections are 40 nM and 160 nM, respectively.

Figure 2.6 is the measurement of TI in the Galveston Bay sample with a salinity of 18, Table 2.4. Chromatogram “a” is the blank. The sample has been diluted 12.2 times and is shown in the “b” chromatogram with no Γ addition. The “c” chromatogram is the sample with an addition of 20 nM of Γ in a 0.1M NaCl solution, and the additions to the “d” and “e” injections are 40 nM and 160 nM, respectively. Peak heights for “a” through “e” are 3 (n=2), 158 (n=2), 312, 813, and 1583 μ AU, respectively. Again, for the graph of peak height as a function of concentration, the equation for the linear regression is $y = 8.7x + 239.6$ ($R^2 = 0.94$). This yields an initial sample TI concentration of 27.6 nM, which results in an actual sample TI of 337.9 nM after multiplying by the dilution factor, DF, 12.2. The TI value of 337.9 nM is + 1.9% of the average value for this sample, 331.5 nM, shown in Table 4. No correction was made for the blank value.

The fresh surface and ground water results given in Table 2.5 are generally within the range of the literature values presented in Table 2.1 (Moran et al., 2002; 1997; Oktay et al., 2001; Santschi et al., 2000; Schink et al., 1995a).

Figure 2.7 shows an overlay of chromatograms that depicts the standard additions method for determining Γ concentration in a surface water sample from the Trinity River near its mouth at the Galveston Bay, Table 2.5.

Table 2.5. Iodine speciation in surface and ground waters from central and southeastern Texas. Gorman Springs and CO₂ Alley (Gorman Cave) are in the Colorado Bend State Park. The Trinity River is the major inflow into Galveston Bay.

Station	Location	Date	DOC (μM)	(TI) ^b (nM)	(TII) ^c (nM)	(I) (nM)	(IO ₃ ⁻) (nM)	(DOI) ^d (nM)	% (DOI)
Galveston rain	29.3°N, 94.8°W	Aug. 2001		48.9	24.3	4.9	19.4	24.6	48.0
Gorman springs	30.9°N, 99.8°W	Jan. 2000		118.6	67.3	62.8	4.5	51.3	40.0
CO ₂ Alley	30.9°N, 99.8°W	Jan. 2000		74.0	64.4	40.4	24.0	9.6	13.0
Trinity River	29.8°N, 94.7°W	Sep. 2000	457 ^a	294.7 ^e	187.3	176.1	11.2	107.4	36.4

^a DOC value from K. W. Warnken, unpublished data. ^b (TI): concentration of total iodine; ^c (TII): concentration of total inorganic iodine; ^d (DOI): concentration of dissolved organic iodine; ^e (TI): independently analyzed by ICP-MS and HPLC.

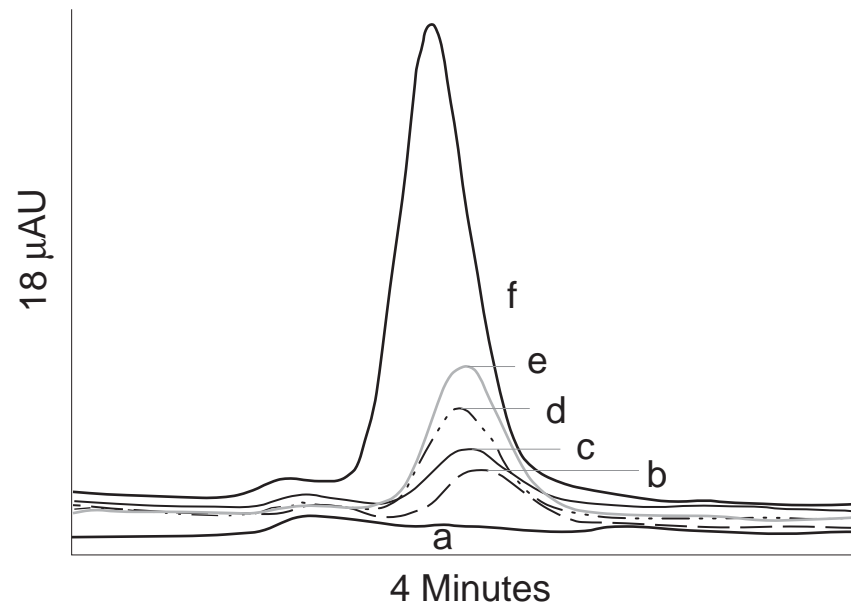


Fig. 2.7. Surface water sample from the Trinity River near its mouth to Galveston Bay, Table 2.5. This overlay of chromatograms depicts the standard additions method for determining I^- concentration. Standard additions were made to a 0.1M NaCl solution, wherein the dilution factor was 10. Chromatogram “a” is the blank and “b” is the sample with no I^- addition. The standard additions of I^- are 3.6 nM (0.6 ppb) for “c”, 17.8 nM for “d”, 35.6 nM for “e”, and 142.6 nM for “f”.

Standard additions were made to a 0.1M NaCl solution, wherein the DF is 10.

Chromatogram “a” is the blank and “b” is the sample with no I⁻ addition. The standard additions of I⁻ are 3.6 nM (0.6 ppb) for “c”, 17.8 nM for “d”, 35.6 nM for “e”, and 142.6 nM for “f”. The chromatogram peak heights for “b” through “f” are 183 (average of 2 runs), 191, 351, 507, and 1551 μ AU, respectively. The linear regression for the plot of the peak height versus the concentration is $y = 9.7x + 170.5$ ($R^2 = 0.9996$). From this plot, the I⁻ concentration in the diluted sample is 17.6 nM (or the intercept divided by the slope). Multiplying this value by the DF, the original sample I⁻ concentration is 176 nM. The peak height value for the blank is 3 μ AU, so no blank correction is needed.

The TI value of 49 nM for the rainwater sample from Galveston, Texas, was higher than the previously published value of 12 nM from the same location. Seasonal variations depending on local weather conditions can contribute to greater concentrations of iodine due to the close proximity of the sampling location to the ocean, the source region for atmospheric iodine. The surface water value from Gorman Springs of 119 nM and the ground water value from CO₂ Alley, Gorman Cave, of 74 nM were within the range for surface waters of the USA (Moran et al., 2002; 1997). Major variations in TI concentrations are mostly due to evapotranspiration effects (Oktay et al., 2001), and also due to release from source rocks, variable Eh/pH conditions, sorption to soil minerals, complexation with organic matter, or imbalance of natural salts due to poor irrigation practices in arid climates (Moran et al., 2002; 1999). The Colorado Bend State Park area, from which these waters are from, is in an arid region. Therefore, TI values higher than the median are expected due to evapotranspiration effects (Oktay et

al., 2001). The Gorman Springs sample collection site has algae, aquatic plants, and swimming organisms. It is reasonable then that the water in the springs shows more DOI than the CO₂ Alley cave water that has been filtered through alluvial sands and karstic gravels during its percolation from the surface to the cave. With the exception of the rain sample, all fresh water samples also showed relatively high iodide to iodate concentration ratios, likely due to biological activities and biogeochemical processes in soils.

CONCLUSIONS

We describe here a new and sensitive method for the detection of iodine species at nanomolar concentrations in different aquatic systems, and to quantitatively measure organic iodine. The method has a useful linear range from 1 to 150 nM that is applicable to fresh, estuarine, and seawater samples. The detection limit for iodide, taken as 3 times standard deviation, was found to be less than 1 nM (0.2 ppb), with a relative standard deviation of 3% for all waters, using standard additions to an iodide solution of 20 nM in 0.1 M NaCl.

Recovery for total inorganic and organic iodine species was validated through the use of the certified reference material SRM 1549 powdered milk, the methods of standard additions and reference standards, and by comparison to results from total iodine determinations by ICP-MS.

CHAPTER III

¹²⁹IODINE: A NEW HYDROLOGIC TRACER FOR AQUIFER RECHARGE
CONDITIONS INFLUENCED BY RIVER FLOW RATE AND
EVAPOTRANSPIRATION

INTRODUCTION

Background

Iodine is a biophilic element supplied to the land surface through atmospheric deposition of sea spray, particularly near coastal regions, and from weathering of marine shales where iodine is concentrated in organic matter. It is involved in the geochemical cycling of organic matter through the reductive or oxidative formation of carbon – iodine bonds in aromatic and protein compounds (Summers et al., 1989; Christiansen and Carlsen, 1991; Carlsen et al., 1992; Warwick et al., 1993; Edmonds and Morita, 1998; Warner et al., 2000). The most common species of iodine in the aquatic environment is iodate (IO_3^-), the thermodynamically stable form of iodine, prevalent in alkaline soils and seawater. Organic forms of iodine can be found in air, soils, and in fresh, estuarine and surface ocean waters (Oktay et al., 2001; Schwehr and Santschi, 2003).

Iodide (I^-) occurs in reducing environments that may also be acidic. In ground waters, after infiltration through organic matter and microbial-reducing surface soils, the most prevalent species in ground water generally becomes I^- (Sheppard et al., 1995;

Langmuir, 1997; Fabryka-Martin, 2000). I^- has a conservative geochemical behavior similar to that of chloride, as it bonds to inorganic minerals by a weak, outer sphere electrostatic attraction, so only adsorbs to positively-charged mineral surfaces and is readily displaced by competitive ligand exchange (McBride, 2000). Therefore, the large ionic radius of iodide and its negative charge lowers its adsorption or exchange energy with most mineral surfaces.

The stable isotope, ^{127}I , has a natural abundance of 100%. Most radioisotopes of iodine are short-lived, however, the isotope ^{129}I has a half-life of 15.6 million years. Radiogenic ^{129}I is produced naturally in the atmosphere by cosmic-ray induced spallation of Xenon, and in the subsurface by spontaneous fission of ^{238}U . The surface inventory of naturally produced ^{129}I is 100 kg (Yiou et al., 1995; Raisbeck et al., 1999), and due to a half-life much longer than the residence time (τ) of surface environmental compartments, this isotope is well-mixed in the surface soil compartment ($\tau \sim 1000$ y) (Kocher, 1982), the surface ocean ($\tau \sim 100$ y for the mixed layer, depth 0 to ~ 100 m) (Raisbeck et al., 1995; Libes, 1992), and the atmosphere ($\tau \sim 11$ -18 days) (Rahn et al., 1976). Anthropogenic sources of ^{129}I include an added 150 kg (Eisenbud and Gesell, 1997) through atmospheric bomb testing during 1945 –1965, and 2360 kg from nuclear fuel reprocessing at Cap de La Hague, France, and Sellafield, England, during 1966 – 1997 (Raisbeck et al., 1999). Further monitoring of anthropogenic ^{129}I production will continue to be important as in 1990, it was estimated about 5660 kg of ^{129}I stored in spent reactor fuel had not yet been reprocessed (Ernst et al., 2002). These anthropogenic

sources of ^{129}I overwhelm the natural sources, and thus provide a high concentration point source for tracer applications of the isotopic ratio $^{129}\text{I}/^{127}\text{I}$ (Raisbeck et al., 1995; Schink et al., 1995a; 1995b; Santschi et al., 1996; 1999; Moran et al., 1997; 1999a; 1999b).

Because atmospheric input of ^{129}I in the USA is mostly from European reprocessing plant emissions (Raisbeck et al., 1995; Moran et al., 1999a; 1999b; Fehn and Snyder, 2000), which have been relatively constant in the 1990s (Szidat et al., 2000; Schnabel et al., 2001), this should allow the interpretation of variations in ^{129}I concentrations as an indicator for watershed or aquifer processes. The objective of this study is to understand the observed variations in ^{129}I concentrations and $^{129}\text{I}/^{127}\text{I}$ ratios in young ground waters of the aquifer system of Orange County, California, where groundwater flow for recently recharged water is well defined from previous studies.

Geohydrology of the study site

The Los Angeles-Orange County coastal plain basin is a synclinal structure formed by intense folding and faulting during collision of continental plates. The folded igneous, metamorphic, and sedimentary rock outcrop around the basin as the San Gabriel Mountains to the northwest and the San Bernardino Mountains to the north. Thousands of feet of unconsolidated alluvial sediments fill the basin and an uplift subdivides the basin into effectively two northwest-trending basinal areas, the Upper and Lower Basins. The Santa Ana River drains an area of about 5840 km² that comprises the

Upper Basin, cuts the uplift between the two adjacent basins and continues through the Lower Basin with little or no coastal barrier to the Pacific Ocean (Planert and Williams, 1995).

The Lower Basin is encompassed by the Orange County basin and its aquifers. The Orange County ground water basin, about 906 km², is bordered by the Coyote and Chino Hills to the north, the Santa Ana Mountains to the northeast, and the Pacific Ocean to the southwest (OCWD, 1999). The Orange County basin is further subdivided into the Forebay (recharge) Area to the northeast and the Pressure (confined) Zone to the southwest. The study area is in the Forebay Area, (Fig. 3.1).

Runoff from precipitation in the surrounding mountains provides flow to the Santa Ana River and percolation through stream beds into the basin aquifer system of continental and marine deposits of sand and gravel interbedded with discontinuous lenses of low permeability clays and silts. Natural ground water flow is perpendicular to the long axis of the Los Angeles-Orange County coastal plain basin with discharge to the Pacific Ocean. High demand for water as early as the 1930's caused tremendous draw-down in ground water wells and subsequent salt water intrusion, so management of water resources became necessary. Recent ground water flow is from artificial recharge spreading ponds to withdrawal areas, with barriers to salt water intrusion through injection wells for reclaimed wastewater.

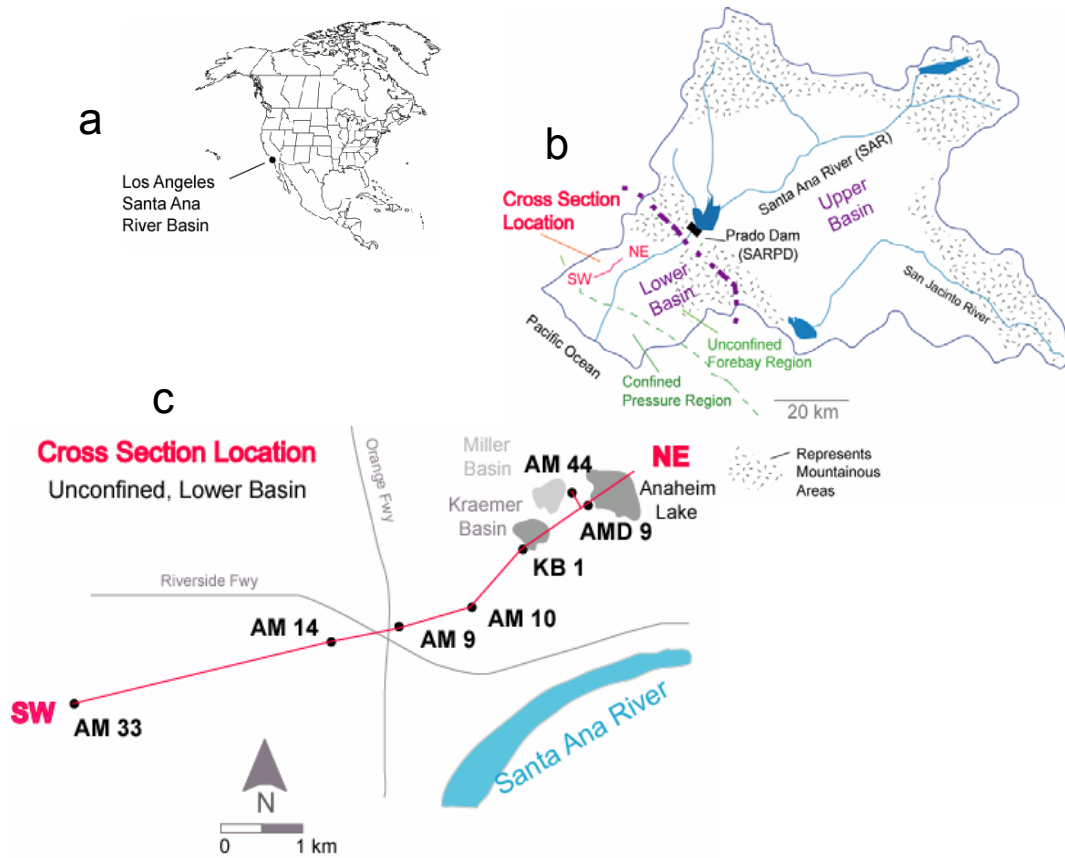


Fig. 3.1. Map showing (a) the general location of the study area, the Santa Ana River Basin; (b) the Santa Ana River Basin indicating the Unconfined Forebay recharge area, the Santa Ana River, Prado Dam, Anaheim Lake and Kraemer Basin, and the location of the cross section shown in Fig. 3.2; and (c) a detailed map showing the cross section location.

Annual precipitation, from November through March, is about 46 cm in the mountains, decreasing to about 35 cm in the basin where most is lost to evapotranspiration. Outflow water at the Prado Dam (SARPD) is the mixture of storm and base flow from the Santa Ana River (SAR) and ~10 to 25% imported water primarily from the Colorado River (COR) (Davisson et al., 1998). Base flow is considered equivalent to reclaimed waste water during dry periods when there is little recharge from storm flow (Davisson et al., 1998).

These waters are diverted to artificial recharge ponds, such as Anaheim Lake and Kraemer Basin, in the Forebay. Replenishment of the aquifer system is from percolation of the water sources from the recharge ponds into permeable sands and gravels. Regionally, ground water flow is locally impeded by discontinuous lenses of clays and silts, faults, or thinning of aquifer beds along structurally upwarped areas, but these restrictions do not form complete barriers; recharge is reported to reach the deepest monitored wells in the Forebay region (about 670 m) (Herndon et al., 1997).

Description of the study site

The study site shows the Forebay recharge area (Fig. 3.1). Aquifer recharge is through waters diverted from the Santa Ana River at the Prado Dam (SARPD) to the Anaheim Lake and Kraemer Basin spreading ponds then along a flow path from these ponds that includes the wells shown on the cross section (Fig. 3.2). Previous studies (Davisson et al., 1996; 1998; 1999a; 1999b) have used a suite of isotopic tracers and geochronometers throughout an extensive network of wells monitored to determine the flow path and turnover times of ground waters. The turnover times or ages of ground water samples from well water involved in this study are given in Table 3.1. The $^3\text{H}/^3\text{He}$ ages were shown to constrain ground water ages older than 1 year (Davisson et al., 1996; 1999a). Ages for waters younger than one year were determined using the measured change in mixing ratios of the $\delta^{18}\text{O}$ of the ground water and the $\delta^{18}\text{O}$ of Colorado River water (Davisson et al., 1999a). Davisson et al. (1999a) identified a relatively rapid flow along a path from Anaheim Lake to wells AM 44, AM 9, AM 14, wherein the linear flow velocity averages 5.1 m d^{-1} and the hydraulic conductivity is $\sim 307 \text{ m d}^{-1}$. A tracer study using sulfur hexafluoride released into the SAR at a location in close proximity to the study area (north of the SAR and extending to less than 0.5 km south of Anaheim Lake) demonstrated a similar linear flow velocity of $\sim 5.5 \text{ m d}^{-1}$ in wells $< 60 \text{ m}$ depth (Gamlin et al., 2001).

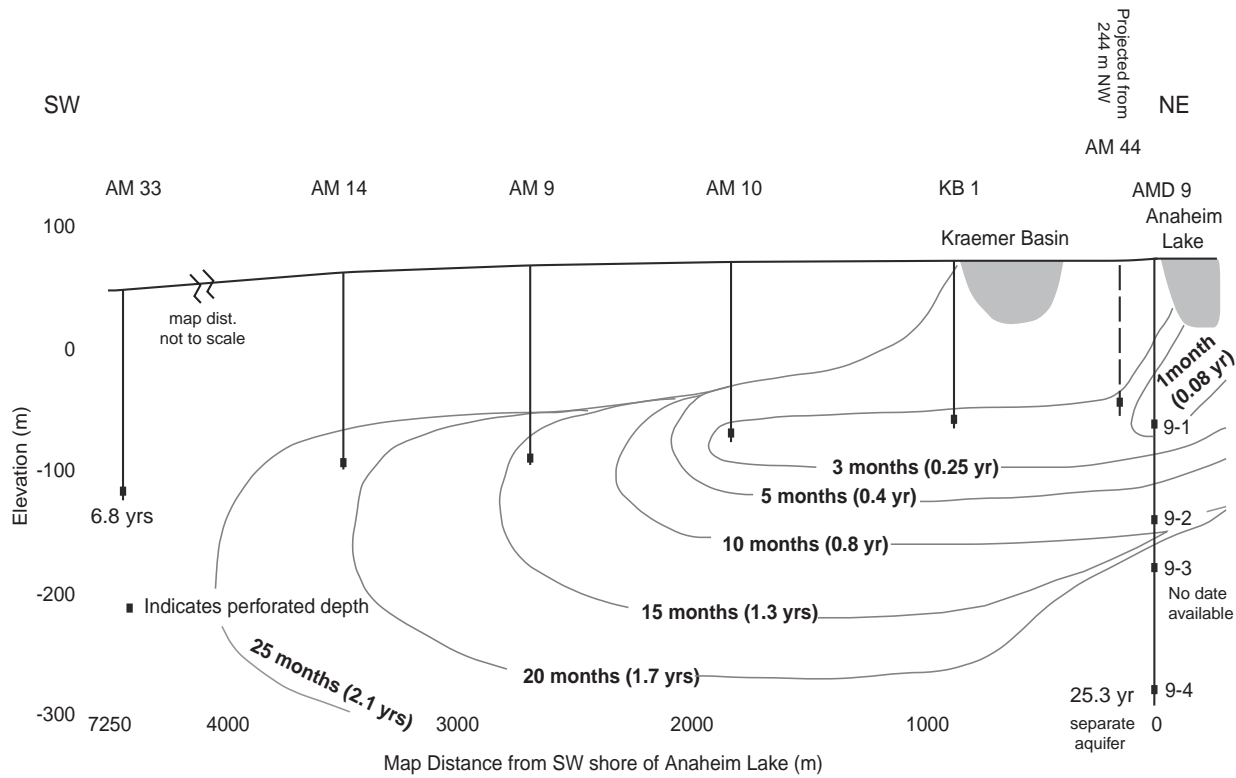


Fig. 3.2. Cross-section showing the study wells and the artificial recharge ponds. Contours represent ground water ages as determined from $^3\text{H}/^3\text{He}$ for waters >1 yr) and $\delta^{18}\text{O}$ and Xe tracer tests. All ground waters are < 10 yrs old with the exception of AMD 9-3, for which there is no water age data available, and AMD 9-4, which is in a separate aquifer system.

Table 3.1. Iodine and water age data for the Orange County study wells.

	AM 33	AM 14	AM 9	AM 10	KB 1	Kraemer Basin	AM 44	Anaheim Lake	AMD 9-1	AMD 9-2	AMD 9-3	AMD 9-4
$^{129}\text{I}/^{127}\text{I}$ (10^{-11})	13.2	8.47	6.11	3.78	2.29	9.88	4.40	5.04	6.89	6.25	8.02	1.74
^{129}I (10^7 atoms/L)	6.63	5.25	3.67	1.77	1.16	4.77	1.83	3.50	5.17	4.07	4.38	0.91
^{127}I (ppb)	22.0 ^a	25.0 ^a	26.8 ^a	25.7 ^a	27.2 ^a	18.3 ^a	24.2 ^b	26	41.1	35.1	31.2	27.3
Ground water age (years)	6.8 ^c	1.9 ^d	1.2 ^d	0.2 ^d	0.1 ^d		0.25 ^e [20%]		0.08 ^e [0%]	0.55 ^e [40%]	n.d. ^f	25.3 ^d
Sample collection date	Aug 99	Aug 99	Aug 99	Sep 99	Aug 99	Aug 99	Aug 99	Sep 99	Sep 99	Sep 99	Sep 99	Sep 99
Date incl. age and travel time ^g	Aug 92	Jun 97	Aug 98	Feb 99	Jan 99	May 99	Feb 99	Jun 99	May 99	Dec 98	n.d.	May 73
TOC (mg/L) ^h	0.89	1.13	0.9 ⁱ	0.89	1.88	3.74	1.19	4.53	2.44	1.76	1.52	1.37
Cl (mg/L) ^h	86.9	73.8	78.8	89	91.6	87.9	103	89.2	105	98.9	86.9	121

^a Independently analyzed by ICP-MS by J. Moran, and by HPLC; ^b analyzed by HPLC (Schwehr & Santschi, 2002); ^c based on $^3\text{H}/^3\text{He}$ data (Clemens-Knott et al., 1998); ^d based on $^3\text{H}/^3\text{He}$ data (Davisson et al., 1999a); ^e based on $\delta^{18}\text{O}$ data (Davisson, 1998) with % mixing in brackets [%]; ^f n.d. represents no data; ^g Water age based on estimated recharge age for Anaheim Lake and Kraemer Basin, see text; ^h aqueous geochemical data from G. Woodside; ⁱ interpolated from monthly measurements preceding and proceeding sample collection.

Clemens-Knott et al. (1999) extended the rapid flow path discussed above to beyond AM 33, displaying an average linear flow velocity of 2.7 m d^{-1} with a hydraulic conductivity of $\sim 200 \text{ m d}^{-1}$. High 'preferential' flow is consistent with the steeply dipping aquifers to the west and southwest near the recharge region. With some distance from recharge, the dip decreases and an increase in consolidation of sediments, dispersivity, and diffusivity are expected to occur with an increase in depth. Therefore, it is not surprising that with an increase in depth, there is a correspondent decrease in flow rates and an increase in water age (Herndon et al., 2003).

The $\delta^{18}\text{O}$ tracer tests showed that the Orange County Water District OCWD KB 1 well and the AM 10 well are likely recharged from Kraemer Basin and not from Anaheim Lake (Davisson, 1998).

The AMD 9 well is a series of nested wells completed at different levels (Fig. 3.2). Anaheim Lake directly recharges wells AMD 9-1 and AMD 9-2. AMD 9-3 is completed in a low permeability zone with no dated waters available, and AMD 9-4 is completed in a separate, older aquifer system with no apparent recharge from Anaheim Lake or Kraemer Basin during the relatively short time of the isotopic tracer tests. The $^3\text{H}/^3\text{He}$ age for water from AMD 9-4 is 25 yrs (Davisson et al., 1999a).

In summary, the Upper Santa Ana River catchment waters are pooled in the Prado Reservoir above the Prado Dam, where flow is diverted from the Santa Ana River and mixed with recycled waste waters and imported waters from the Colorado River. These waters are then spread onto artificial recharge ponds, such as Anaheim Lake and Kraemer Basin. Water from these recharge ponds percolates into a permeable sandy aquifer system at a rate such that there is a complete turnover for these ponds several times annually. The study wells supplied by this artificial recharge are within a flow path demonstrating high hydraulic conductivity and water turnover of less than ten years, with the exception of AMD 9-4, which is in a separate aquifer system and has a water age of 25 years.

METHODOLOGY

Water samples

Three to 5 Liters of water were collected from all wells in August and September 1999 (Table 3.1). The samples were collected by and received through collaboration with the Orange County Water District and the Lawrence Livermore National Laboratory, respectively. Upon receipt, the samples were preserved by the addition of 10 mM HSO₃ reductant per liter to prevent possible volatilization of elemental gaseous iodine. Aliquots of 5 mL were used for measurement of total ¹²⁷I by HPLC and ICP-MS (Schwehr and Santschi, 2003). The bulk of the samples were then transferred into acid-

cleaned polypropylene bottles, sealed with parafilm, and stored at room temperature in the dark.

Processing water samples for $^{129}\text{I}/^{127}\text{I}$

The sample processing for $^{129}\text{I}/^{127}\text{I}$ isotopic iodine ratio determination includes sample pre-concentration for ease of iodine extraction and subsequent decrease of required reagents, reduction of I_2 and IO_3^- to I^- , recovery of iodine from decomposition of organic iodine forms, liquid-liquid extraction of iodine as the sum of all potential iodine species from the sample, and preparation of AgI targets for AMS measurement.

The first stage of sample preparation was a volume reduction from 3 to 5 L to ~500 mL by distillation by rotary evaporation. The pre-concentrated solutions were placed in Teflon bottles, with the addition of 2 to 4 mg of Woodward iodine, a low concentration carrier (iodine $^{129}\text{I}/^{127}\text{I}$ ratio of 80×10^{-15}). Next, 5M NaOH was added to adjust the pH to 14. The sample solutions were then oxidized by chlorination with 250 μL of fresh 4 to 6% NaClO, ultrasonicated for 3 hours at 40°C and left in the 40°C bath overnight. Testing of this high pH chlorination treatment for organic matter oxidation yielded recoveries of ~98% iodine from known concentrations of the destruction-resistant L-thyroxine compound. The sample solutions were then cooled to room temperature, treated with 5 mL 1M HSO_3^- and 10 mL 1M $\text{NH}_2\text{OH}\cdot\text{HCl}$, and ultrasonicated again for 1.5 hrs at 40°C, re-cooled, after which the pH was adjusted to 6.5 with HNO_3 (Gabay et al., 1974; Szidat et al., 2000; Schnabel et al., 2001). The Teflon bottles were then sealed with parafilm and refrigerated until extraction.

For the solvent extraction procedure, the pre-concentrated sample was placed in a 1000 mL separatory funnel. The solution was acidified to a pH of 1 with 6M HNO₃, equilibrated with ~10 mL CCl₄ and repetitive additions of 5 mL 30% H₂O₂, under shaking and venting, until the CCl₄ turned pink from the dissolution of I₂. The pink CCl₄ solution was reserved in an acid-cleaned Teflon beaker, and covered with a Teflon watchglass. Further additions of CCl₄ and H₂O₂ were added to the remaining separatory funnel solution, and each successive pink CCl₄ was added to the reserved solvent beaker until no change of color was noted in the CCl₄ (usually after 3 repetitions of solvent extraction). Then, 20 mL of 1 M NH₂OH.HCl and 10 mL CCl₄ were added to the remaining separatory funnel sample solution, which was shaken and vented, as a final check that no oxygenated iodine species remained in the sample. All of the reserved, iodinated CCl₄ fractions were combined and back-extracted into ~15 mL of a freshly made-up aqueous solution of 0.1 M NaHSO₃ and 0.18 M H₂SO₄. The colorless solvent was drawn-off as waste, and the aqueous solution was placed into a conical 50 mL glass centrifuge tube. Then 2 mg of Cl⁻ with a low iodine blank was added to the aqueous back-extract to prevent precipitation of sulfo-silver. Tellurium compounds, often found in sulfo-silver, are interferents to the accelerator mass spectrometry (AMS) measurement. The addition of Cl⁻ also provides a more effective co-precipitation the low concentrations of iodide. A solution of 0.1 M AgNO₃ was added drop-wise during agitation of the back-extract to co-precipitate AgCl (white) and AgI (yellow). To maximize precipitation, the solution was refrigerated overnight. The AgCl was redissolved preferentially by addition of 30% NH₄OH solution, vortexed, centrifuged,

decanted, then rinsed thoroughly with 18.3 MΩ de-ionized water. The remaining AgI pellet was rinsed in ethanol and dried in a dark oven, after which it was weighed, mixed with Ag powder, and analyzed by AMS at the Purdue PRIME Lab.

System blanks for the rotary evaporation and chemical reagent blanks had $^{129}\text{I}/^{127}\text{I}$ values from 20 to 85×10^{-15} , which is in the range of the carrier iodine blank. Consequently, no blank corrections were necessary.

RESULTS AND DISCUSSION

^{129}I and $^{129}\text{I}/^{127}\text{I}$ data

Data for ^{129}I and ^{127}I , along with water ages, are presented for each well and for the recharge ponds in Table 3.1.

The ^{127}I values are within the range of 18.3 to 41.1 ppb with a median value of 28.4 ppb. Further discussion relating to the range of these values is found later in the text.

The ^{129}I values for Anaheim Lake and Kraemer Basin, 3.50×10^7 and 4.80×10^7 atoms/L, respectively, are close to regional riverine concentrations measured in 1995 to 1996, which range from 0.6×10^7 atoms/L in the Sacramento River to 3.20×10^7 atoms/L in the Colorado River (Table 3.2; Moran et al., 2002). Values for ^{129}I in the Mississippi River (8.0 and 5.1 atoms/L for May 1995 and June 1996, respectively) are included for reference (Moran et al., 2002). Although there is no measurement for the Santa Ana

Table 3.2. Comparison of ^{129}I , ^{127}I , Cl concentrations and flux for regional rivers and the recharge ponds.

River or Pond	Date	Discharge (m^3s^{-1})	Discharge (10^{12} L/yr)	Drainage (10^{10} m^2)	^{129}I (10^7 atoms/L)	$^{129}\text{I}/^{127}\text{I}$ (10^{-11})	^{127}I (ppb)	Cl (mg/L)	Flux ^{129}I (10^{18} atoms/yr)
Mississippi ^a	05/95	16400	517.00	327.00	8.00	85.0	19.8	n.d. ^d	41400
Mississippi ^a	06/96	n.d. ^d			5.10	194.0	5.5	n.d. ^d	
Sacramento ^a	12/95	845	26.60	5.00	0.60	80.5	1.6	1.7	160
Colorado ^a	08/96	111	3.50	32.00	3.20	123.2	5.5	57.0	112
SARPD ^b		6.6 ^e	0.21	0.58	4.14 ^f				8.62 ^g
Anaheim Lake ^c	09/99				3.50	5.04	26.0	89.2	
Kraemer Basin ^c	08/99				4.77	9.88	18.3	87.9	

^a ref. (Moran et al., 2002); SARPD refers to Santa Ana River at the Prado Dam, which represents the Upper Santa Ana River Basin drainage; ^c this work; ^d n.d. indicates no data value; ^e median annual flow, including wet and dry water years; ^f average of Anaheim Lake and Kraemer Basin; ^g estimate based on median annual flow for SARPD and using the average ^{129}I value for Anaheim Lake and Kraemer Basin as an estimate for the ^{129}I concentration in the SARPD; compare to the ^{129}I flux of 8.80×10^{18} atoms/yr calculated from an exponential regression of ^{129}I data in Fig. 3.6, discussion in text.

River, the value for the Colorado River is notably close to the ^{129}I value of the recharge ponds, 3.20×10^7 atoms/L.

The recently observed organic nature of much of ^{129}I in surface waters explains the 50% to 70% decrease in ^{129}I values from the surface waters to the nearest wells (Anaheim Lake to AM 44 and Kraemer Basin to KB 1 and to AM 10), which suggests retention due to partitioning into macromolecular organic matter too large or surface reactive to infiltrate into the subsurface waters (Santschi et al., 1999). The increase in ^{129}I from the surface waters to the nested AMD 9 wells is postulated to be due to evapotranspiration effects in the recharge water, and will be explained in more detail below.

The removal of macromolecular organic ^{129}I in recharge waters as they percolate to the ground (well) waters agrees with the ~ 50% surface retention in ^{129}I reported by Santschi et al. (1999) between infiltrating river water and the nearest well in the Glatt River Aquifer observation system in Switzerland. The K_d for iodine in the Santschi et al. (1999) study was 1.0 mL/g. This is consistent with the work of Oktay et al. (2002), wherein about 50% of the ^{129}I in Mississippi River water was found associated with macromolecular organic matter. Furthermore, the study of ^{129}I and ^{127}I partitioning in sandy, glaciofluvial soils on the Canadian Shield also found 43 to 73% of the ^{129}I was organically-bound or in residual mineral fractions, with a K_d for iodine of 1.6 mL/g (Quiroz et al, 2002). However, ^{127}I values do not appear to have noticeably decreased from the source water to the nearest wells, suggesting that ^{129}I and ^{127}I are not in the same chemical form.

Concentrations in total organic carbon (TOC) demonstrate the same trend as the ^{129}I values. TOC in Anaheim Lake and Kraemer Basin at the time of the sample collection was 4.53 and 3.74 mg/L, respectively (Table 3.1). Values for TOC in the wells at the time of the sample collection averaged 1.46 mg/L, with a median of 1.37 mg/L, which also suggests retention of 60 to 70% of TOC, the fraction of macromolecular organic matter one often observes in fresh waters in arid climates (e.g., the mean DOC in rivers located in arid regions is 3 mg/L (Thurman, 1985)). Also, Davisson et al. (1998) has documented 50% TOC removal from a one month old water mass (1.5 mg/L TOC at < 91 m depth) as dated by the $\delta^{18}\text{O}$ tracer, that originated from Colorado River water introduced into Anaheim Lake (3.0 mg/L). The same study also showed ~50% decrease in TOC from recharge water from the Santa Ana River in Anaheim Lake (8.4 mg/L, < 1.0 μm) when sampled in a well (4.1 mg/L from ~64 m depth, < 0.2 μm) after one month. Indeed, some of the reason for artificial recharge is to use the sandy aquifer system as a natural 'filter' to aid in elimination of macromolecular organic colloids, such as the carcinogenic trihalomethanes formed when the waters are disinfected with chlorine compounds.

Table 3.3 shows the statistical minimum, maximum, and median for the TOC in the surface waters of Anaheim Lake and Kraemer Basin, and in the ground waters of the wells studied, for the time period May 1990 through April 2001. The number of samples for each site is also shown. Although not presented, the majority of the sampling was from 1996 through the present, which were wetter years. Additionally, although there are high TOC concentration values in wells AM 9 and AM 10, these represent very few

sample values. All the wells with the exception of the three wells, AMD 9-1, AMD 9-2, and KB 1, show a consistency in TOC values. The median TOC value for the surface waters is 4.72 mg/L and 1.24 mg/L for the ground waters.

Table 3.3. Statistics for TOC (mg/L) from May 1990 through April 2001.
Data provided by G. Woodside, OCWD.

Site ID	Median	Minimum	Maximum	Number of samples
<i>Surface Waters</i>				
Anaheim Lake	5.13	2.82	12.20	118
Kraemer Basin	4.32	2.75	6.56	17
Average	4.72			
<i>Ground Waters</i>				
AM 33	0.78	0.49	1.01	8
AM 14	0.80	0.65	1.13	16
AM 9	1.01	0.70	2.67	67
AM 10	1.09	0.73	4.03	55
KB 1	2.27	1.29	5.07	77
AM 44	1.64	1.08	2.48	67
AMD 9-1	2.46	1.55	4.32	110
AMD 9-2	1.39	0.80	2.89	98
Average	1.24			

Since ^{129}I as IO_3^- and especially macromolecular organo-iodine species are likely retained in surface soils (Santschi et al., 1999; Dissanayake and Chandrajith, 1999; Quiroz et al., 2002), only the more soluble and mobile iodide ion, with its low sorption potential (K_d of ≤ 1 mL/g) in neutral to acidic ground waters, would be expected to

infiltrate into the groundwater (Sheppard et al., 1995; Fukui et al., 1996; Fuhrman et al., 1998; Santschi et al., 1999; Kaplan et al., 2000).

The travel time of 3 months for Santa Ana River at the Prado Dam (SARPD) water to reach spreading ponds was determined by following the measurement of low $\delta^{18}\text{O}$ from a discrete pulse of storm water within the Upper Basin from the SARPD to Anaheim Lake (Davisson et al., 1999a). Consequently, three months have been subtracted from the measured ground water ages to adjust for the travel time between the SARPD to Anaheim Lake, so that a comparison can be made between SAR flow rates and the concentrations of ^{129}I in the well waters. No additional time corrections were made to the age-dated well waters.

Concentrations by evapotranspiration versus dilution by rainfall effects on ^{129}I in infiltrating Santa Ana River water

In the mixing diagram, Fig. 3.3, the relationships are shown between the $^{129}\text{I}/^{127}\text{I}$ ratio and the inverse values of ^{127}I , plotted on a log-log scale to include the diverse range of values determined in US waters. Surface water values are represented as squares. The median value for U.S. rain is clearly the highest isotopic ratio that indicates an atmospheric source for ^{129}I , as transported in the troposphere from the European nuclear reprocessing facilities (Moran et al., 1999a; 1999b). Among the rivers shown, the Mississippi (with values for 1995 and 1996), Colorado, and the Sacramento Rivers show high $^{129}\text{I}/^{127}\text{I}$ values, suggesting that their concentrations are due to drainage from larger

areas, which are 1 to 3 orders of magnitude greater than the drainage for the SARPD (Table 3.2).

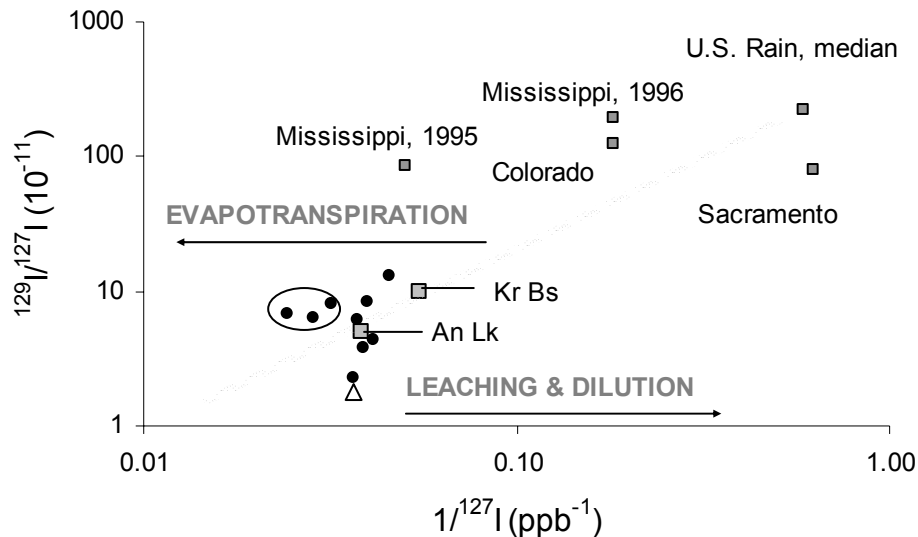


Fig. 3.3. Mixing diagram showing iodine isotopic ratios as a function of the inverse of the stable iodine values for surface and ground waters on a log-log scale. The squares represent values for surface waters, i.e., Anaheim Lake (An Lk), Kraemer Basin (Kr Bs), river drainages, and the median for U.S. rain (Moran et al., 2002). Dots indicate values for the study wells with the AMD 9 perched aquifer wells delineated as a circled group. The triangle is the AMD 9-4 well, which is in an older, deeper aquifer system than the other wells.

Since atmospheric concentrations and input values for ^{129}I from European sources are expected to be roughly constant over the last decade (Szidat et al., 2000), differences in ^{129}I and $^{129}\text{I}/^{127}\text{I}$ values (Fig. 3.3) between the surface water samples of Anaheim Lake and Kraemer Basin and the ground water well values should be due to influences at the time of infiltration. Of course, this assumes that the initial retention of ^{129}I into the groundwater has been constant over time, an assumption that is supported by other observations (see previous section).

Factors affecting the annual input of artificial recharge to the wells are a reflection of factors influencing water quality in the arid Upper SAR Basin, i.e., (1) subsurface aqueous geochemical precipitation or dissolution along the ground water flow path, (2) episodic wetting and drying climatic cycles of the near-surface soils, or (3) mixing effects from other water sources, such as reclaimed waste water and imported water from the Colorado River.

The first factor is unlikely to have affected concentrations of iodine and chlorine species, since, as we have discussed earlier, chloride and iodide exhibit conservative geochemical behavior in the subsurface, in the absence of other sources.

The second factor is considered the most influential. In semi-arid to arid environments such as this region, evapotranspiration (ET) can cause dissolved solutes to concentrate and precipitate as salts during drying cycles (Drever, 1997; Meijer, 2002). Conversely, during wetting cycles, soluble salts are leached and diluted. The degree of dissolution and leaching depends on the amount of meteoric precipitation and the degree of infiltration. We therefore expect chloride and iodide to follow this cyclic geochemical behavior.

The third factor may have some impact, but would seem to be minimal based on the information available. Using the ^{129}I value for the COR (Table 3.2) from Moran et al. (2002) there is little difference in the ^{129}I value for the Anaheim Lake and Kraemer Basin waters which are compared in Section 3.1. However, there are no data available for COR and SARPD for the same year. Intuitively, the COR drainage would experience regional ET effects in the same periods as the SAR. From this premise and

the ^{129}I value that we have, it would be expected that there would be little change in ^{129}I values due to mixing. Correspondingly, the biggest mixing effect due to dilution with COR would result in lower ^{127}I values (COR is 5.5 ppb, study well average is 27.5 ppb) and subsequently in higher $^{129}\text{I}/^{127}\text{I}$ ratios. If the amount of COR water imported is 10 to 25%, this does not result in a change that is significant enough to alter the trends shown by our data. The largest change would show in the isotopic $^{129}\text{I}/^{127}\text{I}$ ratios. Since the figures that follow do not show a trend in the $^{129}\text{I}/^{127}\text{I}$ ratios that displays a noteworthy difference from what is seen in ^{129}I , this concern is not valid. Another topic to address is the contribution of reclaimed waste waters. Davisson et al (1998) maintains that at periods of low recharge from storm flow, the base flow for the SARPD is essentially captured waste waters that have been treated. It is not known what effect reclamation has on the iodine isotopes in this study, but it would seem that there is little effect. The effects due to mixing of SARPD waters with COR and treated waste waters should be addressed in future studies to ascertain its potential importance.

It should be noted that there is a component of human-induced wet-dry cycling within each year. This occurs when the recharge ponds are purposely allowed to dry so that organic matter can be scraped from the bottom to renew infiltration potential. This occurrence is deemed to be of little consequence when compared to the catchment wetting and drying cycles since the Upper SAR is comprised of an area of 5840 km² while the recharge ponds in the study area are ~ 0.6 km² (Miller Basin has not been included in the study, but is included in the pond areal calculation with Anaheim Lake and Kraemer Basin because of its proximity). Therefore, it is anticipated that the natural

climatic geochemical fingerprint of the catchment wetting and drying cycles overwhelms the influence possibly induced by pond wetting and drying. Additionally, even though organic matter is scraped from the pond bottoms, macromolecular retention and micromolecular infiltration of organic forms still exists within the shallow sediments. In support, the experiment by Davisson et al. (1998) where TOC in surface waters and wells measured over a 6 month period (which should include 2 drying cycles with pond-scraping) showed that ~ 50% of the value for TOC in surface recharge waters was measured in well waters at < 90 m depth. The surface water TOC was also larger in size (< 1.0 μm) and younger (3 pmc higher in ^{14}C) than the well water DOC (< 0.2 μm).

Ground water values above the mixing line show concentrations of ^{129}I that are higher than expected from the mixing line due to ET and low annual peak flow for the SAR as a consequence of low storm recharge, and therefore, lack of leached soluble weathering products (Southard, 2000). Below the mixing line, $^{129}\text{I}/^{127}\text{I}$ values are lower due to dilution of ^{129}I during periods of higher SAR annual peak flow (higher storm recharge) and subsequent leaching of halogen ions to greater soil profile depths (Southard, 2000). Another possibility is that ^{129}I is diluted in the subsurface by waters not originating from the recharge ponds. Due to the shallow nature of these aquifers and given that there is no indication of significant mixing from other tracer studies, this aspect is less likely. If subsurface waters do not originate from the ponds, their source is still the catchment with its ET fingerprint. There is no geochemical evidence to indicate that brine waters infiltrate the aquifers in the Forebay Area.

Davisson et al. (1999a) report that excess air (indicated by a high ^4He measured versus ^4He expected for water in equilibrium with atmosphere) and fluctuations in recharge temperatures consistent with those of mean annual soil temperatures indicate the presence of a periodic vadose zone beneath Anaheim Lake. Perched waters should have higher concentrations of solutes, including ^{129}I (and ^{127}I and Cl), than surface waters due to the leaching of salts and ET effects prior to percolation and mixing with other vadose zone waters (Meijer, 2002). It is suggested that levels 1-3 of the AMD 9 nested wells are within a perched aquifer, shown as the circled ground water wells with concentrated $^{129}\text{I}/^{127}\text{I}$ values on the mixing diagram (Fig. 3.3). Viable alternative explanations for higher than expected values for $^{129}\text{I}/^{127}\text{I}$ in the AMD 9-1 through 9-3 wells are:

(1) there are coarser gravels or a macroporous system, allowing higher molecular weight colloidal organic material, rich in ^{129}I , to migrate the relatively short distance from the source than for the other study wells; and

(2) there are older, more enriched waters mixing with these waters, as may be indicated by the older $^3\text{H}/^3\text{He}$ ages than were indicated by the $\delta^{18}\text{O}$ tracer studies.

Note that for explanation (1), an additional mechanism is needed to concentrate ^{129}I , as the ^{129}I in AMD 9-1 is higher than in Anaheim Lake or Kraemer Basin. In the case of explanation (2), the $^3\text{H}/^3\text{He}$ age in AMD 9-1 was 0.4 yrs (Davisson et al., 1999a), whereas the $\delta^{18}\text{O}$ tracer age indicated waters that reflected 100% of the tracer composition (complete mixing) in ~30 days (Davisson, 1998). For well AMD 9-2, the $^3\text{H}/^3\text{He}$ age was 2.7 yrs (Davisson et al., 1999a), whereas the $\delta^{18}\text{O}$ tracer age indicated

waters showing 60% mixing at 200 days (Davisson, 1998). (No water age determination was available for AMD 9-3). Since the $\delta^{18}\text{O}$ tracer ages were considered more accurate than the $^3\text{H}/^3\text{He}$ ages for $\delta^{18}\text{O}$ water ages that were less than 1 yr, we are using the $\delta^{18}\text{O}$ tracer ages (Table 3.1) with no corrections for potential mixing. The % composition due to water mass mixing indicated by the $\delta^{18}\text{O}$ tracer experiments is indicated in brackets in Table 3.1. In some wells within the area, Xe isotopic ratios were used in combination with the $\delta^{18}\text{O}$ tracer tests. The $\delta^{18}\text{O}$ values of the waters (Colorado River) introduced in a controlled recharge were isotopically depleted enough to confidentially determine dilution from the SAR to within 90%. The Xe isotopic ratios were significantly enriched and conservative so that mixtures below 10% could be quantified. While no Xe tracer data was measured in the study wells, other wells within the immediate vicinity of the recharge ponds were tested. This combined $\delta^{18}\text{O}$ and Xe tracer data showed that a well at the southern shore of Anaheim Lake, perforated at ~ 61 m depth, had a water mass age of < 1 month. Also, that a nested series of wells on the western shore of Kraemer Basin indicated water mass ages of 4, 8, 11, and 16 months at perforated intervals centering at approximately 92, 137, 171, and 244 m, respectively (Herndon et al., 2003). These data are integrated into the water mass age contours on the cross section shown in Fig. 3.2, which also honors the age data from the sources indicated in Table 3.1. Also, as discussed in the studies referenced on Table 3.1, the contours also infer that well AM 44 is recharged from Anaheim Lake and that well AM 10 is sourced via Kraemer Basin.

The remaining wells shown on Fig. 3.3 include the three values above the mixing line, showing ET concentration of $^{129}\text{I}/^{127}\text{I}$ corresponding to relatively low SARPD peak

flow. The wells above Anaheim Lake are AM 9, AM 14, and AM 33. Below the mixing line, from Anaheim Lake downward are diluted concentrations of $^{129}\text{I}/^{127}\text{I}$ in wells AM 44, AM 10, and KB 1. The AMD 9-4 water, which is from a separate and deeper aquifer system than the other waters, has a water age of 25 years and a $^{129}\text{I}/^{127}\text{I}$ value that is an order of magnitude less than waters from the other wells. The lower $^{129}\text{I}/^{127}\text{I}$ value is likely a result of the lower atmospheric input from the European nuclear reprocessing facilities 25 years ago, which was at least 50% less for Europe during that time (Buraglio et al., 2001; Hou, 2002). Therefore, since the AMD 9-4 well represents a different $^{129}\text{I}/^{127}\text{I}$ value input and a different aquifer from the other study wells, it is not included on the other plots.

^{129}I and $^{129}\text{I}/^{127}\text{I}$ versus ground water age

The isotopic ratio $^{129}\text{I}/^{127}\text{I}$ and ^{129}I concentrations in the study site wells show a natural logarithmic dependence with the age of the ground waters (Fig. 3.4). The oldest water, AM 33, has the highest concentration, with progressively younger water ages proceeding in the following order: AM 14, AM 9, AMD 9-1 (higher concentration and younger than the trend), AMD 9-2, followed by wells AM 10 and AM 14 in close proximity, and lastly, KB 1. The causes for this relationship likely have nothing to do with the fallout history of ^{129}I during the 1990's, when atmospheric inputs were relatively constant (Moran et al., 1999a; Szidat et al., 2000), but more with the modulation of the fallout signal in the river due to evapotranspiration effects on infiltrating river and lake water concentrations varying with SARPD flow conditions, as elaborated in the following section.

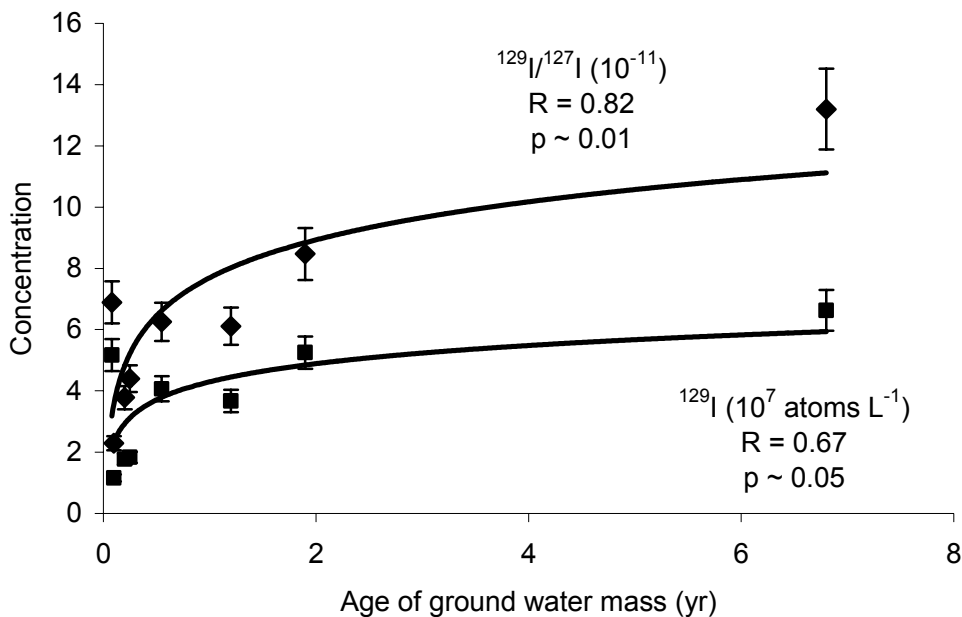


Fig. 3.4. The $^{129}\text{I}/^{127}\text{I} \times 10^{-11}$ and $^{129}\text{I} \times 10^7$ (atoms/L) values for ground waters, as a function of ground water age. Vertical error bars represent 10%.

Catchment drainage response to chloride, ^{129}I , and $^{129}\text{I}/^{127}\text{I}$ ratios

Chloride in river water mostly originates from atmospheric deposition and may therefore be used in analogy to ^{129}I , in the absence of other sources. During times of low storm recharge and subsequent low river flow, one would expect high regional ET and the concentration of solutes, i.e., chloride salts, in near surface waters. Storm runoff and soil infiltration are able to dissolve chloride salts, to be added to the river water.

In the SAR catchment, there is a strong regional response of chloride concentration to flow at the Santa Ana River Prado Dam (SARPD), as shown in Fig. 3.5, with data on flow rates and chloride concentrations $[\text{Cl}^-]$ from the USGS on-line database (USGS, 2002a). During an extended dry period from 1983 to 1992 (these

water years are from Oct.-Sept.), median $[Cl^-]$ ranged from 3.1 meq/L and gradually increased to 3.4 meq/L. The period from 1992 to 1999 included wetter years, therefore having lower median $[Cl^-]$ (1.8 to 2.8 meq/L). The median of minimum values during that time period was 1.4 meq/L (no data are available from 1994 -1995).

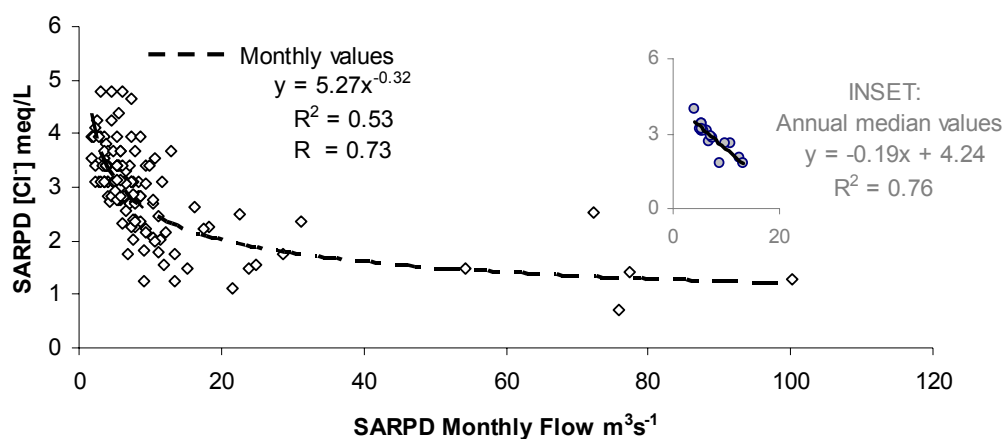


Fig. 3.5. Inverse correlation for chloride concentration (meq/L) in the Santa Ana River at the Prado Dam (SARPd) as a function of discharge at the dam (m^3s^{-1}). The diamonds and the dashed regression line represent monthly values for both flow and $[Cl^-]$. The inset shows the annual median of the monthly values discussed in the text.

The median for the annual peak flow during the dry period is $5.5 m^3s^{-1}$, whereas the median for annual peak flow for the wet period is $40 m^3s^{-1}$, with the maximum peak flow reaching $100 m^3s^{-1}$ in 1992 and $77 m^3s^{-1}$ in 1997. The median annual value for the water years 1979 -1999, covering the combined period of wet and dry years, is a flow rate of $6.6 m^3s^{-1}$ and a Cl^- concentration of 3.1 meq/L. Figure 3.5 shows the inverse correlation between the SARPd Cl^- concentration and the SARPd flow rate. The

monthly values show a power correlation regression, with high $[Cl^-]$ values during low flow, and dropping off to lower $[Cl^-]$ values that show a baseline response with increasing flow. The surface waters from the SARPD represent the response of the Upper Santa Ana River Basin catchment to storm flow. The storm runoff and infiltration from long duration storm events dilute the $[Cl^-]$ and provide recharge to river water and unconfined aquifers. Conversely, $[Cl^-]$ becomes concentrated during low flow and low infiltration from occasional short duration meteoric precipitation in conjunction with ET. This regional relationship is even more strongly established through the correlation of the annual median of the monthly values which eliminates the extreme periods of flow (Inset, Fig. 3.5). The elimination of extreme (high) flow by exclusion of all data with SARPD flow values $> 15 \text{ m}^3 \text{ s}^{-1}$ yields a linear regression ($y = -0.15x + 4$; $R^2 \sim 0.35$) (not shown), similar to that of the annual median values ($y = -0.2x + 4.2$; $R^2 \sim 0.8$).

Fig. 3.6 shows the relationship of $^{129}I/^{127}I$ and ^{129}I values for ground waters, as a function the SARPD mean monthly outflow. The $^{129}I/^{127}I$ ratios and ^{129}I concentrations each show an inverse correlation with outflow. It can be assumed that with a larger ^{129}I data set containing ^{129}I values also during higher riverine flow rates, the plotted relationship would have followed a similar power regression as shown in the SARPD $[Cl^-]$ vs. SARPD flow given in Fig. 3.5. Because, however, the highest flow rates seen in the SARPD occur very infrequently, the ^{129}I data are more representative of typical SAR drainage basin conditions.

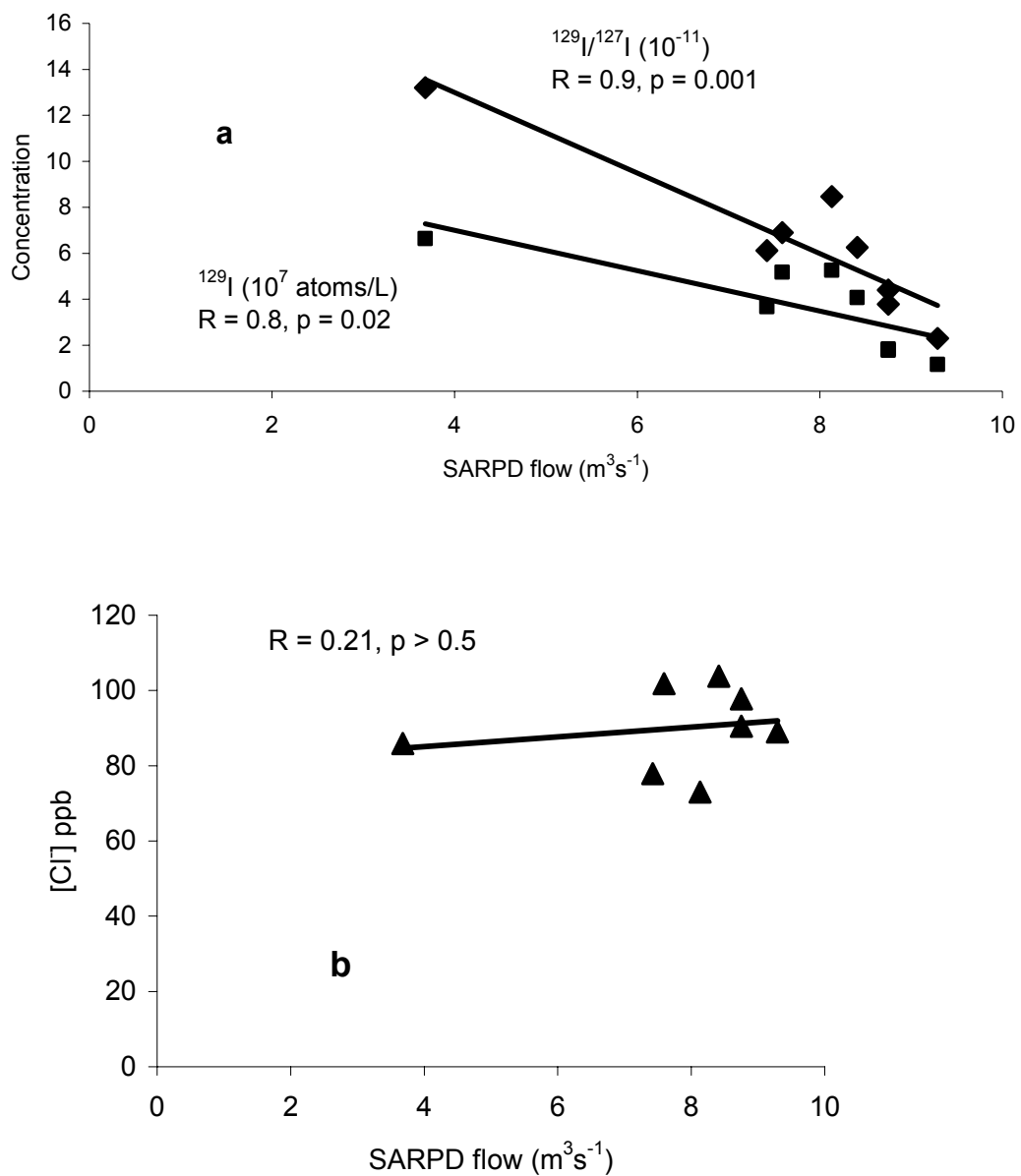


Fig. 3.6. (a) The $^{129}\text{I}/^{127}\text{I} \times 10^{11}$ and ^{129}I (10^7 atoms/L) values for ground waters as a function the Santa Ana River Prado Dam (SARPD) mean monthly outflow (m^3s^{-1}). Vertical error bars represent 10%. (b) Also, shown are the chloride concentrations for the ground waters, yet these show no apparent correlation to SARPD flow.

A similar inverse relationship between iodine isotopic ratios in river water and river flow rate was also reported by Oktay et al. (2001). These authors reported an exponential decrease in ^{129}I and $^{129}\text{I}/^{127}\text{I}$ values in Mississippi River water with increased flow rates ($y = 14.4 * e^{(-3.57x*10E-5)x}$; $R = -0.48$). Furthermore, the ^{129}I concentrations in the river water asymptotically approached the average ^{129}I value for rainwater in the U.S. during the highest river flow rates. Since ^{129}I originates from atmospheric transport from the European nuclear facilities, and the Mississippi drainage covers about 40% of the contiguous U.S., the rainwater ^{129}I concentration was assumed to be close to the source input value.

Using an exponential relationship for the ^{129}I concentration in ground water as a function of SARPD flow (Fig. 3.6a), somewhat analogous to the Oktay et al. (2001) river water study, the relationship would be $y = 22.314 * e^{(-2519)x}$; $R^2 \sim -0.5$. Using this equation to calculate a source input value for ^{129}I in the SARPD, and using the median annual flow rate for the SARPD, $6.6 \text{ m}^3\text{s}^{-1}$, the calculated ^{129}I concentration is 4.23×10^7 atoms/L with a ^{129}I flux from river flow rate is 8.80×10^{18} atoms/yr.

This calculation compares quite favorably to the calculation shown in Table 3.2, where the ^{129}I value used is 4.14×10^7 atoms/L (the average for the ^{129}I values for Anaheim Lake (3.50×10^7 atoms/L) and Kraemer Basin (4.77×10^7 atoms/L)), and the calculated ^{129}I flux from river flow rate is 8.62×10^{18} atoms/yr. The similarity between the ^{129}I value calculated from the exponential relationship in Fig. 3.6 and annual median flow of the SARPD and the average ^{129}I value for the artificial recharge ponds suggests that the concentration of ^{129}I in the river water of the SARPD is indeed inversely

proportional to SARPD flow rate, and that the proportion of ^{129}I removed at the aquifer interface must be constant. The ^{129}I flux from river flow rate thus calculated also compares favorably with that of other rivers considering the relative size of the drainage basin (Table 3.2).

Using a linear relationship for the SARPD (Fig. 3.6a), the isotopic ratio of $^{129}\text{I}/^{127}\text{I}$ shows an even greater significance ($y = -1.75x + 20$; $R^2 \sim 0.8$, $p < 0.005$). The $^{129}\text{I}/^{127}\text{I}$ correlation is notably more significant than the correlation for SARPD $[\text{Cl}^-]$ to SARPD flow rate. Although there is a strong inverse correlation between riverine $[\text{Cl}^-]$ and river flow in the surface river water at the SARPD, such a relationship is not apparent in the ground waters (Fig 3.6b). This suggests that either: (1) the ET signal in $[\text{Cl}^-]$ is dampened or buffered by water-rock reactions in the subsurface, or (2) other factors are at work, and the the ET signal in $[\text{Cl}^-]$ is not as strong as the ET signal in concentrating the ^{129}I and $^{129}\text{I}/^{127}\text{I}$ values.

Regarding the first possibility, Fig. 3.7 shows a strong ground water (GW) buffering of $[\text{Cl}^-]$ in response to $[\text{Cl}^-]$ changes in meteoric precipitation (PPT), while the riverine $[\text{Cl}^-]_{\text{SARPD}}$ changes have a higher slope, and showing a significantly greater response to changes in $[\text{Cl}^-]_{\text{PPT}}$. In consideration of the second possibility, it is suggested that due to a water age shorter than needed for complete equilibration, ^{129}I displays an apparent mobility in ground water that is markedly different from ^{127}I or Cl^- . As mentioned in the discussion regarding Table 3.1, the data suggest that ^{129}I and ^{127}I have a different mobility and are thus not in the same chemical form or equilibrated on

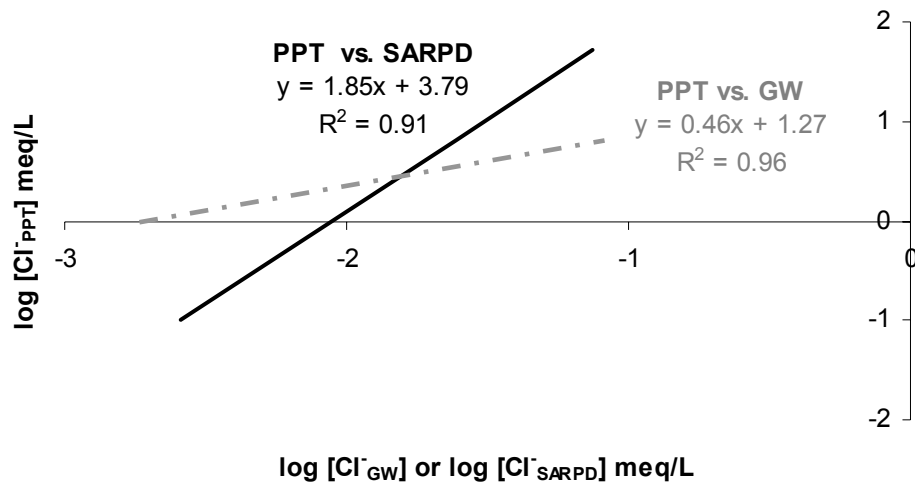


Fig. 3.7. The $\log [\text{Cl}^-]$ (meq/L) in meteoric precipitation (PPT) as a function of the $\log [\text{Cl}^-]$ (meq/L) in ground water (GW) and that of the $\log [\text{Cl}^-]$ (meq/L) in the SARPD. The contrast in slope shows the buffered response in $[\text{Cl}^-]_{\text{GW}}$ to changes in $[\text{Cl}^-]_{\text{PPT}}$. The riverine response in changes of $[\text{Cl}^-]_{\text{SARPD}}$ to $[\text{Cl}^-]_{\text{PPT}}$ is much faster as expected. The buffered response of $[\text{Cl}^-]_{\text{GW}}$ explains the lack of correlation in $[\text{Cl}^-]$ to SARPD flow in Fig. 6. $[\text{Cl}^-]_{\text{PPT}}$ data is for monthly precipitation-weighted concentrations from the National Atmospheric Deposition Program for the water years 1982 to 1999 (NADP/NTN, 2002).

the same time scales. This is supported by Fig. 3.8 which shows that ^{127}I does not correlate to SARPD flow as does ^{129}I in Fig. 3.6a. It should be noted that the two highest concentrations of ^{127}I are from the AMD 9-1 and 9-2 wells and are likely due to percolation and mixing in a localized perched aquifer or infiltration of colloidal organic matter through coarser gravels, as discussed in section 3.2.

Even though there is only circumstantial evidence that ^{129}I is a tracer for river flow rates under circumstances where atmospheric input is constant, as in the 1990's,

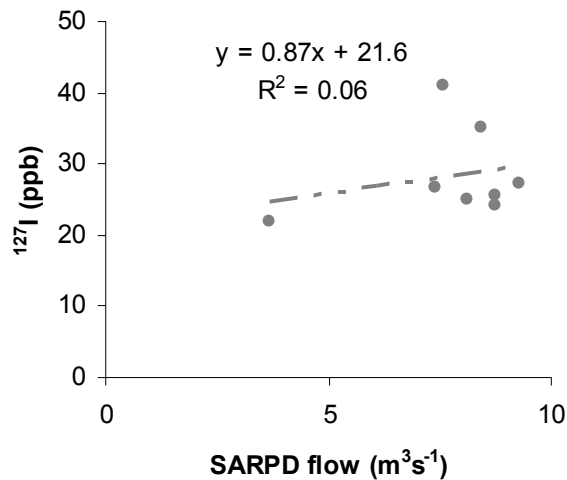


Fig. 3.8. Similar to Fig. 3.6, but showing the correlation of ^{127}I values for ground waters as a function of the Santa Ana River Prado Dam (SARPD) mean monthly outflow (m^3/s). Unlike in the case of ^{129}I , there is no apparent correlation to SARPD flow, suggesting that ^{127}I and ^{129}I have different mobilities in ground water.

such behavior had been demonstrated in other rivers affected by evapotranspiration (Oktay et al., 2001). What will be needed in a future study is to show 1) that the concentration of ^{129}I in the river water of the SARPD is indeed inversely proportional to SARPD flow rate, 2) that the proportion of ^{129}I and ^{127}I that is removed at the pond bottom/aquifer interface is constant, 3) that Cl^- concentrations in the aquifer are buffered against changes from infiltrating river water due to rock dissolution, 4) the contribution of ^{129}I and $^{129}\text{I}/^{127}\text{I}$ concentrations from all input waters, i.e., reclaimed waste waters and imported waters of the Colorado River is minimal, and 5) the potential for use of $^{129}\text{I}/^{127}\text{I}$ as a geochronometer for TOC which may provide a higher constraint on dating organic matter than radiocarbon for ages less than 50 years.

CONCLUSIONS

From measurements of ^{129}I and ^{127}I in wells from Orange County ground water basin fed by the Anaheim Lake and Kraemer Basin recharge ponds, literature values of aquifer water ages based on $^3\text{H}/^3\text{He}$ and $\delta^{18}\text{O}$ data, as well as time-series data of chloride and Santa Ana River flow rates over the past decade, the following conclusions were made:

1) Ratios of $^{129}\text{I}/^{127}\text{I}$ and ^{129}I concentrations in the ground waters increase with aquifer water age, in contrast to the response expected from the constant atmospheric source input over the past decade from European reprocessing plant emissions.

2) The chloride concentrations in the Santa Ana River (SAR) show an inverse relationship to the discharge of the Santa Ana River. This is consistent with the study of Oktay et al. (2001) wherein ^{129}I concentrations and $^{129}\text{I}/^{127}\text{I}$ values are inversely proportional to the river flow rate of the Mississippi.

3) Ratios of $^{129}\text{I}/^{127}\text{I}$ and ^{129}I concentrations in the ground waters are inversely related to the inferred flow of the Santa Ana River at the Prado Dam (SARPD). The inferred flow is defined as the SARPD flow at the date equivalent to the date at the ground water collection time subtracted by the ground water age and the three month travel time from the SARPD to the spreading ponds. Thus, it appears that ^{129}I and $^{129}\text{I}/^{127}\text{I}$ behavior in this aquifer are reflecting the climatic conditions in the semi-arid SAR basin, i.e., concentration of ^{129}I and $^{129}\text{I}/^{127}\text{I}$ during periods of low river flow and evapotranspiration and dilution of ^{129}I and $^{129}\text{I}/^{127}\text{I}$ during storm flow.

This novel application, even though it needs to be tested further, could be useful in determining past hydrological conditions in other, less studied aquifers, in semi-arid basins with populations in need of drinking water and a recharge affected by evapotranspiration.

CHAPTER IV

THE DISSOLVED ORGANIC IODINE SPECIES OF THE ISOTOPIC RATIO OF
 $^{129}\text{I}/^{127}\text{I}$: A NOVEL TOOL FOR TRACING TERRESTRIAL ORGANIC MATTER IN
THE ESTUARINE SURFACE WATERS OF GALVESTON BAY, TEXAS

INTRODUCTION

Anthropogenic ^{129}I can now be found all over the globe (Snyder and Fehn, unpublished), which lead to the use of ^{129}I concentrations to trace the movement of oceanic water masses in the Atlantic Bight (Santschi et al., 1996), in the Gulf of Mexico (Schink et al., 1995b), and in the Arctic ocean (Raisbeck et al., 1995; Carmack et al., 1997; Smith et al 1998; Edmonds et al., 1998; Raisbeck and Yiou, 1999; Cooper et al., 2001; Yiou et al, 2002). Artificial ^{129}I primarily originates from gaseous waste products released by nuclear fuel reprocessing plants in Europe, and transported is to North America within ~ 10 to 18 days (Moran et al., 1997). Concentrations of ^{129}I and $^{129}\text{I}/^{127}\text{I}$ ratios are used as tracers for surface and groundwater interactions (Santschi et al., 1999; Schwehr et al., 2003a). The biophilic nature of iodine is exemplified by the fact that ~ 40 to 75% of the total iodine in fresh and coastal marine waters are found as organic iodine (Oktay et al., 2001; Quiroz et al., 2002; Schwehr et al., 2003a).

Concentrations of ^{129}I and $^{129}\text{I}/^{127}\text{I}$ values are much higher in terrestrial organic matter as compared to marine organic matter, likely due to the greater dilution potential of the ocean (i.e., 100s of m per decade) than the terrestrial system (i.e., 10 cm in soils)

after atmospheric fallout, as well as differences in stable iodine concentrations. For example, the mean concentration values in North American rain water and river water are 3.8×10^{-9} and $(0.1 \text{ to } 3) \times 10^{-9}$, respectively (Moran et al., 1997; 2000; 2002), whereas the value in the surface waters of the Gulf of Mexico is about 65×10^{-12} (Schink et al., 1995b).

The objective of this study is to test the potential use of $^{129}\text{I}/^{127}\text{I}$ in DOI (dissolved organic iodine) to trace terrestrial organic matter in the Galveston Bay estuary. To this end, the goals of this study are to a) develop the appropriate methods to measure DOI in $^{129}\text{I}/^{127}\text{I}$; b) to test how far the elevated values of $^{129}\text{I}/^{127}\text{I}$ in DOI can be followed through a transect of salinity in the Galveston Bay estuary; and c) to compare the results with published data on stable isotopes in dissolved organic matter, i.e., $\delta^{13}\text{C}$, $\delta^{14}\text{N}$ as well as C/N ratios.

METHODOLOGY

Study site

Galveston Bay is a subtropical estuarine environment where the mean annual precipitation is 132 cm and the mean annual temperature is 21°C (data for Houston, Texas from NCDC/NOAA, 2003). The Galveston Bay is a shallow bay with a mean depth of 2 m and diurnal tidal changes of less than 40 cm. Consequently, estuarine circulation is primarily wind-driven (Ward, 1992, as cited in Santschi 1995; Tang et al., 2002). It is the second largest watershed emptying into the Gulf of Mexico, draining a

basin of 46,100 km² into an estuarine area of 1432 km² adjoined by a wetland area of 526 km² (Ward, 1992, as cited in Santschi, 1995; Pinkney et al., 2002).

Freshwater input to the Bay is mainly from the Trinity (83%) and San Jacinto (8%) Rivers, which transport moderate to high loads of terrestrial organic carbon (5-8 mg L⁻¹ C) and suspended particulate matter (4-200 mg L⁻¹) (Guo and Santschi, 1997).

Figure 4.1 is a map of Galveston Bay indicating station locations, with the transect beginning at Station 1, nearest the mouth of the Trinity River, and ending with Station J beyond the jetty of Galveston Bay. Samples were collected December 14, 2001.

Sample collection and storage

Containers and tubing were cleaned and samples prepared as described in Schwehr and Santschi (2003). Briefly, while wearing polyethylene gloves, acid-cleaned containers were triple-rinsed with 18M Ω water (de-ionized water, DIW), then conditioned with a triple-rinse of sample down-current from the collection site. The 10 L sample container was over-filled with surface water, tapped to release any gas bubbles, then over-filled again and sealed. The sealed containers were immediately stored in a dark, insulated cooler filled with ice. Within ~5 hours, all samples were collected and transported to the laboratory where they were filtered through a 0.45 μ m in-line capsule filter assembly. Immediately after filtering, the concentrations of stable iodide, [¹²⁷I-I⁻]; natural total inorganic iodine as the sum of iodide and iodate, [¹²⁷I-TII]; and natural iodate, [¹²⁷I-IO₃⁻], were determined as discussed below.

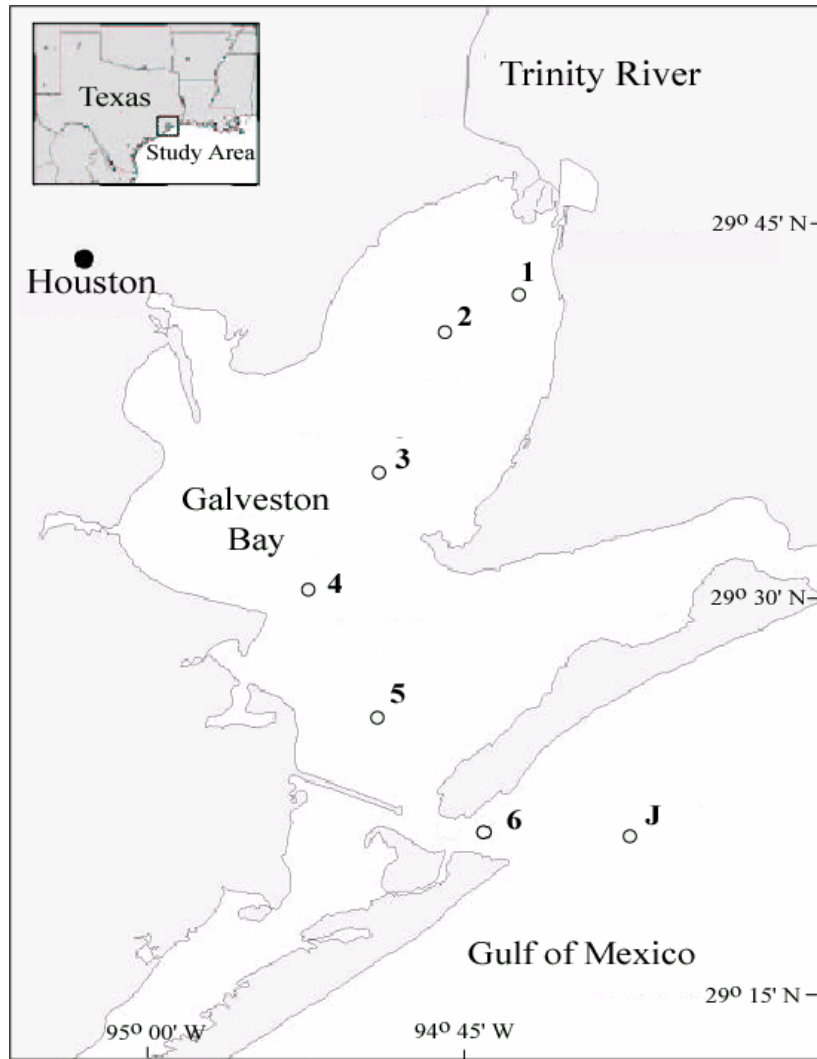


Fig. 4.1 Sampled locations in Galveston Bay Estuary on Dec. 14, 2001.

Simultaneously, $^{129}\text{I}^-$ and $^{129}\text{IO}_3^-$ were separated by anion chromatography in the laboratory. The remaining sample portions for both isotopes for IO_3^- and bulk DOI species were frozen in volumes larger than 250 ml, preferably in 1 L containers for ease of processing and storage. Fractions to be analyzed for TI (both isotopes) were stored refrigerated or in a cool, dark room in containers sealed with parafilm, after the addition of a reducing solution (RS). The RS consisted of 2 ml of $1 \text{ mol L}^{-1} \text{HSO}_3^-$ + 4 ml $1 \text{ mol L}^{-1} \text{NH}_2\text{OH}\cdot\text{HCl}$, adjusted to pH 6.5, per 1 L sample, to prevent loss of volatile iodine species (Szidat et al., 2000). The individual methods used are indicated in the following sections.

Measurement of [^{127}I] concentration and error calculation

The ^{127}I fractions that were measured directly for all samples were total iodine (TI), iodide (I^-), and total inorganic iodine (TII). The iodate (IO_3^-) concentration was also measured directly for samples from Stations 1, 3, 4, and J. All ^{127}I determinations were made as I^- , after the method of Wong and Zhang (1992), by cathodic stripping square wave voltammetry (CSSWV) using standard additions. ^{127}I species in samples from Stations 1, 3, 4, and J were also determined by high performance liquid chromatography (HPLC) using standard additions according to the method of Schwehr and Santschi (2003).

Standard additions were always made with two measurements on the initial dilution and at least two subsequent additions of the working I⁻ standard. This provided a total of at least two sets of standard additions on each fraction for each sample (at least eight measurements per iodine species), with an additional set of standard additions on the station samples duplicated by HPLC (at least 12 measurements per iodine species). For TI, three controls were run with the sample set. These controls were a thyroxine standard and a sample each of Galveston Bay and Trinity waters for which TI was previously determined independently by ICP-MS. The TI concentrations measured by HPLC showed standard deviations that were $\leq 3\%$ of the TI values measured by ICP-MS. The IO₃⁻ concentrations were also indirectly calculated for each sample by the subtraction of I⁻ from TII. Dissolved organic iodine (DOI) was determined as the difference between TI and TII. The maximum standard deviation for any ¹²⁷I species was $< 11 \text{ nmol L}^{-1}$ standard deviation (SD for one sigma) or $< 10\%$ relative standard deviation (RSD) error. This is important when considering DOI values, which were lower in overall concentrations than the other fractions. The % RSD for values of DOI was $\leq 10\%$ for all stations except Station 4, where it was $12 \pm 6 \text{ nmol L}^{-1}$ or a $\sim 50\%$ error, and Station J, where it was $8 \pm 9 \text{ nmol L}^{-1}$ or $\sim 125\%$ error.

Measurement of [¹²⁹I] concentration and error calculation

The procedure used for measuring the concentration of ¹²⁹I species was similar to that of ¹²⁷I, except that it was scaled up to allow processing of larger volume water samples (2 to 5 L). The low concentrations of ¹²⁹I in environmental samples ($\sim 10^7 \text{ atoms L}^{-1}$)

require that measurements be made by an Accelerator Mass Spectrometer (AMS) on 1 to 2 mg of AgI derived from the iodine concentration in large volume water samples.

Anion chromatography was used to separate and concentrate $^{129}\text{I}^-$ and $^{129}\text{I}-\text{IO}_3^-$ according to a modified method of Hou et al. (2001). Both isotopes of I^- were obtained by passing the filtered sample through a column of strong anion exchange resin, AG1-X4 or AG1-X8 (100-200 mesh). The resin had been pre-treated with $2 \text{ mol L}^{-1} \text{ NaNO}_3$ solution, then rinsed with deionized water (DIW) until the effluent did not form a white solution after the addition of AgCl (indicating that the resin was in the NO_3^- form). The treated resin was slurried into a column using 50 g resin per 1 L seawater with a salinity of 35, or 22 g per 1 L seawater with a salinity of 15. The sample was loaded onto the column at a flow rate of 2 ml min^{-1} . When processed in this fashion, I^- was retained on the resin and IO_3^- and most DOI fractions passed into the effluent. The $^{127}\text{I}^-$ concentration in the eluant was monitored as a yield tracer for breakthrough and recovery calculations. Alternatively, $^{125}\text{I}^-$ was added to the sample prior to loading the column to aid in the recovery determination.

After that, the resin column was rinsed with 50 ml $18\text{M}\Omega$ de-ionized water (DIW), which was added to the IO_3^- fraction and RS, then set aside. The resin column was then rinsed with 50 ml $0.1 \text{ mol L}^{-1} \text{ NaNO}_3$ solution to elute Cl^- and Br^- retained on the resin (Hou et al., 1999; 2001), and then with 50 ml $1 \text{ mol L}^{-1} \text{ NaNO}_3$ solution to elute potentially retained DOI (Reifenhauser and Heumann, 1990; Wimschneider and Heumann, 1995). These effluents were discarded. The I^- fraction was eluted after soaking the resin column (fitted with a covered reservoir) overnight in a 200 ml 2%

NaClO solution. The column was then drained and rinsed with two subsequent 50 ml volumes of DIW. All three elutions were combined, and reduced with 40 ml of 1 mol L⁻¹ HSO₃ + 0.18 mol L⁻¹ H₂SO₄ that was then stored in a dark, refrigerated container, sealed with parafilm, for subsequent liquid-liquid extraction.

To obtain IO₃⁻, RS was added to the sample effluent and the first DIW rinse to reduce IO₃⁻ species to I⁻ and the solution was allowed several hours to react to completion. The resin was rinsed with DIW then loaded with the reduced IO₃⁻ fraction. The rinsing and elution process as outlined for the I⁻ fraction was repeated and the final elution was also saved as the IO₃⁻ fraction for liquid-liquid extraction.

The concentration of ¹²⁹I-DOI was obtained as the difference of [¹²⁹I-TI] - ([¹²⁹I-I⁻] + [¹²⁹I-IO₃⁻]). The ¹²⁹I-TI fraction was isolated by adding a measured sample volume to 2.5 L glass bottles fitted with Teflon valves for pressure release. Dehydrohalogenation degrades alkyl and aryl halides. While the majority of DOI probably is aryl iodide (such as proteinaceous or complex humic and fulvic acid forms) and some alkyl iodide (Butler, 1996) which were degraded through acid and alkaline hydrolysis steps, ultrasonication, heating and freezing. This combination of physical and chemical processes was designed to uncoil helices, unfold proteins, break ester bridges, and expose all possible R-I bonds to degradation by dehydrohalogenation.

Dehydrohalogenation was accomplished by adding NaOH (4g per L sample) and ethanol (200 ml per L sample), ultrasonicated at 65°C for 3 hrs, then allowing it to react overnight. These steps were repeated then the sample was reduced with RS and acidified, ultrasonicated at 45°C for 1.5 hrs, and cooled in a freezer. Next, the sample

was warmed gently to room temperature, uncapped, and placed in a boiling water bath for 2 to 3 hrs to drive off the ethanol. After cooling, the sample was then passed through Empore C18 disks under vacuum to remove any remaining refractory substances and then processed through a resin column as described for Γ^- in the preceding discussion. The Empore C18 disks were conditioned prior to use by soaking in methanol overnight and rinsing with DIW. The same three controls as described for the ^{127}I -TI procedure were run in parallel with all ^{129}I samples.

The Γ^- , IO_3^- , and TI (for DOI by difference) fractions were then processed by liquid-liquid extraction by adding a ^{129}I -free carrier solution of $^{127}\text{I}^-$, oxidizing and acidifying the solution with H_2O_2 to transform all iodine species to I_2 , then shaking in a separatory funnel with CHCl_3 so that all I_2 would partition into the organic CHCl_3 phase. This purified I_2 fraction was then back-extracted into a solution of NaHSO_3 and H_2SO_4 , and precipitated into a pellet of AgI . The detailed version of the extractions and precipitation procedures are described elsewhere (Schwehr et al., 2003). The AgI pellet was cleaned, dried, and mixed with a pure Ag powder in preparation for measurement of the $^{129}\text{I}/^{127}\text{I}$ ratio in the iodine species of Γ^- , IO_3^- , and TI (DOI by difference), by the AMS facility at the Purdue PRIME Lab.

The column efficiency was $99 \pm 3\%$ for the recovery of $^{129}\text{I-I}^-$ ($n = 6$) and $^{129}\text{I-IO}_3^-$ ($n = 4$), which is similar to the 97% recovery in the procedure used by Hou et al. (2002) which used an eluant of 800 ml KNO_3 . The dehydrohalogenation efficiencies for $^{129}\text{I-TI}$ were $\geq 97 \pm 3\%$ ($n = 4$). The liquid-liquid extraction recovery was $95 \pm 5\%$ ($n = 5$). The counting error for $^{129}\text{I}/^{127}\text{I}$ by AMS generally averaged $\pm 10\%$ ($n = 18$). Therefore, the final error for $^{129}\text{I-I}^-$ and $^{129}\text{I-IO}_3^-$ after processing through the column, liquid-liquid extraction, and AMS averaged $\pm 12\%$ ($n = 4$). The counting error by AMS for $^{129}\text{I-TI}$ averaged 6% ($n = 4$). Since $^{129}\text{I-DOI}$ was obtained by difference where $[^{129}\text{I-DOI}] = [^{129}\text{I-TI}] - \{[^{129}\text{I-I}^- + ^{129}\text{I-IO}_3^-]\}$, the associated propagated error for $^{129}\text{I-DOI}$ ranged from 14 to 25%, and averaged 21% ($n = 4$). The highest error was associated with AMS counting of the $^{129}\text{I-I}^-$ fraction. Since this error was associated with the lowest concentration distributions for the measured ^{129}I fractions, the error could have been decreased by concentrating a larger volume of sample. Optimal sample volumes to decrease the error for the ^{129}I species in Galveston Bay would have been 1 to 2 L for $^{129}\text{I-TI}$, 5 L for $^{129}\text{I-IO}_3^-$, and 6 L for $^{129}\text{I-I}^-$. The actual volumes used were 1 to 2 L for $^{129}\text{I-TI}$, and 2 to 4 L for $^{129}\text{I-IO}_3^-$ and $^{129}\text{I-I}^-$.

RESULTS AND DISCUSSION

¹²⁷I speciation in Galveston Bay

The ¹²⁷I-TI concentrations in estuarine waters of Galveston Bay, presented in Table 4.1, are similar to literature values for total inorganic iodine concentrations in other coastal waters (Wong and Cheng, 1998; 2001; Abdel-Moati, 1999; Schwehr and Santschi, 2003). Fig. 4.2 shows the distribution of the ¹²⁷I species concentration in the Galveston Bay relative to salinity. All of the iodine species as well as DOC (Table 4.1) display scatter and deviate from conservative behavior in the estuary. Conservative behavior could be expected because the Trinity River, which accounts for an average of 84% of the fresh water input to the Galveston Bay, was at moderately high river discharge, with a mean value of $586 \text{ m}^3 \text{ s}^{-1}$ for December 2001, or ~50% maximum mean monthly flow for the year (the long term monthly mean value during the years 1924 through 2002 is $233 \text{ m}^3 \text{ s}^{-1}$ for the USGS station located at Romayor, Texas (USGS 2002b). Using the Trinity River discharge of $586 \text{ m}^3 \text{ s}^{-1}$, an estuarine surface area of 1432 km^2 , and a mean depth of 2.1 m (Santschi, 1995), the water renewal time for the Galveston Bay during this period would have been about 60 days.

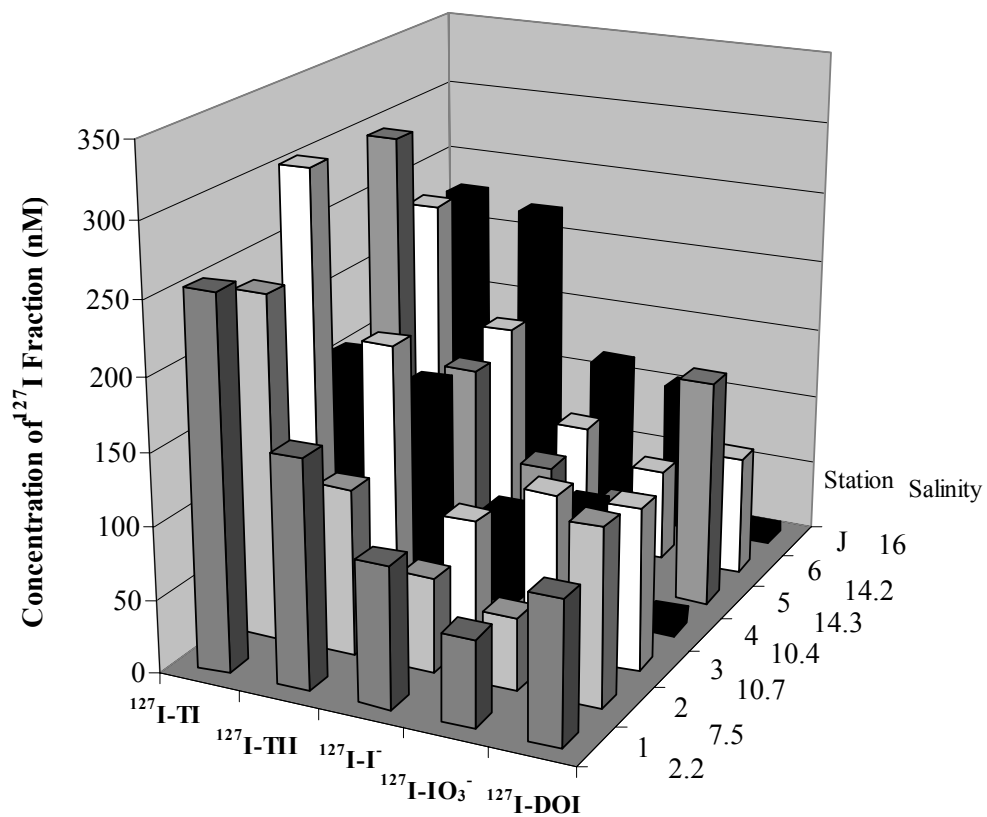


Fig. 4.2. Distribution of ^{127}I species concentrations in the Galveston Bay, December 14, 2001.

Table 4.1. Concentration of ^{127}I species in the surface waters of the Galveston Bay, Dec. 2001.

Station	Salinity ^a	Temperature °C ^a	Sigma- tau ^a	[TI] nM	[TII] nM	[I] nM	[IO ₃ ⁻] nM	[DOI] nM	1 STD for DOI ± nM	% DOI	Chl a ^a μM L ⁻¹	DOC μM C	TI/DOC *10 ⁻⁴
1	2.2	14.7	0.87	255	157	97	60	98	8	38	5.6	473	5
2	7.5	14.8	0.50	237	115	65	50	122	8	52	6.5	353	7
3	10.7	15.0	7.39	305	193	82	111	112	10	37	10.7	281	11
4	10.4	16.3	6.89	159	147	66	81	12	6	8	4.7	537	3
5	14.3	15.8	9.97	297	139	78	61	158	9	53	6.8	443	7
6	14.2	15.3	9.97	234	151	87	64	83	8	36	9.3	365	6
J	16	n.r.	n.r.	228	220	115	105	8	8	3	n.r.	403	6

^a Data provided by J.L. Pinckney and S.E. Lumsden.

A common way to evaluate sources and sinks of dissolved chemical species is to compare its distribution across a salinity gradient with that controlled by mixing only, termed “conservative behavior” (Loder and Reichard, 1981; Cifuentes and Eldridge, 1998; Truesdale and Jones, 2000). Dissolved or filter-passing (0.45 micron) iodine species data from the Bay were thus evaluated in terms of deviations from conservative behavior. A simple linear mixing model was applied to provide estimates for iodine species concentrations under conservative conditions to be compared to measured values. In this approach, the linearly extrapolated values were derived from averages of literature values for the river and ocean end-members, as shown in Table 4.2. For example, the end-member concentrations that were chosen for DOC and for $^{127}\text{I-TI}$ in the Trinity River (TR_M) were $457 \mu\text{mol C L}^{-1}$ and 295 nmol L^{-1} respectively, and $90 \mu\text{mol C L}^{-1}$ and 526 nmol L^{-1} for DOC and $^{127}\text{I-TI}$ in the Gulf of Mexico (GOM_M), respectively

Using these end member concentrations, a linear regression was calculated in the form of a concentration versus salinity regression (Fig. 4.3). Fig. 4.3a displays the DOC trend as a comparison between observed data (squares and solid lines) and expected values for conservative linear mixing (dashed line) between the Trinity River (TR_M) and.

Table 4.2. ^{129}I , ^{127}I , and DOC for the linear mixing model end-members, i.e., the Trinity River and the Gulf of Mexico (GOM).

Sample	Date	Sal	$^{129}\text{I}/^{127}\text{I}$ (10^{-12})	$^{129}\text{I-TI}$ (10^7 at L^{-1})	$^{127}\text{I-TI}$ (nM)	$^{127}\text{I-TII}$ (nM)	$^{127}\text{I-I}^-$ (nM)	$^{127}\text{I-IO}_3^-$ (nM)	$^{127}\text{I-DOI}$ (nM)	DOC $\mu\text{M C}$	Reference
Trinity	Jun 94	n.r. ^a	1093	5.6	79	n.r.	n.r.	n.r.	n.r.	n.r.	Schink et al., 1995b
Trinity	Nov 94	n.r.	1140	5.4	79	n.r.	n.r.	n.r.	n.r.	n.r.	Schink et al., 1995b
Trinity	Jul 95, Jul 93	0								417, 495	Guo and Santschi, 1997
Trinity	Jul 93, Jul 95	0.1, 0								258, 649	Wen et al., 1999
Trinity	Jun 96	n.r.	1100	5.7	87	n.r.	n.r.	n.r.	n.r.	n.r.	Moran et al., 2002
Trinity	Sep 00, Feb 01	0								350, 558	Warnken and Santschi, 2003
Trinity	Sep 00	0	n.r.	n.r.	295	187	176	11	107	457 ^b	Schwehr and Santschi, 2003
Trinity	Dec 01	2.2	406	6.2	255	157	97	60	98	473	This study
TR_M^c		0	333^d	5.9	295	187	176	11	107	457	This study
SW avg. ^e	n.r.	n.r.	n.r.	n.r.	472	n.r.	n.r.	n.r.	n.r.	n.r.	Moran et al., 1997
GOM	92-94	35	n.r.	n.r.	450-550	n.r.	n.r.	n.r.	n.r.	n.r.	Schink et al., 1995b
GOM	Mar 92	35	63	1.67	440	n.r.	n.r.	n.r.	n.r.	n.r.	Schink et al., 1995b
GOM	Apr 94	n.r.	59	1.56	440	n.r.	n.r.	n.r.	n.r.	81	Schink et al., 1995a
GOM	Jul 00	36.7	n.r.	n.r.	526	491	228	263	35	90 ^f	Schwehr and Santschi, 2003
GOM_M^g		35	51	1.62	526	491	228	263	35	90	This study

^a n.r. denotes that the value was not reported; ^b DOC value from K. Warnken, unpublished data. ^c TR_M indicates the values used for the Trinity River in the linear mixing model; ^d value derived by dividing avg. $^{129}\text{I-TI}$ for all '0' salinity measurements by the most reliable value for $^{127}\text{I-TI}$ (295 nM); ^e SW avg. represents seawater average; ^f Data provided by Hung et al., 2003; ^g GOM_M indicates the values used for the Gulf of Mexico in the linear mixing model.

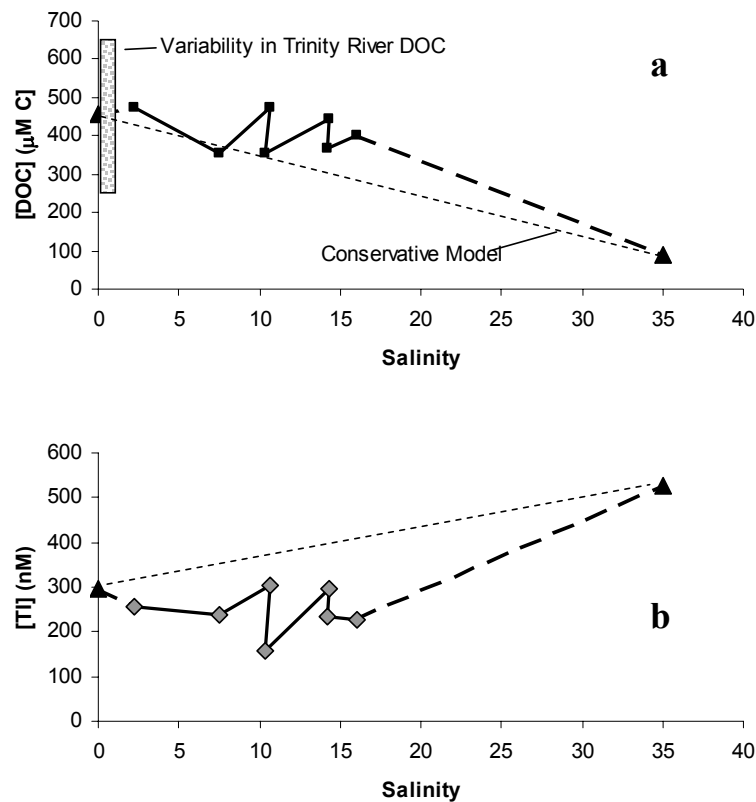


Fig. 4.3 (a) Comparison of observed (squares) and modeled (triangles) data for $[DOC]$ ($\mu M C$). The line of short dashes indicates a conceptual conservative linear mixing between the Trinity River and GOM end-members. The shaded area shows the range of variability for the Trinity River input (Guo and Santschi, 1997; Wen et al., 1999; Tang et al., 2002; Warnken and Santschi, 2003). (b) Comparison of observed transect (diamonds) and modeled (triangles) data for $[TI]$ (nM).

Gulf of Mexico (GOM_M) end-members (triangles). It would appear that the [DOC] is enhanced relative to conservative mixing indicating net sources (Guo and Santschi, 1997; Guo et al., 1999) within Galveston Bay for all stations except Station 3. The non-conservative behavior of DOC and the range of variability in Trinity River DOC ($\pm 43\%$) has been documented before (Guo and Santschi, 1997; Wen et al., 1999; Tang et al., 2002; Warnken and Santschi, 2003). Alternatively, another interpretation is that the measured [DOC] in the estuary are within the variability of the Trinity River input and are therefore conservative. Future research requires measurement of the end member values at the same sampling time as the estuarine transect.

Fig. 4.3b compares the values for conservative linear mixing (dashed line) between the Trinity River and GOM end-members (triangles) to the observed transect data for [TI] (diamonds and solid lines). In contrast to [DOC], [TI] values are depleted relative to conservative mixing, indicating net sinks for TI in the Bay during the time of sampling. The range of variability for TI is also very similar to that of DOC. The variations in observed TI show a very similar trend to those observed for DOC, implying that the same processes affect both quantities; however, changes in TI lag changes in DOC. It is therefore suggested that the scatter in iodine species is related to the patchiness in the distribution of DOC and other species (see below).

Although the patterns in variability (not shown) are different for TII , I^- , and IO_3^- , all three species also show net removal from the Bay water. Station 4 for IO_3^- is the exception, suggesting that IO_3^- was added as a source at this locale. Unlike the other

iodine species, [DOI] has a negative gradient with salinity, indicating a source to the Bay at Station 2 and 3, while showing removal at the other transect sampling points.

Reasons for deviations from expected conservative mixing include 1) analytical error, or 2) processes that influence iodine speciation, i.e., hydrographic mixing that is non-linear across the salinity gradient due to riverine variability (Cifuentes and Eldridge, 1998; Pakulski et al., 2000; Warnken and Santschi, 2003), biotic or abiotic reactions from sediment-water exchange, uptake, release, or remineralization processes. Before one can explore the effects of biogeochemical or hydrological processes, however, one needs to first address the variability due to analytical error.

The iodine fractions that were measured directly for all samples were TI, I⁻, and TII. The IO₃⁻ concentration was also measured directly at Stations 1, 3, 4, and J. All standard deviations were $\leq 3\%$ RSD for direct measurements. IO₃⁻ was also indirectly calculated for each sample by the subtraction of I⁻ from TII. DOI was found as the difference between TI and TII. The maximum standard deviation for any iodine species was $< 11 \text{ nmol L}^{-1}$ SD for one sigma or $< 10\%$ RSD error. This is important when considering the DOI values that were lower in absolute concentrations than the other fractions and calculated by difference. However, the RSD error for DOI was generally still acceptable, i.e., equivalent to $\leq 10\%$, for all stations except Station 4, where DOI was $12 \pm 6 \text{ nmol L}^{-1}$ or a $\sim 50\%$, and Station J, where DOI was $8 \pm 9 \text{ nmol L}^{-1}$ or $\sim 125\%$. Therefore, the magnitude of the analytical error is not sufficient to account for the variability in the range of iodine species concentrations, with the exception of [DOI] at Stations 4 and J.

This interpretation of strong patchiness is further supported by the distribution of nitrogen species, phosphate, silicate, and irradiance (K_d) data provided by J.L. Pinckney and S.E. Lumsden from the same sampling stations (Fig. 4.4). At Station 3 (salinity 10.71), Fig. 4.4, the nitrogen (NH_4^+ and sum of ($\text{NO}_2^- + \text{NO}_3^-$)) and orthophosphate concentrations appear to have been lowered through uptake by the primary producers (as suggested by the higher biomass) and possibly released through remineralization at Station 4 (salinity 10.36). Alternatively, Station 4 could reflect a patch of water that was more heavily influenced by wastewater inputs from local sources. We suggest that the latter interpretation is the most probable given the evidence of non-linear hydrographic mixing (Table 4.1). Interestingly, linear mixing is not observed along the transect as evidenced by the values for salinity, temperature, and sigma-tau (data provided by J.L. Pinckney and S.E. Lumsden) for Stations 3 and 4. For example, Station 4 is farther in distance from the head of the Bay than Station 3, yet the salinity and sigma-tau values were lower and the temperature higher than that of Station 3. This indicates that there is a different water mass, and therefore, non-linear mixing at Station 4.

The distribution of silicate is completely different from that of nitrogen species, orthophosphate, and irradiance, suggesting that its variations are more strongly influenced by other factors, e.g., the abundance of diatoms or benthic fluxes (Warnken et al., 2001). Additionally, the irradiance, K_d , was high at Station 3 indicating higher light absorption which could suggest higher biomass or suspended particulate matter. Furthermore, when concentrations at stations of similar salinity are compared, the % variations in nutrients were extremely large, and thus, were likely indicative of the same

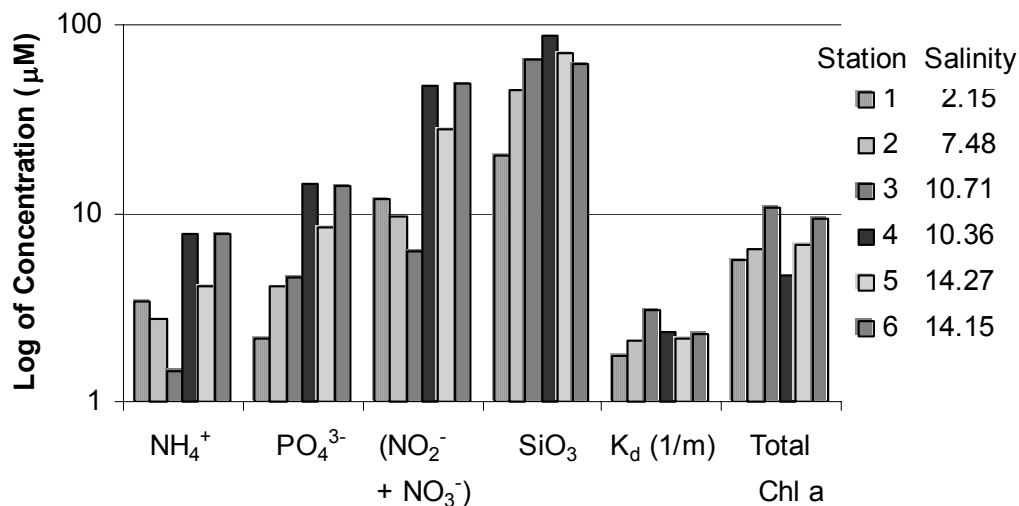


Fig. 4.4. Distribution of nutrient concentrations, irradiance (K_d), and biomass as chl a for the sampled transect of Galveston Bay. Data provided by J.L. Pinckney and S.E. Lumsden.

factors influencing the high variability in the iodine species concentration values, especially considering the modest analytical variability of $\leq 10\%$. Specifically, the salinity difference between Stations 3 and 4 was very small, only $\sim 3\%$, but the % variability between these nearby stations was 215% for orthophosphate, 430% for NH_4^+ , and 650% for $(\text{NO}_2^- + \text{NO}_3^-)$. Similarly, the relative salinity difference between Stations 5 and 6 was 1%, yet the % nutrient variability was 65%, 90%, and 75%, for PO_4^{3-} , NH_4^+ , and $(\text{NO}_2^- + \text{NO}_3^-)$, respectively.

Nutrient data also relate to the unusually low DOI value at Station 4.

Unfortunately, no ancillary nutrient data are available for Station J. Although there is no significant correlation between DOI and chl a or DOC concentrations, there is a fairly consistent TI/DOC ratio of 0.0006 ± 0.0002 across Galveston Bay (Table 4.1).

Dissolved organic iodine (DOI) values, as a percentage of TI, are higher than those reported for other coastal waters, but similar to those of Galveston Bay during a previous sampling period. The DOI concentrations ranged from about 3% to 53% of the TI, with an average DOI value of 85 nmol L^{-1} , or 32% of TI, and a median value of 98 nmol L^{-1} or 35% of TI. Comparison of data on chl a and TI/DOC ratios in Table 4.1 show that there was a high biomass and high nutrient concentrations at Station 3 and Station 4, again indicating either intensive remineralization at this station, or more likely, a patch of water influenced by local waste water discharge.

¹²⁹I speciation in Galveston Bay

The following notation was used: $^{129}\text{I-TI}$, $^{129}\text{I-TII}$, $^{129}\text{I-I}^-$, $^{129}\text{I-IO}_3^-$ and $^{129}\text{I-DOI}$, which represent the fractions of ^{129}I in total iodine, total inorganic iodine, iodide, iodate, and dissolved organic iodine, respectively. The distribution for ^{129}I speciation versus station number and salinity is shown in Figure 4.5 and Table 4.3.

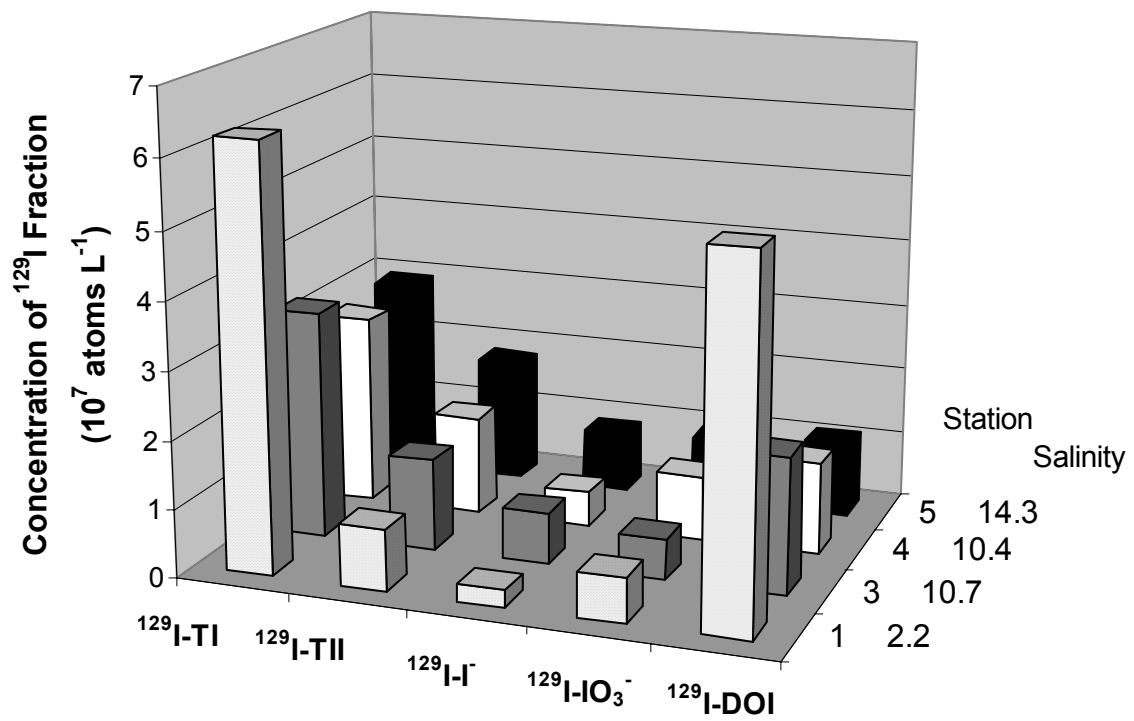


Fig. 4.5. Distribution of ^{129}I species concentrations in Galveston Bay, December 14, 2001.

Table 4.3. Concentration of ^{129}I and $^{129}\text{I}/^{127}\text{I}$ species in the surface waters of the Galveston Bay, Dec. 2001.

Station	Salinity	$^{129}\text{I-TI}$ (10^7 at L^{-1}) ^a	$^{129}\text{I-TII}$ (10^7 at L^{-1}) ^b	$^{129}\text{I-I}^-$ (10^7 at L^{-1}) ^a	$^{129}\text{I-IO}_3^-$ (10^7 at L^{-1}) ^a	$^{129}\text{I-DOI}$ (10^7 at L^{-1}) ^b
1	2.2	6.2	0.86	0.24	0.62	5.4
2	7.5			0.55		
3	10.7	3.4	1.3	0.76	0.52	2.1
4	10.4	2.8	1.4	0.51	0.90	1.4
5	14.3	2.9	1.8	0.87	0.91	1.1
J	16			0.72		
Station	Salinity	$^{129}\text{I}/^{127}\text{I-TI}$ (10^{-12}) ^a	$^{129}\text{I}/^{127}\text{I-TII}$ (10^{-12}) ^b	$^{129}\text{I}/^{127}\text{I-I}^-$ (10^{-12}) ^a	$^{129}\text{I}/^{127}\text{I-IO}_3^-$ (10^{-12}) ^a	$^{129}\text{I}/^{127}\text{I-DOI}$ (10^{-12}) ^b
1	2.2	406	91	41	170	912
2	7.5			142		
3	10.7	183	110	153	78	309
4	10.4	295	159	128	184	1913
5	14.3	163	212	184	248	119
J	16			105		

^a measured directly. ^b calculated by difference.

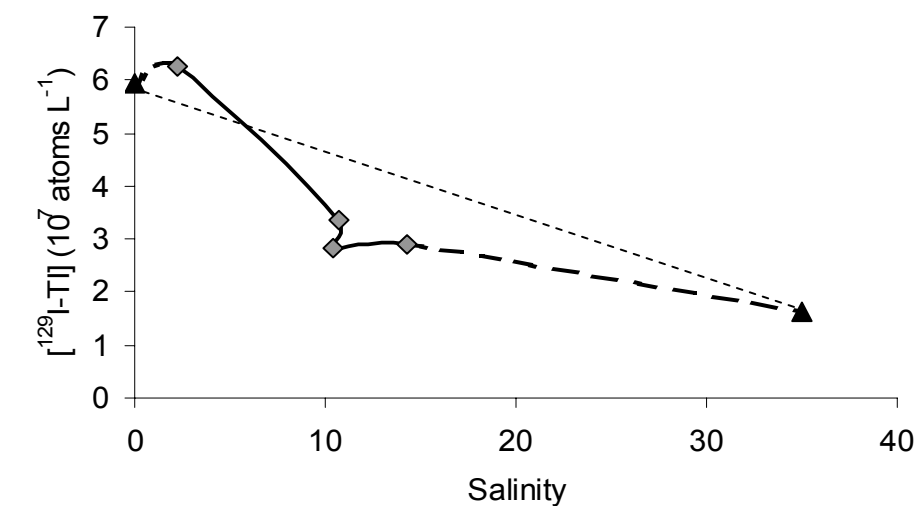
The measured $^{129}\text{I-TI}$ value of 6.2×10^7 atoms L^{-1} from a sample taken near the Trinity River is only slightly higher than the $^{129}\text{I-TI}$ value of 5.7×10^7 atoms L^{-1} given in Moran et al. (2001). The former study used H_2O_2 to convert DOI into inorganic forms of iodine. It is well-documented that many oxidation methods used for the decomposition of organic iodine are not quantitative and are compound-dependent (Wong and Cheng, 1998; 2001; Schwehr and Santschi, 2003; Santschi and Schwehr, 2003). Thus, it is possible that incomplete digestion of DOI by previous research is the reason for their somewhat lower value. Since the $^{129}\text{I-DOI}$ fraction is 87% of the $^{129}\text{I-TI}$ at this station, this would suggest that the majority of the riverine $^{129}\text{I-DOI}$ is labile enough to have

been decomposed by the H_2O_2 method. It is plausible that once C-I bonds are cleaved in the H_2O_2 method and the iodine species are oxidized to I_2 , the I_2 partitions into the organic solvent used in the liquid-liquid extraction before new DOI species are reformed.

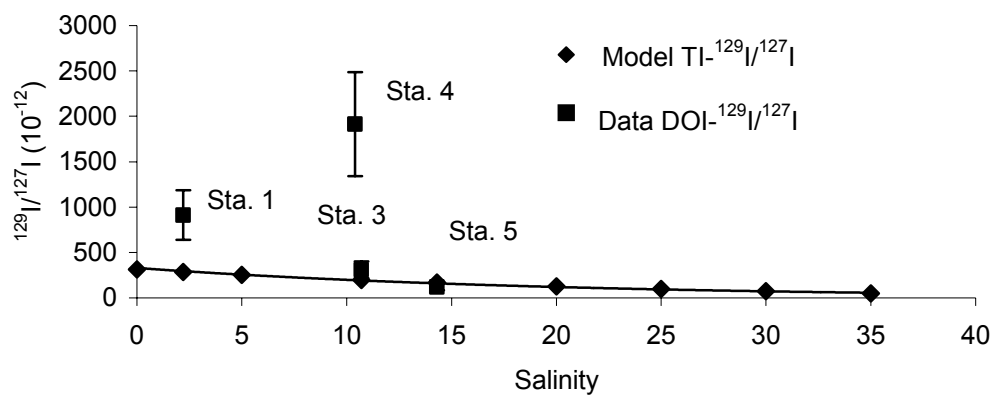
As for the stable iodine species, a simple model of conservative linear mixing was used for comparison purposes to measured $^{129}\text{I}/^{127}\text{I}$ and $^{129}\text{I}\text{-TI}$ values. The compiled literature values for the model end-members, TR_M and GOM_M , are 5.9×10^7 atoms L^{-1} for TR_M and 1.62×10^7 atoms L^{-1} for GOM_M (Table 4.3). The concentrations of ^{127}I species from Schwehr and Santschi (2003) were selected because it is the only consistent and reliable data for this area. These $^{127}\text{I}\text{-TI}$ values were obtained using standard additions, calibrated against the iodine concentration in a certified reference material (SRM 1549, powdered milk), and were measured independently by ICP-MS (Schwehr and Santschi, 2003). The different values for $^{129}\text{I}\text{-TI}$, i.e., from the various literature data summarized in Table 4.2, are all within the analytical error, so the average of these values was used for TR_M and GOM_M . It should be noted that the $^{129}\text{I}\text{-TI}$ value for this study (6.2×10^7 atoms L^{-1}) was not included in the average value of $^{129}\text{I}\text{-TI}$ for GOM_M as the salinity at this station was not '0' as required for the assumption that the different iodine species and isotopes for the end-member values were fully equilibrated in the water. The $^{129}\text{I}/^{127}\text{I}$ value of 333×10^{-12} for the TR_M was derived by dividing the average $^{129}\text{I}\text{-TI}$ for all '0' salinity measurements by the most reliable value for $^{127}\text{I}\text{-TI}$, 295 nM, as explained above.

Measured values of $^{129}\text{I}/^{127}\text{I}$ (Table 4.3) are compared with those derived from a linear mixing model (dashed lines) (Fig. 4.6a). The observed $^{129}\text{I-TI}$ distribution (Fig. 4.6a) shows non-conservative behavior, with the river-influenced Station 1 indicating the presence of a source for $^{129}\text{I-TI}$, while the other stations are showing net removal from the estuary.

$^{129}\text{I}/^{127}\text{I}$ values for the different iodine species are plotted as a function of salinity in Fig. 4.6b. This diagram depicts the relationship of DOI- $^{129}\text{I}/^{127}\text{I}$ concentrations (as squares), and TI- $^{129}\text{I}/^{127}\text{I}$ values (shown as diamonds) with salinity, and compares them to conservative mixing behavior. To develop the $^{129}\text{I}/^{127}\text{I}$ ratio mixing model values, concentration vs. salinity equations were calculated separately for $^{129}\text{I-TI}$ and for $^{127}\text{I-TI}$ to pass through the end-member concentrations (Table 4.3). The TI- $^{129}\text{I}/^{127}\text{I}$ values were then derived by dividing each $^{129}\text{I-TI}$ value by its corresponding $^{127}\text{I-TI}$ value for a particular salinity. The values for TI- $^{129}\text{I}/^{127}\text{I}$, which used the $^{127}\text{I-TI}$ value (295 nmol L⁻¹) for the TR_M from Schwehr and Santschi (2003) for predicted conservative linear mixing, are shown as a dark dashed line with grey diamonds. It is evident that the $^{127}\text{I-TI}$ values (295 and 255 nmol L⁻¹) have increased in this most recent sampling expedition, when compared to earlier times (79 nmol L⁻¹ in 1994 and 87 nmol L⁻¹ in 1996; Table 4.3). As a comparison, the white diamonds and grey dashed line indicate the model for TI- $^{129}\text{I}/^{127}\text{I}$ values using the average $^{127}\text{I-TI}$ value (84 nmol L⁻¹) from the earlier work. Provided $^{127}\text{I-TI}$ values are of the order of 200 nmol L⁻¹, then DOI- $^{129}\text{I}/^{127}\text{I}$ concentrations are non-conservative and significantly elevated.



(a)



(b)

Fig. 4.6. Comparison of observed (diamonds and solid lines) and modeled (triangles and dashed lines) data for (a) $^{129}\text{I-TI}$ and (b) $^{129}\text{I}/^{127}\text{I}$ for TI.

These elevated values can thus be used to trace terrestrial organic matter through the upper reaches of the Bay, at salinities < 10 , e.g., at Station 1. The isotopic ratio of DOI- $^{129}\text{I}/^{127}\text{I}$ may also be used to trace biogeochemical processes in estuaries as indicated by the elevated DOI- $^{129}\text{I}/^{127}\text{I}$ value at Station 4 that suggests strong terrestrial influence, most likely through wastewater input. This salinity zone of 0 to ~ 15 ppt appears to be the zone most strongly dominated by terrestrial species. For example, Guo and Santschi (1997) showed that macromolecular organic matter ≥ 10 kDa in Galveston Bay is mostly removed in this salinity zone, and Guo et al. (2003) demonstrated that terrestrial influence of colloidal macromolecular organic compounds, as traced by $\delta^{13}\text{C}$, $\delta^{14}\text{N}$ and C/N ratios, does not extend beyond 20 ppt, in agreement with our data.

Fig. 4.7 is a mixing diagram for the values of the isotopic ratio $^{129}\text{I}/^{127}\text{I}$ (10^{-12}) plotted against $1/^{127}\text{I}$ (ppb^{-1}). Values are shown for $^{129}\text{I}/^{127}\text{I}$ (10^{-12}) median of U.S. rains (diamond), U.S. rivers (circle), and the Gulf of Mexico (GOM, triangle) are all for the iodine species TI for both isotopes. The squares indicate the observed data values for the species DOI for both isotopes. This plot emphasizes the terrestrial source of DOI for Stations 4 and 1, which compare to mixing between U.S. rains and rivers. Stations 3 and 5 show values approximating the ocean waters of GOM with limited dilution from U.S. rivers.

Other studies of inorganic ^{129}I speciation in seawater

Currently, we know of only one other study of ^{129}I speciation in seawater. Hou et al. (2001) measured concentrations for inorganic $^{129}\text{I-TII}$, $^{129}\text{I-I}^-$, and $^{129}\text{I-IO}_3^-$ in surface

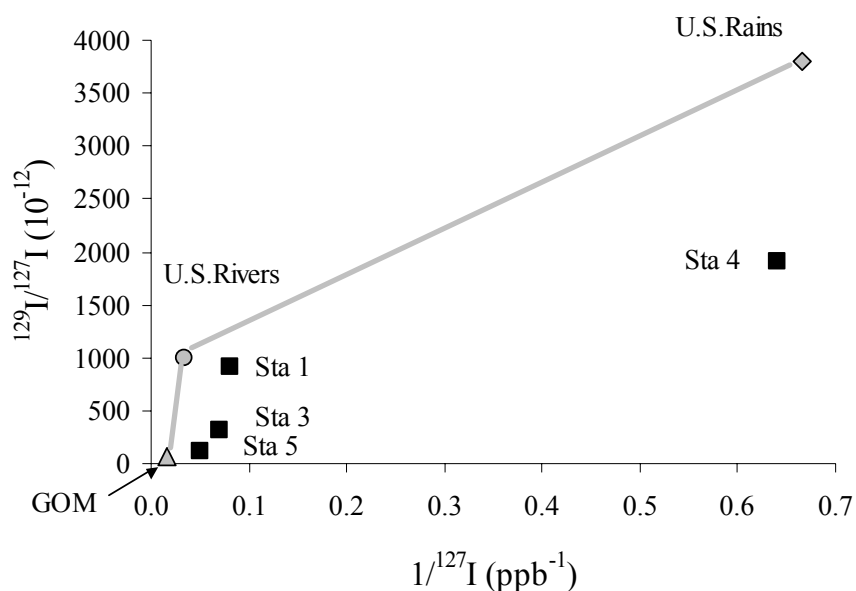


Fig. 4.7. Mixing diagram for the values of the isotopic ratio $^{129}\text{I}/^{127}\text{I}$ (10^{-12}) plotted against $1/^{127}\text{I}$ (ppb⁻¹). Values are shown for $^{129}\text{I}/^{127}\text{I}$ (10^{-12}) median of U.S. rains (diamond), U.S. rivers (circle), and the Gulf of Mexico (GOM, triangle) are all for the iodine species TI for both isotopes. The squares indicate the observed data values for the species DOI for both isotopes. This plot emphasizes the terrestrial source of DOI for Stations 4 and 1, which compare to mixing between U.S. rains and rivers. Stations 3 and 5 show values approximating the ocean waters of GOM with limited dilution from U.S. rivers.

and bottom waters of the Kattegat and Baltic Seas. Salinities ranged from 7.5 to ~35 in waters that have open ocean characteristics wherein the inorganic species are conservative with salinity. We have shown that the inorganic speciation of our iodine values is strongly influenced by estuarine processes at Stations 3 and 4, so it follows that our data can be different from the more open ocean stations of Hou et al (2001).

Another difference in the Hou et al (2001) data is that the concentrations of ^{129}I there are several orders of magnitude higher than in North American waters. This is

expected since the Kattegat and Baltic Seas are much closer to the source of ^{129}I emissions from Sellafield and La Hague than Galveston Bay.

CONCLUSIONS

Values for $^{129}\text{I}/^{127}\text{I}$ in terrestrial organic matter are greatly elevated over those from marine systems. The question in this research was if isotope ratios of iodine, a biophilic element, can be used to trace terrestrial organic matter across an estuary, similar to carbon isotopes. Novel analytical techniques of $^{129}\text{I}/^{127}\text{I}$ ratio determination in DOI and the other iodine species, utilizing dehydrohalogenation, anion chromatography, HPLC and AMS techniques, were developed and applied to samples from a transect across Galveston Bay, Texas. Results indicate that elevated $^{129}\text{I}/^{127}\text{I}$ values in DOI from terrestrial sources are significant up to salinity of about 15, similar to previously described stable isotope signals of DOM ($\delta^{13}\text{C}$, $\delta^{14}\text{N}$ and C/N ratios) in this estuary (Guo et al., 1997, 2003). $^{129}\text{I}/^{127}\text{I}$ ratios in the other iodine species, e.g., iodide and iodate, did not show this feature, indicating fast isotopic and chemical equilibration between the two isotopes among the different inorganic species in the estuary. Future research should include measurement of the end-member values during the same collection period as the estuarine transect sampling. Additionally, a time series input of $^{129}\text{I}/^{127}\text{I}$ values, especially for $^{129}\text{I}/^{127}\text{I}$ -DOI during different discharge periods for the Trinity River, would document input variability to the Galveston Bay estuary.

CHAPTER V

CONCLUSIONS AND RECOMMENDATIONS FOR FUTURE RESEARCH

CONCLUSIONS

Conclusions for methodology of measurement of ^{127}I species

This is a description of a new and sensitive method for the detection of iodine species at nanomolar concentrations in different aquatic systems, and to quantitatively measure organic iodine. The method has a useful linear range from 1 to 150 nM and is applicable to fresh, estuarine, and seawater samples. The detection limit for iodide, defined as 3 times the standard deviation of the instrument detection limit, was less than 1 nM (0.2 ppb), with a relative standard deviation of 3% for all waters. Recovery for total inorganic and organic iodine species was validated through the use of the certified reference material SRM 1549 powdered milk, the methods of standard additions, and by comparison to results for total iodine determinations by ICP-MS.

Conclusions for the measurement of the $^{129}\text{I}/^{127}\text{I}$ for the TI species in a fresh water aquifer system

From measurements of ^{129}I and ^{127}I in wells from Orange County ground water basin fed by the Anaheim Lake and Kraemer Basin recharge ponds, literature values of aquifer residence times based on $^3\text{H}/^3\text{He}$ and $\delta^{18}\text{O}$ data, as well as time-series data of chloride and Santa Ana River flow rates over the past decade, the following conclusions were drawn:

$^{129}\text{I}/^{127}\text{I}$ ratios as well as ^{129}I concentrations in well water increase with aquifer water residence times, which is not likely to be a result of changes in the source function, since the low concentrations of ^{129}I from European reprocessing plant emissions have been shown to be about constant over the past decade. This behavior of ^{129}I is ascribed to the inverse relationship between ^{129}I concentration and river flow rate previously documented for ^{129}I in the Mississippi River [Oktay et al., 2001], for example, and for chloride in the Santa Ana River. Thus, it appears that ^{129}I behavior in this aquifer that is being recharged by ponds fed mainly by rivers draining semi-arid basins showing evapotranspiration effects, can be used as a hydrological tracer for past river flow conditions in the recharge area. This novel application, even though it needs to be tested further, could be useful in determining past hydrological conditions in other, less studied aquifers, in semi-arid basins with populations in need of drinking water with recharge areas affected by evapotranspiration. Additionally, the behavior of ^{129}I and total organic carbon (TOC) showed higher concentration in surface waters than in the youngest ground waters. This behavior follows natural filtration of macromolecular

organic matter with percolation through soils. The interpretation is supported by the documented study showing that larger size fractions of TOC and younger ^{14}C -age dated TOC present in surface waters than in the aquifer waters.

Conclusions for the determination of the concentration of $^{129}\text{I}/^{127}\text{I}$ for the TI species in an estuarine environment

$^{129}\text{I}/^{127}\text{I}$ ratios in terrestrial organic matter are greatly elevated over those from marine systems. The question in this research was if isotope ratios of iodine, a biophilic element, can be used to trace terrestrial organic matter across an estuary, similar to carbon isotopes. Novel analytical techniques of $^{129}\text{I}/^{127}\text{I}$ ratio determination in DOI and the other iodine species, utilizing dehydrohalogenation, anion chromatography, HPLC and AMS techniques, were developed and applied to samples from a salinity transect across Galveston Bay, Texas. Results indicate that elevated $^{129}\text{I}/^{127}\text{I}$ ratios in DOI from terrestrial sources are noticeable up to salinity of about 15, similar to previously described stable isotope signals of DOM in this estuary (Guo et al., 1997, 2003). $^{129}\text{I}/^{127}\text{I}$ ratios in the other iodine species, e.g., iodide and iodate, did not show this feature, indicating fast isotopic and chemical equilibration between the two isotopes among the different inorganic species in the estuary.

Summary of conclusions

Based on the biophilic nature of iodine and the elevated concentration of ^{129}I due primarily to atmospheric emissions of nuclear fuel reprocessing facilities in Europe, the hypotheses have been confirmed that $^{129}\text{I}/^{127}\text{I}$ values have tracer applications and potential for geochronometry of organic matter. Significant developments from this study are: 1) a new method to determine ^{127}I concentrations and species that is an order of magnitude more sensitive than other methods and can be used for all matrices of natural waters; 2) a new technique using dehydrohalogenation to decompose organic iodine quantitatively for both iodine isotopes; 3) the first reported values of ^{129}I -DOI and $^{129}\text{I}/^{127}\text{I}$ -DOI are published herein; 4) a new tracer application ground water relative to the inferred flow volume in the catchment basin where the values of $^{129}\text{I}/^{127}\text{I}$ are concentration during evapotranspiration cycles and diluted during storm cycles; 5) as hypothesized, ^{129}I has a different mobility and thus, perhaps a different chemical form than ^{127}I and Cl in the Orange County, California, aquifer system; 6) it was inferred that with known localized inputs, ^{129}I could be used as a geochronometer of organic matter based on the apparent similar behaviors of TOC and ^{129}I concentrations, i.e., they follow an equivalent trend to TOC concentrations (reduced concentrations from surface water to ground waters by 50-75%) and the TOC decreased in size and increased in ^{14}C -age with travel from surface to ground water; and 7) since terrestrial organic matter is more highly enriched in ^{129}I than marine organic matter (due to source pathways of ^{129}I biogeochemical cycling), $^{129}\text{I}/^{127}\text{I}$ -DOI can be used to trace terrestrial organic matter in estuaries where salinity is less than 15.

RECOMMENDATIONS FOR FUTURE RESEARCH

To use $^{129}\text{I}/^{127}\text{I}$ values as a tracer, certain tracer prerequisites must be met. These prerequisites are that 1) the ^{129}I input source location is known; 2) the ^{129}I input concentration function is known; 3) the $^{129}\text{I}/^{127}\text{I}$ values trace a single process with a known time scale; 4) the isotope ^{129}I is equilibrated with ^{127}I , or the extent of non-equilibration is defined; and 5) the chemical speciation and geochemical properties for iodine and its species are known. The first item is known; the nuclear fuel reprocessing facilities of the Hague in France and Sellafield in Great Britain. For the second item, localized input functions of ^{129}I concentrations over time need to be determined, particularly since $^{129}\text{I}/^{127}\text{I}$ values are distributed with latitude and distance from the European sources (Snyder and Fehn, unpublished). Items 3 and 4 have been addressed in the case studies presented in Chapters III and IV, but further testing of these concepts under a variety of conditions and the ancillary data (discussed in these Chapters) would confirm the utility of these tracer applications.

For the last item the kinetics of equilibration with ^{127}I and transformations of ^{129}I is not well-known. Knowledge of the speciation and transport of ^{129}I and ^{127}I , which reflects differences in equilibration times within environmental archives, needs to be greatly improved. ^{129}I appears to undergo a number of biological and physical transformations potentially changing from an organic to an inorganic form (or vice versa) several times. Over time scales of months to years, ^{129}I tends to end up in a more refractory organic matter pool. During the formation of organo-iodine species,

microorganisms (bacteria and phytoplankton) appear to bind iodine in kinetically faster reactions into nitrogen-rich compounds, i.e., proteins. These microbially produced nitrogen-rich compounds are more labile, and might have a shorter lifetime (days to weeks), before they are converted into more refractory compounds such as humic-acid-type molecules. In the upper water column, photochemical and other oxidation reactions continually destroy and produce organo-iodine species through radical reactions contributing to the channeling of ^{129}I into a rather refractory organic matter pool. Thus, over time scales of 1 day to a few months, iodine ends up in nitrogen-rich compounds, while on time scales of 1-10 years, labile organo-iodine compounds will evolve into more stable and more refractory organic compounds.

Once the localized input functions for ^{129}I concentrations and the kinetics of equilibration and transformation are determined, $^{129}\text{I}/^{127}\text{I}$ values may even provide a geochronometer for organic molecules formed or altered in the past 50 years (since the advent of bomb-testing).

REFERENCES

- Abdel-Moati M.A.R. (1999) Iodine speciation in the Nile River estuary. *Mar. Chem.* **65**, 211-225.
- Baker A.R. (2002) Air-sea exchange of iodine. School of Environ. Sci., Univ. of East Anglia, United Kingdom. URL: <http://www.uea.ac.uk/~e780/airseaiod.htm>.
- Baker A.R., Thompson D., Campos M.L.A.M., Parry S.J., and Jickells T.D. (2000) Iodine concentration and availability in atmospheric aerosol. *Atmosph. Environ.* **34**, 4331-4336.
- Baskaran M., Asbill S., Santschi P.H., Brooks J., Champ M., Adkinson D., Colmer M.R., and Makeyev V. (1996) Pu, ¹³⁷Cs and excess ²¹⁰Pb in Russian Arctic sediments. *Earth Planet. Sci. Lett.* **140**, 243-257.
- Baskaran M., Asbill S., Santschi P.H., Davis T., Brooks J., Champ M., Makeyev V., and Khlebovich V. (1995) Distribution of ^{239,240}Pu and ²³⁸Pu concentrations in sediments from the Ob and Yenisey Rivers and the Kara Sea. *Applied Radiation and Isotopes* **46/11**, 1109-1119.
- Beasley T.M., Cooper L.W., Grebmeier, J.M., Kilius L.R., and Synal H-A. (1997) ³⁶Cl and ¹²⁹I in the Yenisei, Kolyma, and ackenzie Rivers. *Environment* **31**, 1834-1836.
- Bichsel Y. and von Gunten U. (1999) Determination of iodide and iodate by ion chromatography with postcolumn reaction and UV/Visible detection. *Anal. Chem.* **71**, 34-38.
- Bichsel Y. and von Gunten U. (2000) Formation of iodo-trihalomethanes during disinfection and oxidation of iodide-containing waters. *Environ. Sci. Technol.* **34**, 2784-2791.
- Brandao A.C.M., Buchberger W.W., Butler E.C.V., Fagan P.A., and Haddad P.R. (1995) Matrix elimination ion chromatography with postcolumn reaction detection for the determination of iodide in saline waters. *J. Chromatogr. A* **706**, 271-275.
- Buldini P.L., Ferri D., and Sharma J.L. (1997) Determination of some inorganic species in edible vegetable oils and fats by ion chromatography. *J. Chromatogr. A* **789**, 549-555.

- Buraglio N., Aldahan A., Possnert G., and Vintersved I. (2001) I-129 from the nuclear reprocessing facilities traced in precipitation and runoff in northern Europe. *Environ. Sci. Technol.* **35**, 1579-1586.
- Butler E.L. (1986) Methyl-iodide and iodine in the marine atmosphere. Ph.D. Dissertation, University of Rhode Island, R.I.
- Butler E.C.V. (1996) The analytical chemist at sea: measurements of iodine and arsenic in marine waters. *Trends in Analytical Chemistry* **15**, 45-52.
- Carlsen L., Lassen P., Christiansen J.V., Warwick P., Hal A., and Randall A. (1992) Radio-labelling of humic and fulvic materials for use in environmental studies. *Radiocimica Acta* **58/59**, 371-376.
- Christiansen J.V. and Carlsen L. (1991) Enzymatically controlled iodination reactions in the terrestrial environment. *Radiochimica Acta* **52/53**, 327-333.
- Cifuentes L.A. and Eldridge P.M. (1998) A mass- and isotope-balance model of DOC mixing in estuaries. *Limnol. Oceanogr.* **43**, 1872-1882.
- Clemens-Knott D., Foster J.H., Yoshiba G., Davisson M.L., Hudson G.B., and Beiriger J. (1998) Hydrogeochemical study of waters on the lower Forebay region of the Santa Ana River. In *Report on Coastal Groundwater Basin, Orange County, California*, pp. 16, Orange County Water District, Ca.
- Cochran J.K., Moran S.B., Fisher N.S., Beasley T.M., and Kelley J.M. (2000) Sources and transport of anthropogenic radionuclides in the Ob River system, Siberia. *Earth Planet. Sci. Lett.* **179**, 125-137.
- Cooper L.W., Beasley T.M., Zhao X.L., Soto C., Vinogrova K.L., and Dunton K.H. (1998) Iodine-129 and plutonium isotopes in arctic kelp as historical indicators of transport of nuclear fuel reprocessing wastes from mid-to-high latitudes in the Atlantic Ocean. *Marine Biology* **131**, 391-399.
- Cooper L.W., Hong G.H., Beasley T.M., and Grebmeier J.M. (2002) Iodine-129 concentrations in marginal seas of the North Pacific and Pacific-influenced waters of the Arctic Ocean. *Mar. Poll. Bulletin* **42**, 1347-1356.
- Davisson M.L. (1998) Final results of Anaheim Lake tracer study. In *Report to OCWD*, pp. 5, Orange County Water District, California.

- Davisson M.L., Hudson G.B., Herndon R., Niemeyer S., and Beiriger J. (1996) Report on the feasibility of using isotopes to source and age-date groundwater in Orange County Water District's Forebay region. In *Lawrence Livermore National Laboratory UCRL-ID-123953*, pp. 31, Orange County, California.
- Davisson M.L., Hudson G.B., Herndon R., and Woodside G. (1999a) Report on isotope tracer investigations in the Forebay of the Orange County Groundwater Basin: Fiscal years 1996 and 1997. In *Lawrence Livermore National Laboratory UCRL-ID-133531*, pp. 44, Orange County Water District, California. URL website: <http://www.llnl.gov/tid/lof/documents/pdf/235457.pdf>.
- Davisson M.L., Vengosh A., and Bullen T. (1999b) Tracing waste-water in river and ground water of Orange County using boron isotopes and general geochemistry. In *Lawrence Livermore National Laboratory UCRL-ID-133529*, pp. 44, Orange County Water District, California.
- Davisson M.L., Hudson G.B., Moran J.E., and Niemeyer S. (1998) Isotope tracer approaches for characterizing artificial recharge and demonstrating regulatory compliance. In *Annual UC Water Reuse Res. Conf., June 4-5*, pp.7, Monterey, Cal. URL website: <http://www.llnl.gov/tid/lof/documents/pdf/233183.pdf>.
- Dissanayake C.B. and Chandrajith, R. (1999) Medical geochemistry of tropical environments. *Earth-Science Reviews* **47**, 219-258.
- Drever J.I. (1997) Evaporation and saline waters; cyclic wetting and drying. In *Geochemistry of Natural Waters: Surface and Groundwater Environments*, pp. 335-336, New Jersey, Prentice-Hall.
- Edmonds J.S. and Morita M. (1998) The determination of iodine species in environmental and biological samples (Technical report). *Pure Appl. Chem.* **70**, 1567-1584.
- Eisenbud M. and Gesell T. (1997) Terrestrial and aquatic pathways. In *Environmental Radioactivity: From Natural, Industrial, and Military Sources*, Fourth Edition, pp. 656, San Diego, Academic Press.
- Fabryka-Martin J. (2000) Iodine-129 as a groundwater tracer. In *Environmental Tracers in Subsurface Hydrology*, pp. 504-510, Boston, Kluwer Acad. Publ.

- Fabryka-Martin J., Bentley H., Elmore D., and Airey P.L. (1985) Natural iodine-129 as an environmental tracer. *Geochim Cosmochim Acta* **49**, 337.
- Farrenkopf A.M. and Luther III G.W. (2002) Iodine chemistry reflects productivity and denitrification in the Arabian Sea: evidence of flux for dissolved species from sediments of western India into the OMZ. *Deep-Sea Res. II* **49**, 2303-2318.
- Farrenkopf A.M., Luther G.W., Truesdale V.W., and Van Der Weijden C.H. (1997) Sub-surface iodide maxima: evidence for biologically catalyzed redox cycling in Arabian Sea OMZ during the SW intermonsoon. *Deep-Sea Res. II* **6-7**, 1391-1409.
- Fehn U., Holdren G.R., Elmore D., Brunelle T., Teng R.T.D., and Kubik P.W. (1986) Determination of natural and anthropogenic ^{129}I in marine sediments. *Geophys. Res. Lett.* **13**, 137-139.
- Fehn U. and Snyder G. (2000) ^{129}I in the southern hemisphere: global redistribution of an anthropogenic isotope. *Nuclear Instruments Methods B* **172**, 366-371.
- Frechou C., Calmet D., Bertho X., and Gaudry A. (2002) $^{129}\text{I}/^{127}\text{I}$ ratio measurements in bovine thyroids from the North Cotentin area (France). *Sci. Tot. Environ.* **293**, 59-67.
- Fuhrmann M., Bajt S., and Schoonen M.A.A. (1998) Sorption of iodine on minerals investigated by X-ray absorption near edge structure (XANES) and ^{125}I tracer sorption experiments. *Applied Geochem.* **13**, 127-141.
- Fukui M., Fujikawa Y., and Satta N. (1996) Factors affecting interaction of radioiodide and iodate species in soil. *J. Environ. Radioactivity*, **31**, 199-216.
- Gabay J.J., Paperiello C.J., Goodyear S., Daly J.C., and Matuszek J.M. (1974) Method for determining Iodine-129 in milk and water. *Health Physics*, **26**, 89-96.
- Gamlin J.D., Clark J.F., Woodside G., and Herndon R. (2001) Large-scale tracing of ground water with sulfur hexafluoride. *Jour. of Environ. Eng.*, **127**, 171-174.

- Guo L. and Santschi P.H. (1997) Isotopic and elemental characterization of colloidal organic matter from Chesapeake Bay and Galveston Bay. *Mar. Chem.* **59**, 1-15.
- Guo, L., Santschi P. H., and Bianchi T. S. (1999). Dissolved organic matter in estuaries of the Gulf of Mexico. In *Biogeochemistry of Gulf of Mexico Estuaries* (eds. T.S. Bianchi, J.R. Pennock, and R. Twilley) pp 269-299, John Wiley & Sons.
- Guo L., Tanaka N., Schell D.M., and Santschi P.H. (2003) Nitrogen and carbon isotopic composition of HMW dissolved organic matter in marine environments. *Mar. Ecol. Progr. Ser.*, **252**, 51-60.
- Hauschild J., Aumann D.C. (1985) Iodine-129 and natural iodine in tree rings in the vicinity of a small nuclear fuels reprocessing plant. *Naturwissenschaften* **72**, 270-271.
- Herndon R.L., Brukner D., and Sharp G., (1997) Groundwater systems in the Orange County Groundwater Basin. In *TIN/TDS Task Force 2.2 Report*, pp. 11, Orange County Water District, Cal.
- Herndon R.L., Woodside G.D., Davisson M.L., and Hudson G.B. (2003) Successful use of isotopes to estimate groundwater ages and flow paths in Orange County, California, *Ground Water*, In review.
- Heumann K.G. (1993) Determination of inorganic and organic traces in the clean room compartment of Antarctica. *Analytica Chimica Acta* **283**, 230-245.
- Heumann K.G., Gallus S.M., Radlinger G., and Vogl J. (1998) Accurate determination of element species by on-line coupling of chromatographic systems with ICP-MS using isotope dilution technique. *Spectrochim. Acta B* **53**, 273-287.
- Hou X., Chai C., and Qian Q. (1997) Study on the chemical species of iodine in some seaweeds. I. *Sci. Tot. Environ.* **204**, 215.
- Hou X., Dahlgaard H., and Nielsen S.P. (2001) Chemical speciation analysis of ¹²⁹I in seawater and a preliminary investigation to use it as a tracer for geochemical cycle study of stable iodine. *Mar. Chem.* **72**, 145-155.
- Hou X.L., Dahlgaard H., Nielsen S.P., and Kucera J. (2002) Level & origin of Iodine-129 in the Baltic Sea, *J. Environ. Radioactivity* **61**, 331-343.

- Hou X., Yan X., and Chai C. (2000) Chemical species of iodine in some seaweeds. II. Iodine-bound biological macromolecules. *J. Radioanalyt. Nucl. Chem.* **245**, 461-467.
- Hu W., Haddad P.R., Hasebe K., Tanaka K., Tong P., and Khoo C. (1999) Direct determination of bromide, nitrate, and iodide in saline matrixes using electrostatic ion chromatography with an electrolyte as eluant. *Anal. Chem.* **71**, 1617-1620.
- Hung C-C., Guo L., Santschi P.H., Alvarado-Quiroz N., Haye J., and Walsh I.D. (2002) *Mar. Chem.* Submitted.
- Hussain A., Jona J., Yamada A., and Dittert L. (1995) Chloramine-T in radiolabeling techniques. *Analytical Biochem.* **224**, 221-226.
- Ito K. (1997) Determination of iodide in seawater by ion chromatography. *Anal. Chem.* **69**, 3628-3632.
- Ito K. (1999) Semi-micro ion chromatography of iodide in seawater. *J. Chromatogr. A* **830**, 211-217.
- Kaplan D.I., Serne R.J., Parker K.E., and Kutnyakov I.V. (2000) Iodide sorption to subsurface sediments and illitic minerals. *Environ. Sci. Technol.*, **34**, 399-405.
- Kekli A., Aldahan A., Meili M., Possnert G., Buraglio N., and Sepanauskas R. (2003) ^{129}I in Swedish rivers: distribution and sources. *Sci. Tot. Environ.* In press.
- Kocher D.C. (1982) On the long-term behaviour of iodine-129 in the terrestrial environment. In *Environmental Migration of Long-lived Radionuclides*, pp. 669-679, Vienna, IAEA.
- Kolb C.E. (2002) Iodine's air of importance. *Nature* **417**, 597-598.
- Krupp G. and Aumann C. (1999) Iodine-129 in rainfall over Germany. *J. Environ. Radioactivity*, **46**, 287-299.
- Langmuir D. (1997) The redox behavior of natural systems. In *Aqueous Environmental Geochemistry*, pp. 403-430, New Jersey, Prentice Hall.
- Lassen P., Carlsen L., Warwick P., Randall A., and Zhao R. (1994) Radioactive labeling and characterization of humic materials. *Environment International* **20**, 127-134.

- Libes S.M. (1992) Residence times and steady state. In *An Introduction to Marine Biogeochemistry*, pp. 357-359, New York, Wiley.
- Loder T.C. and Reichard R.P. (1981) The dynamics of conservative mixing in estuaries. *Estuaries* **4**, 64-69.
- Lopez-Gutierrez J.M., Garcia-Leon M., Garcia-Tenorio R., Schnabel C., Suter M., Synal H-A., and Szidat S. (2000) $^{129}\text{I}/^{127}\text{I}$ ratios and ^{129}I concentrations in a recent sea sediment core and in rainwater from Sevilla (Spain) by AMS. *Nucl. Instr. Meth. Phys. Res. B*, **172**, 574-578.
- Lopez-Gutierrez J.M., Garcia-Leon M., Schnabel C., Schmidt A., Michel R., Synal H-A., and Suter M. (1999) Determination of ^{129}I in atmospheric samples by accelerator mass spectrometry. *Appl. Rad. Isotopes* **51**, 315-322.
- Luther G.W., Wu J., and Cullen J.B. (1995) Redox chemistry of iodine in seawater: frontier molecular orbital theory considerations. *Advances in Chemistry Series*, **244**, 135-155.
- Luther III G.W. and Campbell T. (1991) Iodine speciation in the water column of the Black Sea. *Deep-Sea Res. II* **38**, S875-S882.
- Luther III G.W., Ferdelman T., Culberson C.H., Kostka J., and Wu J. (1991) Iodine chemistry in the water column of the Chesapeake Bay – evidence for organic iodine forms. *Estuar., Coastal., Shelf Sci.* **32**, 267-279.
- Martin M.W. (1999) Selectivity of some ion chromatography stationary phases for small anions in solvent-water mixtures with hydroxide. *Microchem. J.* **62**, 203-222.
- McBride M.B. (2000) Chemisorption and precipitation reactions. In *Soils* (ed. M.E. Sumner) pp. B-265-302, Boca Raton, CRC Press.
- Meijer A., (2002) Conceptual model of the controls on natural water chemistry at Yucca Mountain, Nevada. *Applied Geochemistry* **17**, 793-805.
- Moran J.E., Oktay S.D., and Santschi P.H. (2002) Sources of Iodine and ^{129}I Iodine in Rivers. *Wat. Res. Res.* **38**, 1149, DOI: 10.1029/2001WR00062, 24-1 to 24-10.

- Moran J.E., Oktay S.D., Santschi P.H., and Schink D.R. (1997) Surface ¹²⁹Iodine/¹²⁷Iodine ratios: Marine vs. terrestrial. In *Applications of Accelerators in Research and Industry* (eds. J.L. Duggan and I.L. Morgan), pp. 807-810, New York, AIP Press.
- Moran J.E., Oktay S.D., Santschi P.H., and Schink D.R. (1999a) Atmospheric dispersal of ¹²⁹Iodine from European nuclear fuel reprocessing facilities. *Environ. Sci. Tech.* **33**, 2536-2542.
- Moran J.E., Oktay S., Santschi P.H., Schink D.R., Fehn U., and Snyder G. (1999b) World-wide redistribution of ¹²⁹Iodine from nuclear fuel reprocessing facilities: Results from meteoric, river, and seawater tracer studies. IAEA-SM-354/101.
- Moran J.E., Teng R.T. D., Rao U., and Fehn U. (1995) Detection of iodide in geologic materials by high-performance liquid-chromatography. *J. Chromatogr. A* **706**, 215-220.
- Moran S.B., Cochran J.K., Fisher N.S., and Kilius L.R. (1995) ¹²⁹I in the Ob River. In *Environmental Radioactivity in the Arctic* (eds. P. Strand and A. Cook), pp. 75-78 Ostersund, Norway, Norwegian Radiation Protection Authority.
- NADP/NTN (2002) National Atmospheric Deposition Program/National Trends Network monthly precipitation-weighted concentrations for the water years from 1982 to 1999 for the station # CA42 Tanbark Flat, Calif., <http://nadp.sws.uiuc.edu/sites/siteinfo.asp?id=CA42&net=NTN>, unpublished.
- NCDC, NOAA, 2003. National Climate Data Center of the National Oceanographic and Atmospheric Administration web site for Houston, Texas. <http://lwf.ncdc.noaa.gov/oa/climate/research/cag3/V1.html>.
- Nisizawa K. (1979) Pharmaceutical studies on marine algae in Japan. In *Marine Algae in Pharmaceutical Science*. p. 243-310, New York, De Gruyter.
- O'Dowd C.D., Jimenez J.L., Bahreinl R., Flagan R.C., Seinfeld J.H., Hameri K., Pirjola L., Kulmala M., Jennings S.G., and Hoffmann T. (2002) Marine aerosol formation from biogenic iodine emissions. *Nature* **417**, 632-636.
- OCWD (1999) Orange County Water District, Master Plan Report for 2020, <http://OCWD 2020 rpt\OCWD Online - Year 2020 Master Plan Study.htm>.

- Oktaý S.D., Santschi P.H., Moran J.E., and Sharma P. (2000) The ^{129}I Iodine Bomb Pulse Recorded in Mississippi River Delta Sediments: Results from Isotopes of I, Pu, Cs, Pb, and C. *Geochim. Cosmochim. Acta* **64**, 989-996.
- Oktaý S.D., Santschi P.H., Moran J.E., and Sharma P. (2001) ^{129}I and ^{127}I transport in the Mississippi River. *Environ. Sci. Technol.* **35**, 4470-4476.
- Ornolfsdottir E.B. (2002) The ecological role of small phytoplankton in phytoplankton production and community composition in Galveston Bay, Texas. Ph.D. Dissertation, Texas A&M University, College Station, TX.
- Pakulski J.D., Benner R., Whitlege T., Amon R., Eadie B., Cifuentes L., Ammerman J., Stockwell D. (2000) Microbial metabolism and nutrient cycling in the Mississippi and Atchafalaya River plumes. *Est. Coastal Shelf Science* **50**, 173-184.
- Pantsar-Kallio M. and Manninen P.K.G. (1998) Speciation of halogenides and oxyhalogens by ion chromatography- inductively coupled plasma mass spectrometry. *Anal. Chim. Acta* **360**, 161-166.
- Paul M., Fink D., Hollos G., Kaufman S.A., Kutschera W., and Magaritz M. (1987) Measurement of ^{129}I concentrations in the environment after the Chernobyl reactor accident. *Nucl. Instrum. Meth. Phys. Res. B* **29**, 341-345.
- Pinkney J.L., Ornolfsdottir E.B., and Lumsden S.E. (2002) Estuarine phytoplankton group-specific response to sublethal concentrations of the agricultural herbicide, atrazine. *Mar. Pollution Bull.* **44**, 1109-1116.
- Planert M. and Williams J.S. (1995) Los Angeles-Orange County coastal plain aquifer system. In HA 730-B: California, Nevada; USGS Groundwater Atlas of the United States, http://capp.water.usgs.gov/gwa/ch_b/B-text4.html.
- Quiroz N.G.A., Kotzer T.G., Milton G.W., Clark I.D., and Bottomley D. (2002) Partitioning of ^{127}I and ^{129}I in an unconfined glaciofluvial aquifer on the Canadian Shield. *Radiochim. Acta* **90**, 1-10.

- Rädlinger G. and Heumann K.G. (2000) Transformation of iodide in natural and waste water systems by fixation on humic substances *Environ. Sci. Technol.* **34**, 3932 – 3936.
- Rahn K.A., Borys R.D., and Duce R.A. (1976) Tropospheric halogen gases – inorganic and organic components. *Science* **192**, 549-550.
- Raisbeck G.M. and Yiou F. (1999) ^{129}I in the oceans: origins and applications. *Sci. Tot. Environ.* **237**, 31-41.
- Raisbeck G.M., Yiou F., Zhou Z.Q., and Kilius L.R. (1995) ^{129}I from nuclear fuel reprocessing facilities at Sellafield (U.K.) and La Hague (France); potential as an oceanographic tracer. *J. Marine Systems* **6**, 561-570.
- Rao U., Fehn U., Muramatsu Y., McNeil H., Sharma P., and Elmore D. (2002) Tracing the history of nuclear releases: Determination of ^{129}I in tree rings. *Environ. Sci. Technol.* **36**, 1271-1275.
- Reifenhauser C. and Heumann K.G. (1990) Development of a definitive method for iodine speciation in aquatic systems. *Fresenius J. Anal. Chem.* **336**, 559-563.
- Rue E.L., Smith G.J., Cutter G.A., and Bruland K.W. (1997) The response of trace element redox couples to suboxic conditions in the water column. *Deep-Sea Res. I* **44**, 113-134.
- Santschi P.H. (1995) Seasonality in nutrient concentrations in Galveston Bay. *Mar. Environ. Res.* **40**, 337-362.
- Santschi P.H., Oktay S., Moran J.E., and Schwehr K.A. (2000) ^{129}I as an environmental tracer. Extended Abstract for invited pres., NRC5, 5th Int. Conf. Nucl. Radiochem. Pontresina, Switzerland.
- Santschi P.H., Moran J.E, Oktay S., Hoehn E., and Sharma P. (1999) ^{129}I Iodine: A new tracer for surface water/groundwater interaction. *IAEA-SM-361*, 10.
- Santschi P.H., Schink D.R., Corapcioglu O., Oktay-Marshall S., Fehn U., and Sharma P. (1996) Evidence for elevated levels of Iodine-129 in the deep Western Boundary Current in the Middle Atlantic Bight. *Deep-Sea Res. I* **43**, 259-265.

- Santschi P.H. and Schwehr K.A. (2003) $^{129}\text{I}/^{127}\text{I}$ as a new environmental tracer or geochronometer for biogeochemical or hydrodynamic processes in the hydrosphere and geosphere: the central role of organo-iodine. *Sci. of Total Environ.* In press, Corrected proof, 1-15.
- Schall C., Heumann K.G., and Kirst G.O. (1997) Biogenic volatile organoiodine and organobromine hydrocarbons in the Atlantic Ocean from 42°N to 72°S. *Fresenius J. Anal. Chem.* **359**, 298-305.
- Schink D.R., Santschi P.H., Corapcioglu O., Oktay S., and Fehn U. (1995a) Prospects for "iodine-129" dating of marine organic matter using AMS. *Nucl. Instr. and Methods in Phys. Res. B* **99**, 524-527.
- Schink D.R., Santschi P.H., Corapcioglu O., Sharma P., and Fehn U. (1995b) ^{129}I in Gulf of Mexico waters. *Earth Planet. Sci. Lett.* **135**, 131-138.
- Schmidt A., Schnabel C., Handl J., Jalpb D., Michel R., Synal H.-A., Lopez J.M., and Suter M. (1998) On the analysis of iodine-129 and iodine-127 in environmental materials by accelerator mass spectrometry and ion chromatography. *Sci.Tot. Environ.* **223**, 131-156.
- Schnabel C., Lopez-Gutierrez J.M., Szidat S., Sprenger M., Wernli J., Beer J., and Synal H.A. (2001) On the origin of I-129 in rain water near Zurich, *Radiochim. Acta* **89**, 815-822.
- Schwehr K.A. and Santschi P.H. (2003) A sensitive determination of iodine species, including organo-iodine, for fresh water and seawater samples using high performance liquid chromatography and spectrophotometric detection. *Analytica Chim. Acta*, **482**, 59-71.
- Schwehr K.A., Santschi P.H., Moran J.E., and Elmore, D. (2003) ^{129}I Iodine: A new hydrological tracer for aquifer recharge conditions influenced by river flow rate variations and evapotranspiration. *Appl. Geochem.*, Submitted.
- SeEVERS R. H., and Counsell R.E. (1982) Radioiodination techniques for small organic molecules. *Chem. Rev.* **82**, 575-590.
- Sheppard M.I., Thibault D.H., McMurry J., and Smith P.A. (1995) Factors affecting the soil sorption of iodine. *Water Air and Soil Pollution*, **83**, 51-67.

- Skoog D.A., West D.M., and Holler F.J. (2000) Evaluation of analytical data. In *Analytical Chemistry*, 7th Edition, pp. 700, Philadelphia, Saunders College Pub.
- Smith J.N., Ellis M., and Kilius L.R. (1998) ^{129}I and ^{137}Cs tracer measurements in the Arctic Ocean. *Deep-Sea Res. I* **45**, 959-984.
- Snyder G. and Fehn U. (2003) Global distribution of ^{129}I in rivers and lakes: Implications for iodine cycling in surface reservoirs. Unpublished manuscript.
- Southard R.J. (2000) Aridisols. In *Soils* (ed. M.E. Sumner), pp. E-321-327, Boca Raton, CRC Press.
- Spokes L.J. and Liss P.S. (1996) Photochemically induced redox reactions in seawater, II. nitrogen and iodine. *Mar. Chem.* **54**, 1-10.
- Stutz J. (2000) Influence of halogen oxides on tropospheric ozone. Dept. of Atmospheric Sciences, UCLA, URL: <http://www.atmos.ucla.edu/~jochen/research/hox/hox.html>.
- Summers R.S., Fuchs F., and Sontheimer H. (1989) The fate and removal of radioactive iodine in the aquatic environment. *Am. Chemical Society, Symposium Series* **219**, 623-636.
- Szidat S. (2000) Grundlagen der Radioökologie des ^{129}I . Ph.D. Dissertation, Zentrum fuer Strahlenschutz und Radioökologie (ZSR), University of Hannover, Germany.
- Szidat S., Schmidt A., Handl J., Jakob D., Botsch W., Michel R., Synal H.A., Schnabel C., Suter M., Lopez-Gutierrez J.M., and Stade W. (2000) Iodine-129: sample preparation, quality control and analyses of pre-nuclear materials and of natural waters from Lower Saxony, Germany, *Nuclear Instruments Methods B* **172**, 699-710.
- Tang D., Warnken K.W., and Santschi P.H. (2002) Distribution and partitioning of trace metals (Cd, Cu, Ni, Pb, Zn) in Galveston Bay waters. *Mar. Chem.* **78**, 29-45.
- Thurman E.M. (1985) Organic carbon in natural waters: amount, origin, and classification. In *Organic Geochemistry of Natural Waters*, p. 1-65, Boston, Kluwer Academic.

- Tian R.C. and Nicolas E. (1995) Iodine speciation in the northwestern Mediterranean Sea: method and vertical profile. *Mar. Chem.* **48**, 151-156.
- Truesdale V.W. and Jones K. (2000) Steady-state mixing of the iodine in shelf seas off the British Isles. *Continental Shelf Res.* **20**, 1889-1905.
- Truesdale V.W., Nausch G., and Baker A.R. (2001) The distribution of iodine in the Baltic Sea during summer. *Mar. Chem.* **74** (2-3), 87-98.
- Tsukada H., Ishida J. and Narita O. (1991) Particle-size distributions of atmospheric I-129 and I-127 aerosols. *Atmos. Environ.* **25A**, 905-908.
- UNSCEAR. (1982) Report by the United Nations Scientific Committee on the Effects of Atomic Radiation to the General Assembly of the United Nations, New York.
- USGS (2002a) United States Geological Survey monthly stream flow statistics for California Station # 11074000, Santa Ana River below the Prado Dam, <http://waterdata.usgs.gov/ca/nwis/monthly>, unpublished.
- USGS (2002b) United States Geological Survey water data for Trinity River gauging station #08066500 (Romayor, Texas). WWW page, <http://tx.waterdata.usgs.gov>.
- Wagner M.J.M., Dittrich-Hannen B., Synal H-A., Suter M., and Schotterer U. (1996) Increase of ^{129}I in the environment. *Nucl Instrum Meth Phys Res B* **113**, 490-494.
- Wakeham S.G. (1999) Monocarboxylic, dicarboxylic and hydroxy acids released by sequential treatments of suspended particles and sediments of the Black Sea. *Org. Geochem.* **30**, 1059-1074.
- Ward G.H. (1992) The prediction problems for salinity intrusion. In *Proc. 2nd State of the Bay Symposium*, ed. R.W. Jensen, R. W. Kiesling & F.S. Shipley. Galveston Bay National Estuary Program Publication GBNEP-23, pp. 315-326.
- Warner J.A., Casey W.H., and Dahlgren R.A. (2000) Interaction kinetics of I_2 (aq) with substituted phenols and humic substances. *Environ. Sci. Technol.* **34**, 3180-3185.

- Warnken K.W., Gill G.A., Griffin L.L, and Santschi P.H. (2001) Sediment-water exchange of Mn, Fe, Ni and Zn in Galveston Bay, Texas. *Mar. Chem.* **73**: 215-231.
- Warnken K.W. and Santschi P.H. (2003) Biogeochemical behavior of organic carbon in the lower Trinity River downstream of the Lake Livingston Reservoir Texas, USA). *Water Res. Res.*, Submitted.
- Warnken K.W., Tang D., Gill G.A., and Santschi P.H. (2000) Performance optimization of a commercially available iminodoacetate resin for the determination of Mn, Ni, Cu, Cd, and Pb by on-line preconcentration inductively coupled plasma-mass spectrometry. *Anal. Chim. Acta* **423**, 265-276.
- Warwick P., Zhao R., Higgs J.J.W., Smith B., and Williams, G.M. (1993) The mobility and stability of iodine-humic and iodine-fulvic complexes through sand. *Sci. Total Environ.* **130/131**, 459-465.
- Wayne R.P., Poulet G., Biggs, P., Burrows, J.P., Cox, R.A., Crutzen, P.J., Haymann, G.D., Jenkin, M.E., Le Bras, G., Moortgat, G.K., Platt, U., and Schindler, R.N. (1995) Halogen oxides: radicals, sources and reservoirs in the laboratory and in the atmosphere. *Atmosph. Environ.* **29**, 2675-2884.
- Wen L.S., Santschi P.H., Gill G., and Paternostro C. (1999) Estuarine trace metal distributions in Galveston Bay: Importance of colloidal forms in the speciation of the dissolved phase. *Mar. Chem.* **63** (3-4), 185-212.
- Wimschneider A. and Heumann, K.G. (1995) Iodine speciation in size fractionated atmospheric particles by isotope dilution mass spectrometry. *Fresenius J. Anal. Chem.* **353**, 191-196.
- Wong G.T.F. (1991) The marine geochemistry of iodine, *Rev. Aquatic Sci.* **4**, 45-73.
- Wong G.T.F. (2001) Coupling iodine speciation to primary, regenerated or "new" production: a re-evaluation. *Deep-Sea Research, Part I* **48**, 1459-1476.
- Wong G.T.F. and Cheng X.H. (1998) Dissolved organic iodine in marine waters: determination, occurrence and analytical implications. *Mar. Chem.* **59**, 271-281.

- Wong G.T.F. and Cheng X.H. (2001) The formation of iodide in inshore waters from the photochemical decomposition of dissolved organic iodine. *Mar. Chem.* **74**, 53-64.
- Wong G.T.F. and Hung C. (2001) Speciation of dissolved iodine: integrating nitrate uptake over time in the oceans. *Cont. Shelf Res.* **12** (5/6), 717-733.
- Wong G.T.F., Piumsomboon A.U., and Dunstan, W.M. (2002) The transformation of iodate to iodide in marine phytoplankton cultures. *Mar. Ecol. Prog. Series* **237**, 27-39.
- Wong G.T.F. and Zhang L.S. (1992) Chemical removal of oxygen with sulfite for the polarographic or voltammetric determination of iodate or iodide in seawater. *Mar. Chem.* **38**, 109-116.
- Yiou F., Rasbeck G.M., Shou Z.Q., and Kilius L.R. (1994) ^{129}I from nuclear fuel reprocessing; potential as an oceanographic tracer. *Nucl. Instrum. Methods B* **92**, 436-439.
- Yoshida S. and Muramatsu Y. (1995) Determination of organic, inorganic and particulate iodine in the coastal atmosphere of Japan. *J. Radioanalyt. Nucl. Chem.* **196**, 295-302.
- Zellmer D.L., (1998) Standard addition. Dept. of Chem., Cal. St. Univ. at Fresno, URL:
<http://crystal.biol.csufresno.edu:8080/~davidz/Chem106/StdAddn/StdAddn.html>, copyrighted.
- Zika R.G., Moffett J., Cooper W.J., Petasne R., and Saltzmann E. (1985) Spatial and temporal variations of hydrogen peroxide in Gulf of Mexico Waters. *Geochim. Cosmochim. Acta* **49**, 1173-1184.

VITA

Kathleen A. Schwehr

Home Phone: 281-334-0903
 E-mail: k_schwehr@hotmail.com
 POB 862
 Kemah, TX 77565

Research Interests

Isotope and aqueous geochemistry. Biogeochemical cycling and speciation of iodine in natural fresh waters, coastal, and open marine systems. Colloids. Applications of stable and radioisotopic tracers.

Education and Awards

Ph.D. Chemical Oceanography, Texas A&M University, 2004
 Texas Institute of Oceanography Graduate Student Fellowship, 2001
 Texas Water Research Institute/ USGS Grant, 2000
 Travel Grants from Ocn. Grad. Council, Mar. Sci. Res. Adv. Board, Mooney Foundation
 M.S. Geology, University of Houston, August 1998
 Amoco Graduate Fellowship for Outstanding Performance
 Sigma Xi Research Grant
 Houston Coastal Center Grant
 B.S. Geophysical Engineering, Montana College of Mineral Science and Technology, 1982

Professional Experience

Graduate Research Associate, Texas A&M University, 1998 – present, Dr. Peter Santschi, Advisor
 Graduate Research Associate, University of Houston, 1996, Dr. Siechi Nagihara
 Graduate Research Associate, University of Houston, 1994-1996, Dr. James Lawrence, Advisor
 Geophysicist, Exploration and Development, Union Oil of California, Midland, TX., 1982-1992,
 Bryan Lee, Supervisor

Research Publications

Schwehr, K.A. and P.H. Santschi, 2003. A sensitive determination of iodine species in fresh or seawaters using high performance liquid chromatography and spectrophotometric detection. *Anal. Chim. Acta* 482, 59-71.
 P.H. Santschi and Schwehr, K.A., 2003. $^{129}\text{I}/^{127}\text{I}$ as a new environmental tracer or geochronometer for biogeochemical or hydrodynamic processes in the hydrosphere and geosphere: the central role of organo-iodine. *Science of the Total Environment (In Press)*.
 Schwehr, K.A., Santschi, P.H., J.E. Moran, and D. Elmore, 2003. ^{129}I iodine: A new hydrologic tracer for aquifer recharge conditions influenced by river flow rate and evapotranspiration, Orange County, Calif. *Applied Geochem.* (submitted).
 Schwehr, K.A. Santschi, P.H., and D. Elmore, 2003. The dissolved organic iodine species of the isotopic ratio $^{129}\text{I}/^{127}\text{I}$: A novel tool for tracing terrestrial organic matter in the estuarine surface waters of Galveston Bay, TX. *Limnol. Oceanogr.* (submitted).

Professional Societies and Academic Services

American Geophysical Union
 American Society of Limnology and Oceanography
 Geological Society of America
 TX A&M University, Oceanography Graduate Council, Executive Board, 2000 to 2004
 TX A&M University, Galveston Graduate Student Council, Treasurer, 1999
 Permian Basin Geophysical Society, 2nd Vice President, Treasurer, Secretary, 1982-1992